

PYROLYSIS AND COMBUSTION BEHAVIOUR OF VARIOUS FUELS IN OXYGEN-  
ENRICHED AIR AND CO<sub>2</sub> ATMOSPHERES

A THESIS SUBMITTED TO  
THE GRADUATE SCHOOL OF NATURAL AND APPLIED SCIENCES  
OF  
MIDDLE EAST TECHNICAL UNIVERSITY

BY

NUR SENA YÜZBAŞI

IN PARTIAL FULFILLMENT OF THE REQUIREMENTS  
FOR  
THE DEGREE OF MASTER OF SCIENCE  
IN  
CHEMICAL ENGINEERING

FEBRUARY 2011

Approval of the thesis:

**PYROLYSIS AND COMBUSTION BEHAVIOUR OF VARIOUS FUELS IN OXYGEN  
ENRICHED AIR AND CO<sub>2</sub> ATMOSPHERES**

submitted by NUR SENA YÜZBAŞI in partial fulfillment of the requirements for the degree of **Master of Science in Chemical Engineering Department, Middle East Technical University** by,

Prof. Dr. Canan Özgen

Dean, Graduate School of **Natural and Applied Sciences**

\_\_\_\_\_

Prof. Dr. Deniz Üner

Head of Department, **Chemical Engineering**

\_\_\_\_\_

Prof. Dr. Nevin Selçuk

Supervisor, **Chemical Engineering Dept., METU**

\_\_\_\_\_

**Examining Committee Members:**

Prof. Dr. Hayrettin Yücel

Chemical Engineering Dept., METU

\_\_\_\_\_

Prof. Dr. Nevin Selçuk

Chemical Engineering Dept., METU

\_\_\_\_\_

Prof. Dr. Necati Özkan

Polymer Science and Technology Dept., METU

\_\_\_\_\_

Asst. Prof. Dr. Görkem Külah

Chemical Engineering Dept., METU

\_\_\_\_\_

Dr. Yusuf Göğebakan

MIMAG-SAMKO Energy Technologies

\_\_\_\_\_

**Date:**

07.02.2011

**I hereby declare that all information in this document has been obtained and presented in accordance with academic rules and ethical conduct. I also declare that, as required by these rules and conduct, I have fully cited and referenced all material and results that are not original to this work.**

Name, Lastname: Nur Sena Yüzbaşı

Signature:

## **ABSTRACT**

### **PYROLYSIS AND COMBUSTION BEHAVIOUR OF VARIOUS FUELS IN OXYGEN-ENRICHED AIR AND CO<sub>2</sub> ATMOSPHERES**

Yüzbaşı, Nur Sena

M. Sc., Department of Chemical Engineering

Supervisor: Prof. Dr. Nevin Selçuk

February 2011, 122 pages

Oxy-fuel combustion technology, which is based on burning coal in a mixture of oxygen and recycled flue gas (RFG), is suggested as one of new promising technologies for capturing CO<sub>2</sub> from power plants.

In this thesis study, the pyrolysis and combustion behaviour of various fuels including imported coal, petroleum coke, two different types of indigenous lignites, olive residue and their blends with different proportions in air and oxy-fuel conditions were investigated by using non-isothermal thermogravimetric method (TGA) coupled with Fourier-transform infrared (FTIR) spectrometer.

Pyrolysis tests were carried out in nitrogen and carbon dioxide environments, which are the main diluting gases of air and oxy-fuel environment, respectively. Pyrolysis results reveal that weight loss profiles are similar up to high temperature zone in both pyrolysis environments, indicating that CO<sub>2</sub> behaves as an inert gas in this temperature range. However, further weight loss takes place in CO<sub>2</sub> atmosphere



after 700°C due to CO<sub>2</sub>-char gasification reaction which is observed in pyrolysis of all fuel samples.

Combustion experiments were carried out in four different atmospheres; air, oxygen-enriched air environment (30 % O<sub>2</sub> – 70 % N<sub>2</sub>), oxy-fuel environment (21 % O<sub>2</sub> – 79 % CO<sub>2</sub>) and oxygen-enriched oxy-fuel environment (30 % O<sub>2</sub> – 70 % CO<sub>2</sub>). Combustion experiments show that replacing nitrogen in the gas mixture by the same concentration of CO<sub>2</sub> does not affect the combustion process significantly but leads to slight delay (lower weight loss rate and higher burnout temperature) in combustion. Overall comparison of weight loss profiles shows that higher oxygen content in the combustion environment is the dominant factor affecting the combustion rather than the diluting gas. As O<sub>2</sub> concentration increases profiles shift through lower temperature zone, peak and burnout temperatures decrease, weight loss rate increases and complete combustion is achieved at lower temperatures and shorter times.

Pyrolysis and combustion behaviour of three different fuel blends were also investigated. Results reveal synergistic interactions in combustion tests of all blends in all combustion environments.

During pyrolysis and combustion tests gaseous products CO<sub>2</sub>, CO, H<sub>2</sub>O, CH<sub>4</sub>, SO<sub>2</sub> and COS were identified in flue gas and analyzed by using FTIR. Results indicate that higher CO and COS formation take place during pyrolysis tests due to gasification reaction in CO<sub>2</sub> atmosphere at high temperature zone. Gaseous species evolution trends in combustion tests are found specific for each fuel. However, evolution trends slightly shift to lower temperatures in oxygen-enriched conditions.

**Keywords:** Oxy-fuel combustion, oxygen-enriched combustion, CO<sub>2</sub> capture, TGA-FTIR, coal blends, lignite-biomass blends.

## ÖZ

# **OKSİJENCE ZENGİN HAVA VE CO<sub>2</sub> ORTAMINDA ÇEŞİTLİ YAKITLARIN PİROLİZ VE YANMA ÖZELLİKLERİNİN İNCELENMESİ**

Yüzbaşı, Nur Sena

Yüksek Lisans, Kimya Mühendisliği Bölümü

Tez Yöneticisi: Prof. Dr. Nevin Selçuk

Şubat 2011, 122 sayfa

Kömürün, oksijen ve geri dönüşümlü baca gazı (RFG) karışımında yanmasına dayanan oksiyakıt yanma teknolojisi, enerji santrallerinden CO<sub>2</sub> gazının yakalanması için günümüzde umut vaat eden yeni teknolojilerden biri olarak önerilmektedir.

Bu tez çalışmasında, ithal kömür, petrokok, yerli linyitler, pirina ve bu yakıtları içeren çeşitli karışımların, hava ve oksiyakıt koşullarında piroliz ve yanma davranışları termogravimetrik analiz yöntemi (TGA) ve buna bağlı olan Fourier dönüşümü kızılötesi spektrometresi (FTIR) kullanılarak incelenmiştir.

Piroliz testleri hava ve oksiyakıt koşullarının seyreltici gazları olan sırasıyla azot ve karbon dioksit ortamlarında gerçekleştirilmiştir. Piroliz testlerinde elde edilen sonuçlara göre, kütle kayıp profillerinin her iki piroliz ortamında da yüksek sıcaklıklara kadar benzer davranışlar sergilediği görülmüş ve bu durum CO<sub>2</sub> gazının bu sıcaklık aralığında inert bir gaz şeklinde hareket ettiğini göstermiştir.

Ancak karbon dioksit ortamında 700°C'den sonra kömür-CO<sub>2</sub> gazlaşma reaksiyonu sebebiyle kütle kaybının devam ettiği görülmüştür.

Yakma testleri ise hava, oksijence zengin hava ortamı (30 % O<sub>2</sub> – 70 % N<sub>2</sub>), oksi-yakıt ortamı (21 % O<sub>2</sub> – 79 % CO<sub>2</sub>) ve oksijence zengin oksi-yakıt ortamı (30 % O<sub>2</sub> – 70 % CO<sub>2</sub>) olmak üzere dört farklı atmosferde yapılmıştır. Yakma testlerinde elde edilen sonuçlar yanma atmosferindeki azot gazının, aynı hacimdeki karbon dioksit gazıyla yer değiştirilmesi sonucunda yanma prosesinin belirgin bir şekilde etkilenmediğini; ancak CO<sub>2</sub> gazının yanmada bir miktar gecikmeye (kütle kayıp hızında düşüş ve tam yanma sıcaklığında artış) yol açtığı göstermiştir. Kütle kayıp profillerinin karşılaştırılması sonucunda, yanma prosesine N<sub>2</sub> gazının CO<sub>2</sub> ile yer değiştirmesinden ziyade, en baskın etkenin yanma atmosferindeki yüksek oksijen konsantrasyonu olduğu anlaşılmıştır. Oksijen konsantrasyonunun artmasıyla yanma profilleri daha düşük sıcaklıklara doğru kaymış, maksimum kütle kayıp hızları artmış ve bu noktaya denk gelen maksimum sıcaklıklar düşmüş, tam yanmaya daha düşük sıcaklıklarda ve daha kısa sürede ulaşılmıştır.

Yapılan çalışmada üç farklı çeşit yakıt karışımının da piroliz ve yanma özellikleri incelenmiştir. Buna göre karışımı oluşturan yakıtların tüm ortamlardaki yanma testleri sırasında etkileştiği (sinejik etki) görülmüştür.

Piroliz ve yanma testleri sonucunda, baca gazında CO<sub>2</sub>, CO, H<sub>2</sub>O, CH<sub>4</sub>, SO<sub>2</sub> ve COS tespit edilmiş ve FTIR yöntemi kullanılarak analiz edilmiştir. Piroliz testlerinde, CO<sub>2</sub> ortamında gerçekleşen gazlaşma reaksiyonu sonucunda CO ve COS gazlarının yüksek sıcaklıklarda belirgin bir şekilde arttığı görülmüştür. Yakma testlerinde yakıtların yapısına göre farklı oluşum profilleri elde edilmiştir. Yanma sırasında tespit edilen gazların yüksek oksijen konsantrasyonuna sahip ortamlarda daha düşük sıcaklıklarda oluştuğu söylenebilir.

**Anahtar Kelimeler:** Oksi-yakıt yanma, oksijence zengin ortamda yanma, CO<sub>2</sub> yakalama, TGA-FTIR, kömür karışımları, linyit-biyokütle karışımları.

*To my great family and knowledge*

## ACKNOWLEDGEMENTS

I would like to express my deepest sense of gratitude to my supervisor Prof. Dr. Nevin Selçuk for giving me chance to be her first student graduated from another university. I am appreciating to her for sincere support, valuable guidance and important advises about everything throughout this study.

Financial support of TUBITAK through 109M401 project is gratefully acknowledged. I would like to thank to Prof. Dr. Hayrettin Yücel and Prof. Dr. Necati Özkan for their support in my experimental set-up in METU Central Laboratory. Moreover, special thanks goes to Saniye Ebru Deniz and Ayşe Nur Özkan for their help in my TGA-FTIR experiments; Kerime Güney, and Aydın Köse from Norm Lab. for fuel analysis tests. I would also like to thank to Gürsel Ulutuncel from Tetra Teknolojik Sistemler Ltd. Şti. and Bilal Bayram from Terra Lab. for installation of the experimental set-up.

Many thanks to my dear roommates Güzide Aydın and Mehmet Yusuf Kaptan due to their support, encouragement and help during this thesis study. I would like to thank to my fellows Eda and Berk, my wise friend Emre Yılmaz, Wisconsin couple Emre and Bahar, Emre Tatlı, Merve, Gamze, my Iraqi friend Baraa, İrem, Didem, Seda, my old friends; Didem, Gülcan, Erinç, Burak, Hilmi, my Spanish girls; Görkem, Simay, Tuğba and all my other friends that I am not able to mention in a page of acknowledgement. My special thanks goes to my patient dearest Çağrı for his endless support and hopeful point of view in all situations.

I want to express my deepest pleasure to my mother Zehra Yıldız and father Kazım Ünal Yüzbaşı, for their sacrifices, unshakable faith in me, valuable advises and endless support. They are my luck. Many thanks to my hero brother Veysel Sinan, his dear wife Esra and my potential nephews.

## TABLE OF CONTENTS

<b>ABSTRACT .....</b>	<b>iv</b>
<b>ÖZ .....</b>	<b>vi</b>
<b>ACKNOWLEDGEMENTS .....</b>	<b>ix</b>
<b>TABLE OF CONTENTS.....</b>	<b>x</b>
<b>LIST OF TABLES .....</b>	<b>xiii</b>
<b>LIST OF FIGURES .....</b>	<b>xiv</b>
<b>CHAPTERS.....</b>	<b>1</b>
<b>1 INTRODUCTION.....</b>	<b>1</b>
1.1 GENERAL .....	1
1.2 AIM AND SCOPE OF THE THESIS .....	3
<b>2 BACKGROUND AND LITERATURE REVIEW .....</b>	<b>5</b>
2.1 GENERAL .....	5
2.2 PATHWAYS TO CAPTURE CO <sub>2</sub> .....	5
2.3 OXY-FUEL COMBUSTION TECHNOLOGY .....	8
2.4 OXY-FUEL COMBUSTION STUDIES BY THERMOGRAVIMETRIC ANALYSIS.....	11
<b>3 EXPERIMENTAL .....</b>	<b>16</b>
3.1 GENERAL .....	16
3.2 MATERIALS .....	16
3.3 EXPERIMENTAL SET-UP .....	20
3.4 EXPERIMENTAL METHOD .....	21
<b>4 RESULTS AND DISCUSSION .....</b>	<b>24</b>

4.1	GENERAL .....	24
4.2	IMPORTED COAL .....	25
4.2.1	<i>Pyrolysis of Imported Coal</i> .....	25
4.2.2	<i>Combustion of Imported Coal</i> .....	29
4.3	PETCOKE.....	34
4.3.1	<i>Pyrolysis of Petcoke</i> .....	34
4.3.2	<i>Combustion of Petcoke</i> .....	38
4.4	LIGNITE I.....	42
4.4.1	<i>Pyrolysis of Lignite I</i> .....	42
4.4.2	<i>Combustion of Lignite I</i> .....	46
4.5	LIGNITE II.....	51
4.5.1	<i>Pyrolysis of Lignite II</i> .....	51
4.5.2	<i>Combustion of Lignite II</i> .....	54
4.6	OLIVE RESIDUE .....	58
4.6.1	<i>Pyrolysis of Olive Residue</i> .....	58
4.6.2	<i>Combustion of Olive Residue</i> .....	61
4.7	IMPORTED COAL – PETROLEUM COKE – LIGNITE I BLEND (BLEND I) .....	65
4.7.1	<i>Pyrolysis of Blend I</i> .....	65
4.7.2	<i>Combustion of Blend I</i> .....	70
4.8	PETROLEUM COKE – LIGNITE II BLEND (BLEND II).....	76
4.8.1	<i>Pyrolysis of Blend II</i> .....	76
4.8.2	<i>Combustion of Blend II</i> .....	81
4.9	LIGNITE I - OLIVE RESIDUE BLEND (BLEND III) .....	86
4.9.1	<i>Pyrolysis of Blend III</i> .....	87
4.9.2	<i>Combustion of Blend III</i> .....	92
<b>5</b>	<b>CONCLUSIONS.....</b>	<b>97</b>
5.1	GENERAL .....	97
5.2	SUGGESTIONS FOR FUTURE WORK.....	99

<b>REFERENCES .....</b>	<b>100</b>
<b>APPENDIX A. PILOT SCALE CARBON CAPTURE AND STORAGE PROJECTS .....</b>	<b>107</b>
<b>APPENDIX B. PUBLISHED PAPER .....</b>	<b>112</b>
<b>APPENDIX C. FTIR PROFILES OF IMPORTED COAL.....</b>	<b>120</b>



## LIST OF TABLES

### TABLES

Table 3.1: Fuel Analyses .....	18
Table 4.1: Pyrolysis Characteristics of Imported Coal.....	26
Table 4.2: Combustion Characteristics of Imported Coal .....	31
Table 4.3: Pyrolysis Characteristics of Petcoke .....	35
Table 4.4: Combustion Characteristics of Petcoke .....	39
Table 4.5: Pyrolysis Characteristics of Lignite I .....	43
Table 4.6: Combustion Characteristics of Lignite I.....	47
Table 4.7: Pyrolysis Characteristics of Lignite II .....	52
Table 4.8: Combustion Characteristics of Lignite II.....	55
Table 4.9: Pyrolysis Characteristics of Olive Residue .....	59
Table 4.10: Combustion Characteristics of Olive Residue .....	62
Table 4.11: Pyrolysis characteristics of blend I and its parent fuels .....	66
Table 4.12: Combustion characteristics of blend I and its parent fuels .....	72
Table 4.13: Pyrolysis characteristics of blend II and its parent fuels .....	77
Table 4.14: Combustion characteristics of blend II and its parent fuels .....	83
Table 4.15: Pyrolysis characteristics of blend III and its parent fuels .....	88
Table 4.16: Combustion characteristics of blend III and its parent fuels .....	93
Table A.1: Large-Scale Power Plant Carbon Capture and Storage Projects.....	108
Table A.2: Pilot Scale Power Plant Carbon Capture and Storage Projects .....	111

## LIST OF FIGURES

### FIGURES

Figure 1.1: World CO <sub>2</sub> emissions by sector in 2008 [4].....	2
Figure 2.1: Pathways to capture CO <sub>2</sub> .....	7
Figure 2.2: Possible configuration of a coal-fired oxy-fuel power plant.....	9
Figure 3.1: Schematic diagram of the experimental setup.....	21
Figure 4.1: TGA and DTG profiles of imported coal during pyrolysis in N <sub>2</sub> and CO <sub>2</sub> atmospheres .....	26
Figure 4.2: Formation profiles of evolved gases during pyrolysis tests of imported coal. ....	28
Figure 4.3: TGA and DTG profiles of imported coal in different combustion atmospheres .....	29
Figure 4.4: Formation profiles of evolved gases during combustion tests of imported coal .....	33
Figure 4.5: TGA and DTG profiles of petcoke during pyrolysis in N <sub>2</sub> and CO <sub>2</sub> atmospheres .....	34
Figure 4.6: Formation profiles of evolved gases during pyrolysis tests of petcoke... ..	37
Figure 4.7: TGA and DTG profiles of petcoke in different combustion atmospheres .....	38
Figure 4.8: Formation profiles of evolved gases during combustion tests of petcoke .....	41
Figure 4.9: TGA and DTG profiles of lignite I in N <sub>2</sub> and CO <sub>2</sub> atmospheres.....	42
Figure 4.10: Formation profiles of evolved gases during pyrolysis tests of lignite I.. ..	45
Figure 4.11: TGA and DTG profiles of lignite I in different combustion atmospheres .....	46
Figure 4.12: Formation profiles of evolved gases during combustion tests of lignite I .....	50

Figure 4.13: TGA and DTG profiles of lignite II in N <sub>2</sub> and CO <sub>2</sub> atmospheres.....	51
Figure 4.14: Formation profiles of evolved gases during pyrolysis tests of lignite II.	53
Figure 4.15: TGA and DTG profiles of lignite II in different combustion atmospheres .....	54
Figure 4.16: Formation profiles of evolved gases during combustion tests of lignite II .....	57
Figure 4.17: TGA and DTG profiles of olive residue in N <sub>2</sub> and CO <sub>2</sub> atmospheres .....	58
Figure 4.18: Formation profiles of evolved gases during pyrolysis tests of olive residue.....	60
Figure 4.19: TGA and DTG profiles of olive residue in different combustion atmospheres .....	61
Figure 4.20: Formation profiles of evolved gases during combustion tests of olive residue.....	64
Figure 4.21: TGA and DTG profiles of Blend I in N <sub>2</sub> and CO <sub>2</sub> atmospheres .....	65
Figure 4.22: Pyrolysis profiles of blend I and its parent fuels in N <sub>2</sub> and CO <sub>2</sub> environments .....	67
Figure 4.23: Formation profiles of evolved gases during pyrolysis tests of blend I ..	69
Figure 4.24: TGA and DTG profiles of blend I in different combustion atmospheres	70
Figure 4.25: Combustion profiles of blend I and its parent fuels in different combustion environments .....	73
Figure 4.26: Formation profiles of evolved gases during combustion tests of blend I .....	75
Figure 4.27: TGA and DTG profiles of blend II in N <sub>2</sub> and CO <sub>2</sub> atmospheres.....	76
Figure 4.28: Pyrolysis profiles of blend II and its parent fuels in N <sub>2</sub> and CO <sub>2</sub> environments .....	78
Figure 4.29: Formation profiles of evolved gases during pyrolysis tests of blend II .	80
Figure 4.30: TGA and DTG profiles of blend II in different combustion atmospheres .....	81

Figure 4.31: Combustion profiles of blend II and its parent fuels in different combustion environments .....	84
Figure 4.32: Formation profiles of evolved gases during combustion tests of blend II .....	86
Figure 4.33: TGA and DTG profiles of blend III in N <sub>2</sub> and CO <sub>2</sub> atmospheres.....	87
Figure 4.34: Pyrolysis profiles of blend III and its parent fuels in N <sub>2</sub> and CO <sub>2</sub> environments .....	89
Figure 4.35: Formation profiles of evolved gases during pyrolysis tests of blend III	91
Figure 4.36: TGA and DTG profiles of blend III in different combustion environments .....	92
Figure 4.37: Combustion profiles of blend III and its parent fuels in different combustion environments .....	94
Figure 4.38: Formation profiles of evolved gases during combustion tests of blend III .....	96
Figure B.1: Published Paper .....	113
Figure C.1: FTIR profile of pyrolysis of imported coal in N <sub>2</sub> atmopshere.....	120
Figure C.2: FTIR profile of pyrolysis of imported coal in CO <sub>2</sub> atmopshere. ....	120
Figure C.3: FTIR profile of combustion of imported coal in 21% O <sub>2</sub> – 79% N <sub>2</sub> atmopshere.....	121
Figure C.4: FTIR profile of combustion of imported coal in 21% O <sub>2</sub> – 79% CO <sub>2</sub> atmopshere.....	121
Figure C.5: FTIR profile of combustion of imported coal in 30% O <sub>2</sub> – 70% N <sub>2</sub> atmopshere.....	122
Figure C.6: FTIR profile of combustion of imported coal in 30% O <sub>2</sub> – 70% CO <sub>2</sub> atmopshere.....	122

# CHAPTER 1

## INTRODUCTION

### 1.1 General

Today, energy requirement of the world and demand for electric power continues to increase due to population growth, developments in economy and technology. In electric power production, coal provides the largest share due to its abundant and widely distributed reserves. With 826 billion tonnes of proved coal reserves, coal combustion is expected to dominate the energy production for at least the next few decades [1]. Coal combustion dominates the electricity generation sector worldwide with its 41 % share in fuel sources [2]. Higher prices and lower reserves of oil and natural gas make coal-fired generation economically more attractive especially for coal rich countries.

Significant rise in energy demand leads to increase in anthropogenic CO<sub>2</sub> emissions. Since pre-industrial era, CO<sub>2</sub> level in the atmosphere has increased from 280 ppmv to 388 ppmv [3]. Figure 1.1 compares world CO<sub>2</sub> emissions by sector in 2008. Generation of electricity and heat was the largest CO<sub>2</sub> produced sector, which was responsible for 41 % of the world CO<sub>2</sub> emissions in 2008 [4].

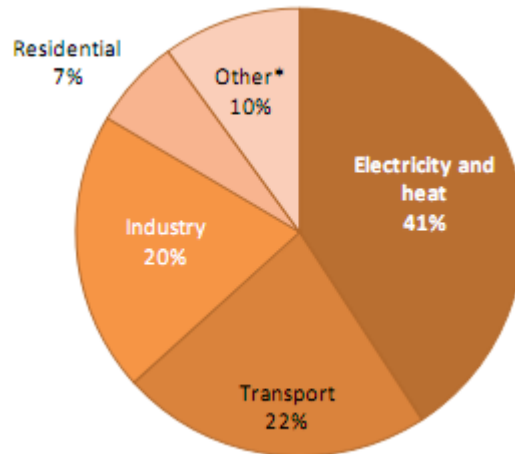


Figure 1.1: World CO<sub>2</sub> emissions by sector in 2008 [4]

Growing concern about greenhouse gas emissions and their potential impact on climate change necessitates reduction of CO<sub>2</sub> emissions from coal fired power plants which accounts for 16 % of world CO<sub>2</sub> emissions [2, 4]. CO<sub>2</sub> emission reduction regulations are driven by international initiatives such as the International Panel on Climate Change (IPCC) and Kyoto Protocol, which was also signed by Turkey in February 2009.

Various solutions can be applied to reduce CO<sub>2</sub> emissions from existing coal fired power plants, such as improving energy efficiency, making use of renewable fuels such as biomass, switching to lower carbon fuels, blend and burn different kinds of solid fuels. However, a significant reduction in CO<sub>2</sub> emissions can be achieved by capturing CO<sub>2</sub> generated from coal utilization from stack gases and storing (sequestering) it [5]. Various technologies and new pathways are being developed for CO<sub>2</sub> capture and storage from coal fired plants. The most attractive technologies for carbon capture and storage (CCS) can be classified in three main categories that are post-combustion, pre-combustion and oxy-fuel combustion [5-8].

Conventional technologies for removing CO<sub>2</sub> from the stack gas in the existing coal fired power plants are expensive since CO<sub>2</sub> is diluted (typically about 14 % by volume on a dry basis). The cost of gas separation can be reduced by increasing the concentration of CO<sub>2</sub> in the flue gas. This can be achieved by increasing the oxygen concentration in the feed stream by using oxy-fuel combustion technology which is based on burning coal in a mixture of oxygen and recycled flue gas (RFG) leading to CO<sub>2</sub> concentrations up to 98 % in the exhaust gas [9]. Many other techno-economic assessment studies reported that oxy-fuel combustion could be demonstrated as cost effective method of CO<sub>2</sub> capture in CCS technologies.

Many laboratory and pilot scale studies were carried out within the last two decades about this technology. These investigations reveal that it is possible to burn coal in O<sub>2</sub>/CO<sub>2</sub> atmosphere. Oxy-fuel combustion technology is a near zero emission technology which can be adapted to both new and existing coal fired power plants. Therefore, oxy-fuel combustion is considered as a favourable option in carbon capture and storage technologies to reduce CO<sub>2</sub> emissions from coal-fired power plants but more research is still required to fully understand this technology.

## **1.2 Aim and Scope of the Thesis**

Oxy-fuel combustion has been studied extensively for pulverized coal combustion, but to date has received relatively less attention for fluidized bed combustion (FBC) systems. Benefits of fluidized bed combustion (FBC) technology such as the ability to burn wide variety of fuels efficiently and to control pollutant emissions without flue gas treatment systems have led to a steady increase in its commercial use over the past decades. Advantage of oxy-fuel firing in FBC technology is that significant reduction in the amount of recycled flue gas can be achieved through the external solid heat exchangers for combustion temperature control [10].

Before firing tests in FBC combustors, combustion characteristics of the various fuels need to be determined under oxy-fuel conditions by using non-isothermal thermo-gravimetric analysis (TGA) technique. TGA is an inexpensive and simple method that has been widely used in studying the pyrolysis and combustion behaviours of fuels and evaluating the relative burning properties of fuel samples [11-17]. In spite of significant ongoing research in this area, there is limited number of studies on oxy-fuel combustion properties of indigenous lignites, biomass, petroleum coke and their blends with various proportions.

Therefore, the objective of this study has been to investigate pyrolysis and combustion behaviour of various fuels in air ( $O_2/N_2$ ) and oxy-fuel ( $O_2/CO_2$ ) conditions by using TGA technique combined with Fourier Transform Infrared (FTIR) spectroscopy to analyze the gaseous species evolved. In an attempt to fulfill this aim, pyrolysis and combustion characteristics of five different types of fuels including imported coal, petroleum coke, two different types of indigenous lignites, olive residue as biomass and their various blends have been studied and reported in this thesis.



## **CHAPTER 2**

### **BACKGROUND AND LITERATURE REVIEW**

#### **2.1 General**

In the first part of this section, carbon capture and storage technologies including pre-, post- and oxy-fuel combustion and their main processes are briefly summarized. In the following part, oxy-fuel combustion, which is the focus of this study, is explained in detail. This section is concluded with the specific oxy-fuel studies that were carried out by using thermogravimetric analysis technique.

#### **2.2 Pathways to Capture CO<sub>2</sub>**

In the past two decades, there has been a growing concern about increase in CO<sub>2</sub> emission and its potential impact on climate change. As coal-fired power plants accounts for about 16 % of CO<sub>2</sub> emissions, researchers have focused on improving clean and efficient technologies in CO<sub>2</sub> reduction in the recent years. There are several options to reduce CO<sub>2</sub> emissions, such as increasing power plant efficiency or using fuels with lower fossil carbon content. However, these options will not achieve the required reductions in CO<sub>2</sub> emissions. The capture of CO<sub>2</sub> from coal-fired systems, that is, Carbon Capture and Storage (CCS) technologies may contribute significantly for solution of this problem. The identified technologies for

carbon capture are classified as post-, pre- and oxy-fuel combustion. Main operations concerned with these technologies are described in Figure 2.1.

*Post-combustion* includes the separation of CO<sub>2</sub> from the flue gas by chemical absorption with chemical solvents and solid minerals such as monoethanolamine (MEA) or a sterically hindered amine (KS-1). Chemically active agents that are used to scrub CO<sub>2</sub> are regenerated by heating to release CO<sub>2</sub>. Considerable energy is required to regenerate these solvents, which leads to 10-14 % points drop in efficiency of power plants. Low concentration of CO<sub>2</sub> in the flue gas (~14 %) results in increase in capture equipment sizes and high capital costs [18, 19].

*Pre-combustion* comprises Integrated Gasification Combined Cycle (IGCC) power plants with carbon capture and storage units. Coal is gasified under high pressure in order to obtain syngas containing CO, CO<sub>2</sub> and H<sub>2</sub>. CO is converted into CO<sub>2</sub> by water-gas shift reaction. CO<sub>2</sub> is separated from the gas and remaining H<sub>2</sub> is used for combustion in a gas turbine. IGCC is considered as a promising technology because of its economics and plant efficiency characteristics; however, it requires high capital costs in plant constructions. Moreover, it is not possible to retrofit existing power plants for IGCC-CCS process [18, 20].

*Oxy-fuel combustion* process is based on increasing the concentration of CO<sub>2</sub> in the flue gas. Conventional technologies for removing CO<sub>2</sub> from the stack gas in the existing coal fired power plants are expensive since CO<sub>2</sub> is diluted (typically about 14 % by volume on a dry basis). The cost of gas separation can be reduced by increasing the concentration of CO<sub>2</sub> in the flue gas. This can be achieved by increasing the oxygen concentration in the feed stream by using oxy-fuel combustion technology which is based on burning coal in a mixture of oxygen and recycled flue gas (RFG) leading to CO<sub>2</sub> concentrations up to 95 % in the exhaust gas. Many other techno-economic assessment studies reported that oxy-fuel combustion should be the most cost and energy efficient technology in CCS.

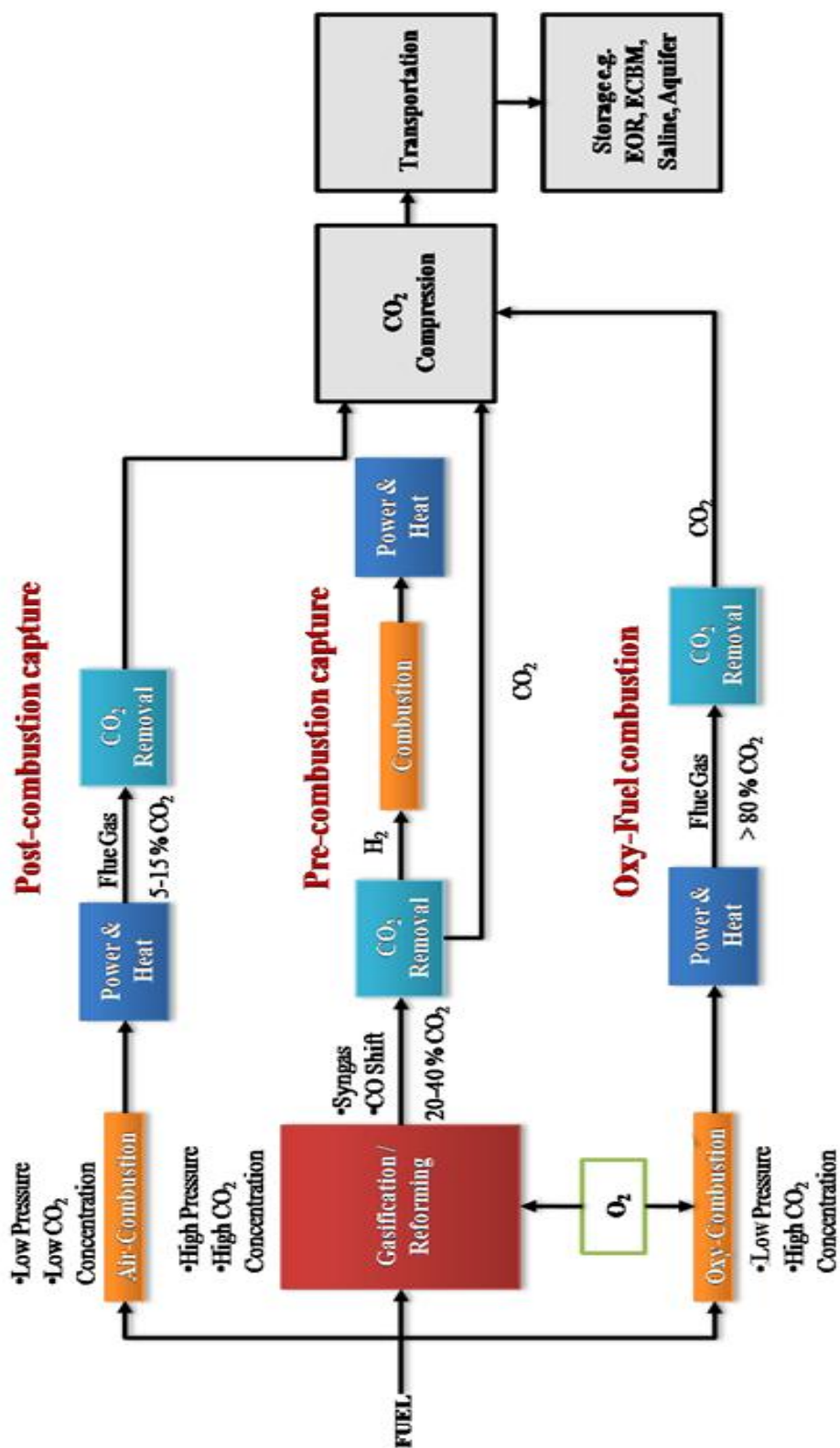


Figure 2.1: Pathways to capture CO<sub>2</sub>.

However, main disadvantage of this technology is the requirement of air separation unit (ASU) for pure O<sub>2</sub> [6, 9, 18, 21-23].

There are no full-scale plants using CCS technologies in operation, however, there is a significant ongoing research in this area. There are many large-scale and pilot scale CCS projects worldwide currently. These projects are listed in Appendix A [18].

Recent techno-economic studies have compared the pre-, post- and oxy-fuel combustion technologies in terms of efficiency, the contributions to increased costs, and the cost of electricity (COE) with a CO<sub>2</sub> tax or penalty. These studies reveal that efficiency penalties vary from 7 % to 10 %. CO<sub>2</sub> compressions and solvent regeneration in post combustion or pure oxygen production in pre- and oxy-fuel combustion systems are the main contributors to efficiency losses. Current knowledge on economical comparisons of these three capture technologies shows that there is no significant difference in cost [18, 20, 22].

As one of three main CO<sub>2</sub> capture approaches, oxy-fuel combustion has received a lot of attention in the recent years as it has potential to produce significantly high CO<sub>2</sub> concentration in the flue gas, which provides easier sequestration of CO<sub>2</sub> from flue gases in coal-fired power plants. Therefore, oxy-fuel combustion, which is considered to be a promising and cost effective option for reduction of CO<sub>2</sub> emissions, is the focus of this study.

### **2.3 Oxy-fuel Combustion Technology**

Oxy-fuel combustion technology has been firstly evaluated by Abraham et al. to produce CO<sub>2</sub> gas for Enhanced Oil Recovery (EOR) in the early eighties [24]. However, after mid-90s, this technology received renewed interest due to growing concern about greenhouse gas emissions.

Oxy-fuel combustion technology involves the combustion of coal in the mixture of oxygen and recycled flue gas (RFG), instead of air, in order to increase concentration of CO<sub>2</sub> in the flue gas for easy separation. CO<sub>2</sub> concentration in the flue gas can be increased from 14 % up to 95 % by volume, with this technology. RFG is used to make up the volume of missing N<sub>2</sub>, control the flame temperature and heat flux profiles [6, 25].

Figure 2.2 demonstrates major process steps of a coal-fired oxy-fuel power plant. Oxygen is separated from air by using air separation unit (ASU). Pure oxygen stream is then mixed with recycled stream of flue gas from the boiler and coal is burned in this resulting gas stream. After combustion in the boiler, the released flue gas is transferred to cleaning equipment. Main cleaning equipments include filter, condenser and flue gas desulphurization (FGD) units for removal of fly ash, water vapour and sulphur, respectively. The cleaned flue gas is partially recycled to boiler and rest of the stream containing clean CO<sub>2</sub> gas is sent to storage units.

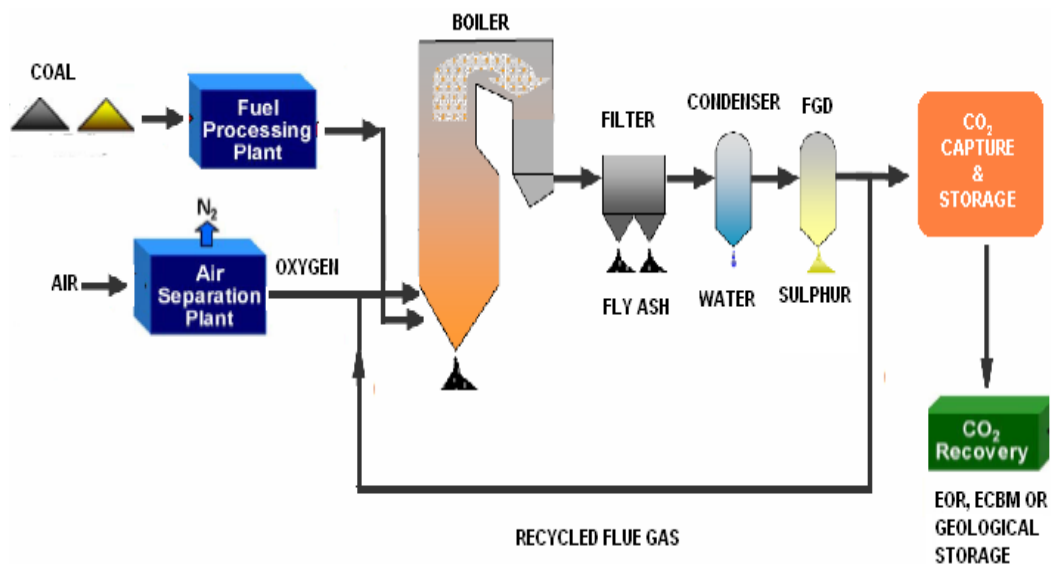


Figure 2.2: Possible configuration of a coal-fired oxy-fuel power plant

Many laboratory and pilot scale studies on oxy-fuel combustion technology have been reported by different researchers and organizations in the open literature up to date. These studies have been summarized by Toftegaard et al. recently, including the information on experimental conditions and aim of each research group [18].

These studies reveal that, oxy-fuel combustion differs from air combustion in combustion characteristics such as burning stability, char burnout, gas temperature profiles and heat transfer due to differences in gas radiative and thermo-physical properties between  $\text{CO}_2$  and  $\text{N}_2$ , which are the main diluting gases in oxy-fuel and air combustion, respectively. Substituting  $\text{CO}_2$  with an equal volume  $\text{N}_2$  leads to larger specific heat capacity in combustion environment that results in lower flame temperatures and delayed combustion in oxy-fuel conditions compared with those in air conditions. Devolatilization, ignition and burnout take place at lower rates in oxy-fuel conditions [6, 23, 26-29]. Previous studies on oxy-fuel combustion mainly revealed that similar temperature profiles with air case are achieved at higher oxygen concentrations between 25 and 42 vol. % depending on fuel and boiler type [9, 23, 30].

Oxy-fuel combustion also differs from air-firing case in gaseous emissions such as;  $\text{CO}$ ,  $\text{NO}_x$ ,  $\text{SO}_2$  and  $\text{SO}_3$ . It has been reported in the literature that increase in  $\text{CO}_2$  concentration in the combustion environment leads to increase in  $\text{CO}$  emissions in the near flame zone which may cause the risk of  $\text{CO}$  corrosion [18, 31]. Numerous studies on  $\text{NO}_x$  emissions in oxy-fuel combustion reveal that it is possible to achieve almost 70-80 % reduction in  $\text{NO}_x$  emissions compared to combustion in air through near elimination of thermal and prompt  $\text{NO}_x$  formation as levels of molecular nitrogen is significantly lower in oxy-fuel conditions [22, 24, 28, 32]. However, increase in oxygen concentration results in higher  $\text{NO}_x$  levels as temperature of combustion environment increases. In order to avoid this effect, various options such as; oxygen staging or increasing oxygen purity is suggested in the open literature [28]. Studies on sulphur oxides shows that release of sulphur from coal is

not affected significantly with the replacement of nitrogen by carbon dioxide. However, sulphur induced corrosion risk appears even at low temperatures (below the acid dew point) in oxy-fuel operation systems including flue gas recirculation without prior  $\text{SO}_2$  removal as the amount of  $\text{SO}_3$  in the boiler can reach high values. Moreover,  $\text{SO}_3$  formation is promoted in oxygen enriched conditions and high water contents in the flue gas if it is recycled before condenser [9, 18, 23].

## **2.4 Oxy-fuel Combustion Studies by Thermogravimetric Analysis**

In the study of Li et al. [25], thermogravimetric technique were used to investigate pyrolysis and combustion behaviour of a pulverized Chinese bituminous coal in oxy-fuel conditions. Effect of pyrolysis environment, oxygen level, particle size and heating rate on pyrolysis and combustion processes and release of gaseous compounds in those conditions were reported. Pyrolysis tests were carried out under  $\text{N}_2$  and 21 %  $\text{N}_2$  – 79 %  $\text{CO}_2$  mixture while combustion tests were performed in air and  $\text{O}_2/\text{CO}_2$  mixtures with oxygen concentrations of 21, 30, 40, and 80 %. For these tests, approximately 10 mg of pulverized coal samples were heated from room temperature to  $1000^\circ\text{C}$  with a heating rate of  $30^\circ\text{C}/\text{min}$  and gas flow rate of 80 ml/min. In order to clarify the effects of heating rate and particle size additional combustion tests were carried out at heating rates of 10, 20,  $30^\circ\text{C}/\text{min}$  and particle sizes < 48, 48 – 74, 74 – 90  $\mu\text{m}$ . Gaseous species evolved in pyrolysis and combustion tests were analysed by using FTIR spectrometer. In  $\text{N}_2/\text{CO}_2$  mixtures, additional gasification stage was observed in pyrolysis profiles of pulverized coal samples at high temperature zone. Under oxygen concentrations corresponding to that of air, combustion was delayed and in elevated oxygen levels, DTG curves shift to lower temperatures. Decrease in particle size led to increase in burning rate and decrease in burnout while heating rate had no significant effect on combustion process.

Liu et al. [33] reported a comparative study on combustion behaviour of two different coal chars in  $O_2/N_2$  and  $O_2/CO_2$  by using thermal analysis methods. Coal chars, which were prepared by using high volatile bituminous coal and anthracite, were burned in the mixtures of  $O_2/N_2$  and  $O_2/CO_2$  with oxygen levels of 3, 6, 10, 21, 30 %. Combustion tests showed that replacing  $N_2$  with the same amount of  $CO_2$  did not result in significant differences in combustion behaviour of char samples as combustion temperature of the sample is controlled by electrical heating in TGA technique. Therefore it was concluded that sample temperature is not affected by combustion environment. Four different methods were used in determination of activation energies of the char samples. Activation energy values were found to be in agreement with those in literature for both bituminous and anthracite chars. Kinetic analysis of the char samples revealed that in oxygen – carbon dioxide mixtures, combustion rate of the char samples were found to vary approximately linearly with the oxygen concentration.

Four different types of Australian coals were analyzed by using drop tube furnace (DTF) to measure coal burnout and thermogravimetric analyzer (TGA) to determine the reactivity of coal/char samples in the study of Rantham and his co-workers. In DTF pyrolysis tests apparent volatile yields of all the four coals were found higher in  $CO_2$  environment compared to those in  $N_2$ . TGA pyrolysis tests revealed similar behaviour up to 1030 K in both  $N_2$  and  $CO_2$  environments. After 1030 K, significant increase in mass loss rate was observed. This significant increase and higher apparent volatile yields in  $CO_2$  atmosphere were attributed to  $CO_2$ -char gasification reaction. DTF combustion tests were carried out in  $O_2/N_2$  and  $O_2/CO_2$  mixtures with oxygen concentrations in the range 3 to 21 % and 5 to 30 %, respectively. In combustion tests, coal burnout was observed to increase in elevated oxygen levels for all four coals. For coals C and D, coal burnouts were observed to be similar in air and oxy-fuel conditions at the same oxygen levels in contrast to coals A and B. For coals A and B higher burnouts were obtained in oxy-fuel conditions compared to that in air conditions. Coal chars were prepared at 1673K in nitrogen environment by using DTF and combusted in TGA for reactivity analysis. TGA combustion tests



were performed in  $O_2/N_2$  and  $O_2/CO_2$  mixtures with oxygen concentrations of 2, 5, 10, 21 and 50 %. Almost identical combustion behaviours were displayed in  $O_2/N_2$  and  $O_2/CO_2$  mixtures at oxygen concentrations of 5 % and above. However, in 2 %  $O_2/CO_2$  conditions, effect of gasification was significant. At elevated oxygen levels, higher maximum reactivity and lower burnout temperatures were obtained [29].

Duan et al. [34] investigated pyrolysis of coals in  $CO_2$  atmosphere to have better understanding of combustion characteristics and gas evolution mechanisms in oxy-fuel conditions by using TGA-FTIR combined system. Formation of  $SO_2$ , and  $NO_x$  related species such as,  $H_2S$ ,  $COS$ ,  $SO_2$ ,  $HCN$  and  $NH_3$  were reported. About 10 mg bituminous coal samples having particle size less than 100  $\mu m$  were used in pyrolysis tests. Samples heated from room temperature to different end temperatures; 700, 800, 900 and 1000°C with different heating rates; 10, 30, 50 and 70°C. TGA tests showed that replacing  $N_2$  with  $CO_2$  in pyrolysis environment had no significant effect on initiation of volatile matter release and rate of weight loss up to 480°C. In  $N_2$  atmosphere, calcite decomposition was observed after 760°C, however, in  $CO_2$  environment, calcite decomposition was prevented. At higher heating rates, volatile yields decreased, however, at higher end temperatures volatile yields increased to due the effect of coal gasification. In FTIR analysis, reactions between  $H_2S$  and  $CO_2$  led to  $COS$  formation in  $CO_2$  atmosphere. Conversion of fuel-N to  $HCN$  was favoured by gasification of char in  $CO_2$  conditions.

In another study of Duan et al. [35] effect of oxy-fuel conditions on sulphur formation behaviour of a bituminous coal and its char displayed in pyrolysis and combustion experiments was reported. Samples were heated from room temperature to 1173 K with a heating rate of 30 K/min. Pyrolysis tests revealed that  $COS$  formation was identified in  $CO_2$  rather than  $N_2$  environment. Higher  $SO_2$  formation was observed when oxygen concentrations were identical in the combustion environment (21 %  $O_2/79$  %  $N_2$  and 21 %  $O_2/79$  %  $CO_2$ ). It was reported that elevated oxygen levels enhance organic sulphur decomposition rate and conversion of  $H_2S$  to  $SO_2$ , which resulted in faster  $SO_2$  formation in oxygen-enriched

environments. X-ray photoelectron spectroscopy (XPS) test results demonstrated that sulphur retention ability increased with the increase in oxygen levels in combustion environment.

In the report of Alstom Power Inc. [36] about engineering feasibility and economics of CO<sub>2</sub> on an existing coal fired plant, TGA tests were performed to obtain reactivity parameters of Conesville and Pittsburgh coals. About 4-6 mg of samples were placed over a pan almost a monolayer in order to mitigate the effects of oxygen mass transfer control phenomena during combustion. In each condition 50 cc/min of analysis gases were mixed with 50 cc/min balance N<sub>2</sub> gas, which was used to protect balance from over heating. Combustion tests were carried out in three different environments; base case (air), constant mass case and constant volume case. Constant mass and volume cases refer to replacement of N<sub>2</sub> with an equal mass and volume of CO<sub>2</sub> gas, respectively. Slight differences in TGA combustion efficiency profiles were reported as experimental error for this type of testing. Peak temperatures obtained from DTG profiles of the coals were found to be in the range of 472 – 479°C for all test conditions. This narrow range was considered to be indicative of similar reactivity characteristics of these two coals in air or any of the O<sub>2</sub>/CO<sub>2</sub> mixture.

Oxy-fuel characteristics and combustion kinetics of high ash Indian coals were studied in TGA by Saravanan and his co-workers [37]. Pyrolysis tests were carried out in N<sub>2</sub> and CO<sub>2</sub> environments while combustion tests were performed in air and O<sub>2</sub>/CO<sub>2</sub> mixtures having oxygen concentrations of 20, 30 and 40 %. Coal samples were heated from room temperature to 1000°C with a heating rate of 10°C/min and gas flow rate was kept at 40 ml/min for each tests. Char-CO<sub>2</sub> gasification was observed above 800°C in pyrolysis tests. Combustion tests showed that two of the coals displayed similar behaviour in 30 % O<sub>2</sub> – 70 % CO<sub>2</sub> mixture with those in air conditions while in the case of the other coal weight loss profiles obtained in air environment laid between weight loss profiles of 20 % O<sub>2</sub> – 80 % CO<sub>2</sub> and 30 % O<sub>2</sub> – 70 % CO<sub>2</sub> mixtures. Therefore, it was concluded that to achieve similar temperature

profiles with air case,  $O_2/CO_2$  proportion need to be considered according to fuel type. In kinetic analysis Arrhenius model was used and calculated activation energies were found within the range from 19 to 33 kJ/mol.

Haykiri-Acma et al. [38] studied reactivity and burnout characteristics of biomass-lignite blends in air and pure oxygen conditions by using TGA and DSC methods. Two different biomass species, sunflower seed shell and hazelnut shell and Soma-Denis lignite were selected for combustion tests. Fuel samples having particle size less than 250 $\mu$ m, was heated from room temperature to 900°C with a heating rate of 40°C/min at a flow rate of 100 ml/min. Biomass-lignite blends were prepared with 5, 10 and 20 wt.% biomass in the blend. It was reported that in pure oxygen maximum weight loss rates shift to lower temperature zone and burnout time shortens. In co-firing tests, presence of biomass led to expected conversion degrees at lower temperatures and better burnout levels. Moreover, excess heat arising from combustion of lignite in pure oxygen could be controlled by co-firing lignite with biomass.

## **CHAPTER 3**

### **EXPERIMENTAL**

#### **3.1 General**

In the first part of this chapter, materials used in pyrolysis and combustion tests and their characteristics including proximate, ultimate and ash analyses are reported. This was followed by description of the experimental set-up and the method in detail.

Experiments have been carried out in Middle East Technical University Central Laboratory within the scope of research project 109M401 financed by The Scientific and Technical Research Council of Turkey (TÜBİTAK).

#### **3.2 Materials**

Five different types of fuels including imported coal, petcoke, two different types of indigenous lignites and olive residue were selected for pyrolysis and combustion tests.

Representative samples of fuels were subjected to proximate, ultimate and ash analysis. Proximate analysis was carried out with LECO TGA-701. Ultimate analysis as performed by using LECO CHNS-932. Calorific values of the fuels were measured

by using AC-500 bomb calorimeter. Analyses were performed according to ASTM standards. The Jeol JSM-6400 scanning electron microscope (SEM) configured with a Noran energy dispersive spectrometer (EDS) was utilised for determination of ash composition. Proximate, ultimate and ash analyses together with calorific values of the fuels are briefly summarized in Table 3.1.

Table 3.1: Fuel Analyses

<b>Proximate Analysis</b>	<b>Imported Coal</b>	<b>Petroleum Coke</b>	<b>Lignite I</b>	<b>Lignite II</b>	<b>Olive Residue</b>
(As received basis, % by wt.)					
Moisture	8.15	0.54	16.35	48.77	6.07
Ash	11.21	3.77	28.78	17.56	4.24
Volatile Matter	18.1	13.51	29.79	22.93	75.69
Fixed Carbon	62.54	82.18	25.08	10.74	14.00
<b>Ultimate Analysis</b>					
(As received basis, % by wt.)					
C	72.87	86.13	37.31	20.40	47.17
H	3.77	3.26	3.30	1.89	5.99
O	2.15	0.00	10.01	9.66	34.78
N	1.63	1.99	0.91	0.70	1.62
S <sub>Combustible</sub>	0.22	4.34	3.33	1.02	0.13
Ash	11.21	3.74	28.78	17.56	4.24
Moisture	8.15	0.54	16.35	48.77	6.07
S <sub>Total</sub>	0.3	4.71	3.49	2.33	0.13
LHV(MJ/kg)	27.04	33.17	9.89	6.34	16.85
<b>Ash Analysis (% by wt.)</b>					
SiO <sub>2</sub>	54.08	9.60	43.13	24.01	31.19
Al <sub>2</sub> O <sub>3</sub>	28.65	2.19	18.20	10.58	5.29
Fe <sub>2</sub> O <sub>3</sub>	5.16	1.62	15.78	5.15	5.17
CaO	2.91	30.57	7.63	25.00	17.52
MgO	0.83	1.19	0.48	4.26	2.51
Na <sub>2</sub> O	0.00	0.00	2.00	0.69	5.21
K <sub>2</sub> O	2.33	0.77	0.63	0.86	27.95
SO <sub>3</sub>	5.08	46.73	11.08	28.68	2.64
TiO <sub>2</sub>	0.96	0.00	1.07	0.78	2.52
NiO	0.00	1.05	0.00	0.00	0.00
V <sub>2</sub> O <sub>5</sub>	0.00	6.28	0.00	0.00	0.00

The imported coal is classified as medium volatile bituminous coal according to its percentage of fixed carbon, calculated on a dry, ash-free basis as stated in the literature [39]. It is a high rank coal that has high calorific value, low volatile matter and oxygen content. Imported coal ash is dominated by oxides of silicon and aluminium.

Petcoke is a carbonaceous solid residual by-product of the oil refining coking process. As crude oil is refined, lighter fractions or products, such as gasoline and jet fuel, are driven off leaving a residual oil of relatively little value. In refineries with cokers, this residual oil is processed further to yield additional amounts of light products, along with petcoke. Petcoke has high calorific value and fixed carbon content; therefore, it is used to make heat recovery in energy production. It has lower ash and higher sulphur contents compared to the other fuels. Absence of inherent oxygen and low volatile matter content result in difficult ignition. Owing to the increasing demand for heavy oil processing the production of petcoke is increasing. High availability, high calorific value and low prices make petcoke attractive as an alternative fuel in energy production [40-42]. Petcoke ash is dominated by CaO and SO<sub>3</sub>. Moreover, NiO and V<sub>2</sub>O<sub>5</sub> are detected in petcoke ash but not in the ashes of other fuels.

Lignite is not only the world's most abundant fossil fuel, but also one of the two major indigenous sources of energy in Turkey with an estimated quantity of 12.4 billion tons of reserves [43]. Therefore, in this study two different kinds of indigenous lignites representing the majority of the reserves are selected for pyrolysis and combustion experiments. Lignite I is a typical indigenous lignite from Çan town of Çanakkale province in Turkey. As can be seen from

Table 3.1, it is characterized by its low calorific value, high ash content and high total sulphur content. Lignite II is another indigenous lignite from Konya province that is characterized by its high moisture content, low calorific value and higher CaO content in its ash.

Biomass is a renewable energy resource as it can be considered as a carbon neutral fuel [44]. Olive residue is selected for pyrolysis and combustion experiments in this study, which is a specific type of biomass from olive oil production process. It is the remaining part of olive after milling and extraction of the olive oil. As Turkey is one of the main olive producers with 774,000 ha of olive groves and 1,464,248 tons of annual production, significant amount of olive residue is produced [45]. Olive residue contains significant amount of oxygen and volatile matter. It has low moisture and ash content.

### **3.3 Experimental Set-up**

In the present work, thermogravimetry (TGA) / differential thermogravimetry (DTG) were used to determine pyrolysis and combustion characteristics of fuel samples. It is a rapid, inexpensive and simple method that has been widely used in studying the pyrolysis and combustion behaviour of various fuels and evaluating the relative burning properties of fuel samples [13, 15, 46, 47]. For determination of evolved gases during pyrolysis and combustion experiments, TGA system was coupled with Fourier transform infrared (FTIR) spectrometer, which has many applications in the open literature [25, 35, 48-52].

Figure 3.1 shows a schematic diagram of the experimental setup consisting of Perkin Elmer Pyris STA 6000 thermo-gravimetric analyzer, Spectrum 1 FTIR spectrometer and a mass flow controller (MFC) for each gaseous species. TGA and FTIR were connected by a heated line with a temperature of 270°C in order to



prevent the condensation of gases. FTIR spectra were collected with  $4\text{ cm}^{-1}$  resolution, in the range of  $4000\text{--}700\text{ cm}^{-1}$  IR absorption band.

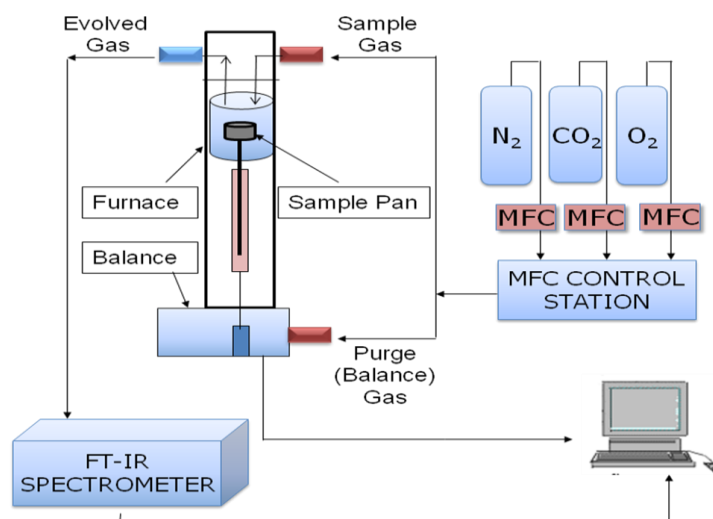


Figure 3.1: Schematic diagram of the experimental setup.

### 3.4 Experimental Method

About 12 mg of coal sample with particle size less than  $100\text{ }\mu\text{m}$  was held initially at room temperature for 1 min and then heated with a heating rate of  $40^{\circ}\text{C}/\text{min}$  from room temperature up to  $950^{\circ}\text{C}$  during each experiment. In pyrolysis tests, samples were held at  $950^{\circ}\text{C}$  for an additional 60 mins. The required combustion environments were formed by mixing two gases in the desired ratio by using two different mass flow controllers in order to regulate the flow rates of the gases. The total gas flow was set to  $70\text{ ml}/\text{min}$  for pyrolysis and  $45\text{ ml}/\text{min}$  for combustion experiments.

Pyrolysis tests were carried out under nitrogen and carbon dioxide atmospheres, which are the diluting gases of air and oxy-fuel environments, respectively. Four

combustion tests were performed in air environment to investigate the effect of combustion environment on burning process. The base case was considered as combustion in air environment. In oxygen-enriched air case the sample is burned in 30 % O<sub>2</sub> – 70 % N<sub>2</sub> atmosphere. In oxy-fuel combustion tests, the volume of N<sub>2</sub> used in the base case was replaced with an equal volume of CO<sub>2</sub>. In the last case, combustion of fuel sample was investigated in oxygen-enriched oxy-fuel environment, that is, in 30 % O<sub>2</sub> – 70 % CO<sub>2</sub> atmosphere.

TGA and DTG profiles obtained during pyrolysis and combustion experiments were used to determine some characteristic parameters such as initial decomposition temperature ( $T_{in}$ ), peak temperature ( $T_{max}$ ), ignition temperature ( $T_{ig}$ ) and burnout temperature ( $T_b$ ).  $T_{in}$  represents the initiation of weight loss and is defined as the temperature at which the rate of weight loss reaches 1 %/min after initial moisture loss peak in DTG profile [12].  $T_{max}$  is the point at which maximum reaction rate occurs. Different from initial decomposition temperature, ignition temperature  $T_{ig}$  is defined as the temperature at which coal starts burning. It is taken as the temperature at which the weight loss curves in the oxidation and pyrolysis experiments diverge [25, 46, 53]. The last characteristic temperature considered is burnout temperature, which represents the temperature where sample oxidation is completed. It is taken as the point immediately before reaction ceases when the rate of weight loss is 1 %/min [13].

Theoretical DTG curves of the blend samples were plotted in order to investigate the interactions between coal and biomass samples and influence of blending on characteristic temperatures. The curves were calculated by applying the additive rule using the profiles of individual components according to their ratio in the blend [54-56].

A linear relation between spectral absorbance at a given wavenumber and concentration of gaseous components is given by Beer's Law. In this study, the points of absorbance at a certain wavenumber are plotted against temperature in order to obtain a formation profile for each evolved gas observed in the spectra

during experiments. The IR wavenumbers of CO<sub>2</sub>, CO, H<sub>2</sub>O, CH<sub>4</sub>, SO<sub>2</sub> and COS are 2360, 2112, 1540, 3016, 1340 and 2042 cm<sup>-1</sup>, respectively. Formation profiles of NO<sub>x</sub> related species such as NO and NO<sub>2</sub> are not reported due to overlap of their absorption bands with the characteristic absorption bands of water in the range of 3900-3500 and 1900-1350 cm<sup>-1</sup>.

## CHAPTER 4

### RESULTS AND DISCUSSION

#### 4.1 General

This study is based on investigation of pyrolysis and combustion behaviour of various fuels in air and oxy-fuel conditions. The effect of diluting gas and oxygen concentration on pyrolysis and combustion characteristics are studied by using TGA-FTIR combined system. In this chapter, TGA-FTIR test results are analyzed by using weight loss and derivative weight loss profiles (TGA/DTG) profiles. Characteristic parameters are calculated by the method defined in Chapter 3 and presented for each fuel and their blend. Moreover, gas formation profiles of the evolved gases identified in FTIR spectra of the fuel samples are also given.

Pyrolysis as the preliminary process of coal combustion plays a crucial role in determining flame stability, ignition, and product distributions [57]. The possible impacts of different gases on pyrolysis process necessitate the investigation of devolatilization behaviour of fuel in both  $N_2$  and  $CO_2$  environments. Devolatilization of fuels may differentiate in volatile composition, volatile yield and possible  $CO_2$  – char reaction at high temperature range. Therefore, pyrolysis tests were carried out under both nitrogen and carbon dioxide atmospheres, which are the diluting gases of air and oxy-fuel environments, respectively.

Oxy-fuel combustion was found to differ from air combustion in heat transfer, combustion characteristics and emissions due to the presence of  $\text{CO}_2$  in high concentrations in oxy-fuel combustion conditions. Therefore, in order to investigate effects of combustion environment, combustion tests were carried out under air (base case), oxygen-enriched conditions (30 %  $\text{O}_2$  – 70 %  $\text{N}_2$ ), oxy-fuel conditions (21 %  $\text{O}_2$  – 79 %  $\text{CO}_2$ ), oxygen-enriched oxy-fuel conditions (30 %  $\text{O}_2$  – 70 %  $\text{CO}_2$ ) for all fuel samples.

## 4.2 Imported Coal

As mentioned previously, imported coal is a high rank, medium volatile bituminous coal with high calorific value and low volatile matter content. Pyrolysis and combustion characteristics of imported coal are explained in the next two sections.

### 4.2.1 Pyrolysis of Imported Coal

Pyrolysis behaviour of imported coal in  $\text{N}_2$  and  $\text{CO}_2$  environments is shown with TGA and DTG curves in Figure 4.1.

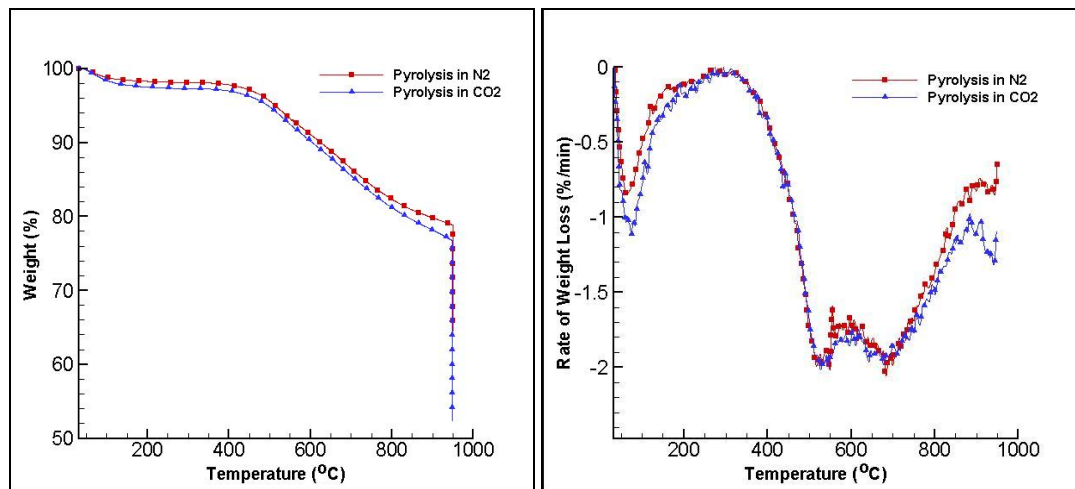


Figure 4.1: TGA and DTG profiles of imported coal during pyrolysis in N<sub>2</sub> and CO<sub>2</sub> atmospheres

As can be seen from figures, similar behaviours are observed in pyrolysis of imported coal samples under N<sub>2</sub> and CO<sub>2</sub> atmospheres up to around 750°C, which indicates that CO<sub>2</sub> behaves as an inert atmosphere until a certain temperature. After moisture release in the first 200°C temperature zone, pyrolysis continues with the release of volatile matter content in the range of 200–750°C. In 250–490°C temperature interval, it is known that primary pyrolysis takes place which includes the release of larger fraction of volatiles, mainly light species and gases; CO<sub>2</sub>, light aliphatic gases, CH<sub>4</sub> and H<sub>2</sub>O. Tar and hydrocarbons evolve between 490 and 640°C. During secondary pyrolysis additional gas formation such as CH<sub>4</sub>, CO and H<sub>2</sub> from ring condensation is mainly observed [17, 57]. The major difference in pyrolysis of imported coal samples in these two different atmospheres is observed after 750°C with the separation of TGA profiles. In 700–950°C temperature range, additional peak is displayed in DTG profile of imported coal obtained in CO<sub>2</sub> atmosphere as shown in Figure 4.1. Sharp peak observed in DTG profile of pyrolysis in CO<sub>2</sub> environment can be attributed to char–CO<sub>2</sub> gasification reaction as also confirmed by higher total weight loss in CO<sub>2</sub> atmosphere as shown in confirmed by other studies [25, 29, 33, 34].

Table 4.1: Pyrolysis Characteristics of Imported Coal

	Pyrolysis in N <sub>2</sub>	Pyrolysis in CO <sub>2</sub>
<b>T<sub>in</sub> (°C)</b>	465.2	463.9
<b>T<sub>max.-1</sub> (°C)</b>	517.0	528.4
<b>T<sub>max.-2</sub> (°C)</b>	-	933.7
<b>(dm/dt)<sub>max.-1</sub> (%/min)</b>	2.0	2.0
<b>(dm/dt)<sub>max.-2</sub> (%/min)</b>	-	1.2
<b>Weight loss up to (%)</b>	21.1	23.2

Formation profiles of evolved gases including  $\text{CO}_2$ ,  $\text{CO}$ ,  $\text{H}_2\text{O}$ ,  $\text{CH}_4$ ,  $\text{SO}_2$  and  $\text{COS}$  during pyrolysis in  $\text{N}_2$  and  $\text{CO}_2$  environments are shown in Figure 4.2.  $\text{CO}_2$  formation displays an increasing trend in the temperature range of 200-950°C, with a maximum absorbance value at around 775°C. This range corresponds to the devolatilization temperature interval as represented in DTG curve of imported coal. Formation of  $\text{CO}_2$  in  $\text{N}_2$  environment is found to be the major contributor to the evolved gases with its highest absorbance intensity.  $\text{CO}$  formation is observed to initiate at around 300°C and continue to evolve up to 700°C.  $\text{CO}$  formation is observed to complete at 850°C in nitrogen atmosphere, while a distinctive increase is observed in formation profile of  $\text{CO}$  due to char- $\text{CO}_2$  gasification reaction in  $\text{CO}_2$  atmosphere. Water vapour shows an increasing trend especially after 700°C. It is considered to be due to effect of side gasification reactions. Methane formation takes place between 400 – 600°C with slightly higher absorbance intensity in  $\text{CO}_2$  environment. In the case of sulphur containing gases,  $\text{SO}_2$  and  $\text{COS}$  formation is identified in the FTIR spectra. Certain amount of  $\text{SO}_2$  is formed in two steps at around 600°C and 900°C. In  $\text{CO}_2$  atmosphere, the absorbance intensity of  $\text{SO}_2$  gas is higher than the one in  $\text{N}_2$  atmosphere; however, similar trends are observed in both atmospheres. As reported in the literature,  $\text{COS}$  is formed by reaction of pyrite or sulphur formed during pyrite decomposition with  $\text{CO}$  [34, 35, 58]. Therefore,  $\text{COS}$  formation is observed to increase significantly with the initiation of gasification reaction in  $\text{CO}_2$  environment. Higher  $\text{CO}$  concentration in pyrolysis environment leads to the formation of  $\text{COS}$  in  $\text{CO}_2$  atmosphere, in contrast to  $\text{N}_2$  atmosphere.

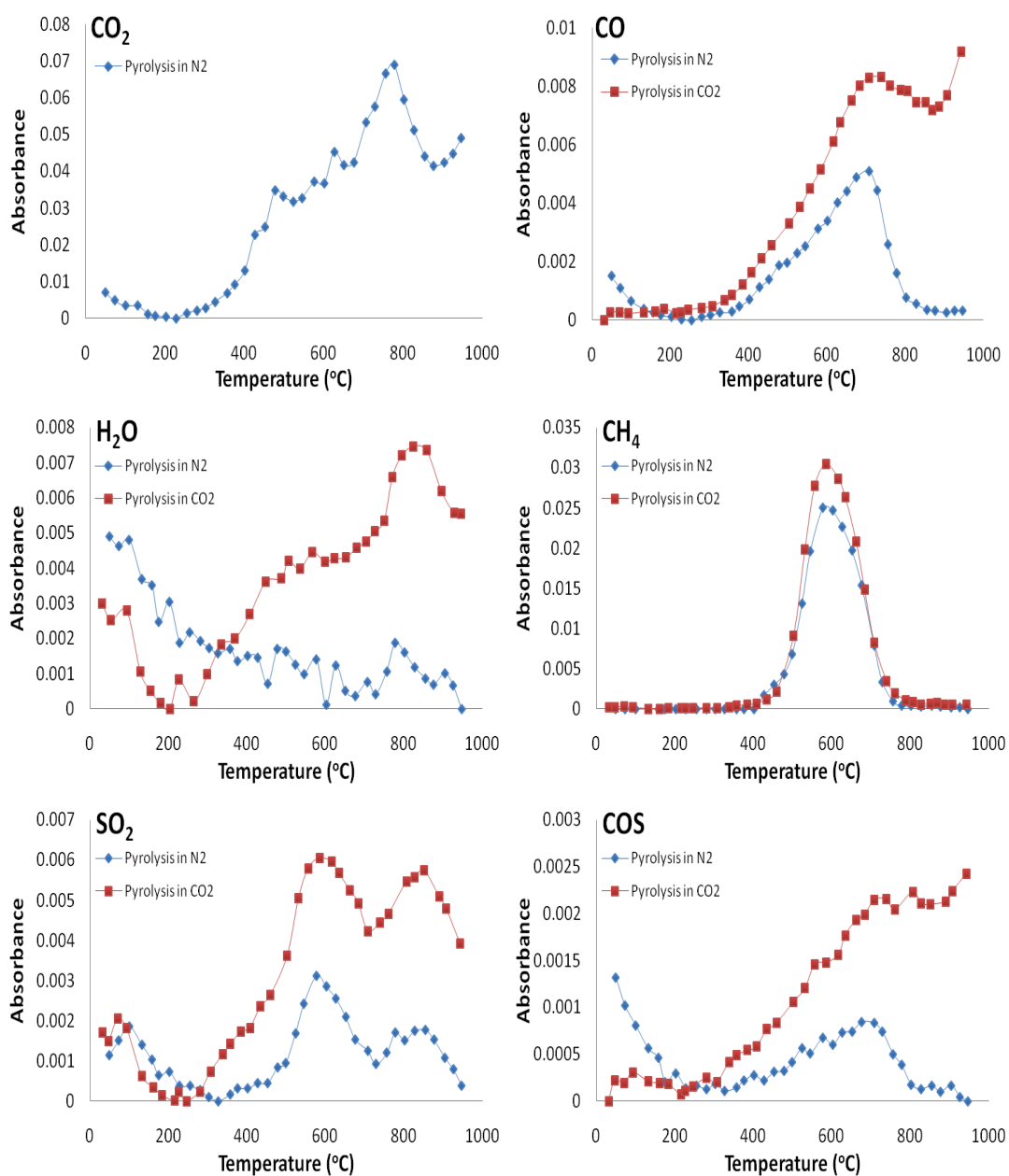


Figure 4.2: Formation profiles of evolved gases during pyrolysis tests of imported coal.



#### 4.2.2 Combustion of Imported Coal

Figure 4.3 shows combustion behaviour of imported coal in air, oxygen-enriched air (30 % O<sub>2</sub> – 70 % N<sub>2</sub>), oxy-fuel environment (21 % O<sub>2</sub> – 79 % CO<sub>2</sub>), and oxygen enriched oxy-fuel environment (30 % O<sub>2</sub> – 70 % CO<sub>2</sub>).

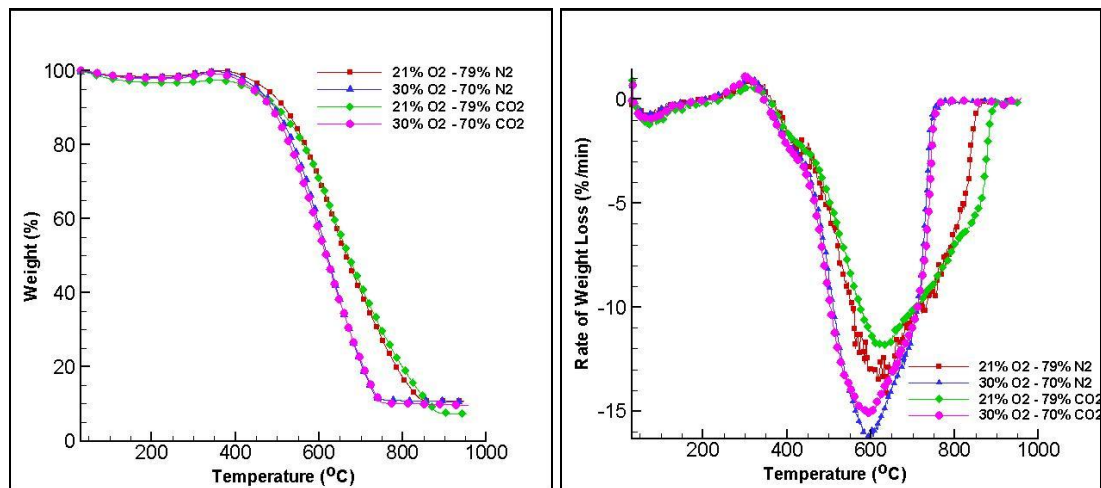


Figure 4.3: TGA and DTG profiles of imported coal in different combustion atmospheres

TGA curves in Figure 4.3 shows that the effect of oxygen concentration is more significant than that of the diluting gas (N<sub>2</sub> or CO<sub>2</sub>) on the combustion profiles. While combustion in O<sub>2</sub>/N<sub>2</sub> and O<sub>2</sub>/CO<sub>2</sub> mixtures with identical oxygen concentrations results in only slight differences in combustion characteristics, elevated oxygen levels in combustion environment shift the weight loss curves to lower temperature zone.

Overall comparison of DTG curves reveal two main weight loss steps in all combustion environments. The first step corresponds to moisture release within the temperature range of 200°C, and the second one accounts for weight loss due to devolatilization of volatile matter and burning of char in the temperature range of

300-850°C. After 200°C, increase to positive values is observed in the rate of weight loss in DTG curves, which is related to the weight gain during heating in the temperature range of 200-400°C [13, 59]. This is considered to be due to oxygen adsorption in the coal structure, which results in formation of oxygenated complex before combustion. In air firing case, as can be seen from the figure, devolatilization and char burning is not sharply separated, however, the shoulder around 400°C can be attributed to volatile release.

Comparison between the DTG curves of imported coal in air and oxy-fuel environments reveals that replacing nitrogen with CO<sub>2</sub> results in lower reactivity and delayed combustion due to lower slope of weight loss rate and higher peak and burnout temperatures. Delayed combustion in CO<sub>2</sub> environment is a physically expected phenomenon that takes place due to higher specific heat of CO<sub>2</sub> leading to lower particle temperature [6, 22, 25]. The shoulder in DTG profile in CO<sub>2</sub> environment after 800°C is also worth noting. This can be attributed to CO<sub>2</sub>-char reaction as also confirmed by findings in the literature [33].

Combustion of imported coal in oxygen enriched air environment displays significantly different behaviour than that in air environment despite the similarity in the shape of DTG profiles. Table 4.2 shows that initial decomposition, peak and burnout temperatures are lower in the oxygen enriched air environment. These lower temperatures are indicative of earlier loss of volatile matter, easier ignition and faster approach to complete combustion, respectively. This is also confirmed by higher reactivity of imported coal in oxygen enriched atmosphere due to higher maximum weight loss rate,  $(dm/dt)_{max}$ , and lower temperature corresponding to the main peak,  $T_{max}$ . It can, therefore, be concluded that imported coal burns hotter and faster in oxygen-enriched environment compared to air environment.

Table 4.2: Combustion Characteristics of Imported Coal

	21 % O <sub>2</sub> -79 % N <sub>2</sub>	30 % O <sub>2</sub> -70 % N <sub>2</sub>	21 % O <sub>2</sub> -79 % CO <sub>2</sub>	30 % O <sub>2</sub> -70 % CO <sub>2</sub>
T <sub>in</sub> (°C)	387.4	376.7	387.0	371.4
T <sub>max.-1</sub> (°C)	618.3	594.9	629.2	591.1
T <sub>b</sub> (°C)	848.4	745.0	885.1	752.0
(dm/dt) <sub>max.</sub> (%/min)	13.3	16.1	11.8	15.0
T <sub>ig</sub> (°C)	446.6	422.0	393.0	420.3
Weight loss up to 950°C ( %)	89.1	89.2	93.3	90.3

The DTG profiles of imported coal in oxygen enriched air and oxygen enriched CO<sub>2</sub> environments reveal close resemblance and slightly lower maximum weight loss rate in the CO<sub>2</sub> environment. Overall comparison of DTG profiles shows that higher oxygen content in the combustion environment is the most effective parameter irrespective of the dilute gas. At higher O<sub>2</sub> concentrations peak and burnout temperatures are lower, weight loss rate is higher and complete combustion is achieved at lower temperatures and shorter time [25, 29, 33, 35, 38, 60]. In oxygen-enriched oxy-fuel conditions, CO<sub>2</sub> gasification shoulder disappears as complete combustion is achieved before 800°C.

Figure 4.4 displays formation profiles of gases evolved in different combustion environments. Gaseous species evolved during combustion tests were found to be CO<sub>2</sub>, CO, H<sub>2</sub>O, CH<sub>4</sub>, SO<sub>2</sub> and COS. CO<sub>2</sub> evolution is observed to initiate at around 300°C and continues up to the end of combustion in air and oxygen-enriched air conditions. Higher oxygen concentration in combustion environment results in shift in CO<sub>2</sub> formation profile to lower temperature zone as elevated oxygen levels lead to faster burning and earlier release of CO<sub>2</sub>. The major contributor to the evolved gases is found to be CO<sub>2</sub> with its higher absorbance intensity. CO formation is

identified between 300-900°C and similar trends are displayed in all combustion conditions. In oxy-fuel environment, CO formation is completed at higher temperatures compared to air conditions, due to effect of gasification reaction. In the first 200°C temperature zone, H<sub>2</sub>O formation is detected due to moisture release in all cases. In the second part, further H<sub>2</sub>O release is observed in all conditions due to coal oxidation reactions. However, H<sub>2</sub>O formation is found to be slightly higher in oxy-fuel conditions. Similar trends are displayed in CH<sub>4</sub> gas evolution profiles 400 – 700°C in all cases. SO<sub>2</sub> gas formation is observed during entire combustion period. COS gas evolves in the temperature range of 300-900°C under all combustion conditions. COS formation is completed in higher temperatures in oxy-fuel case similar to CO formation.

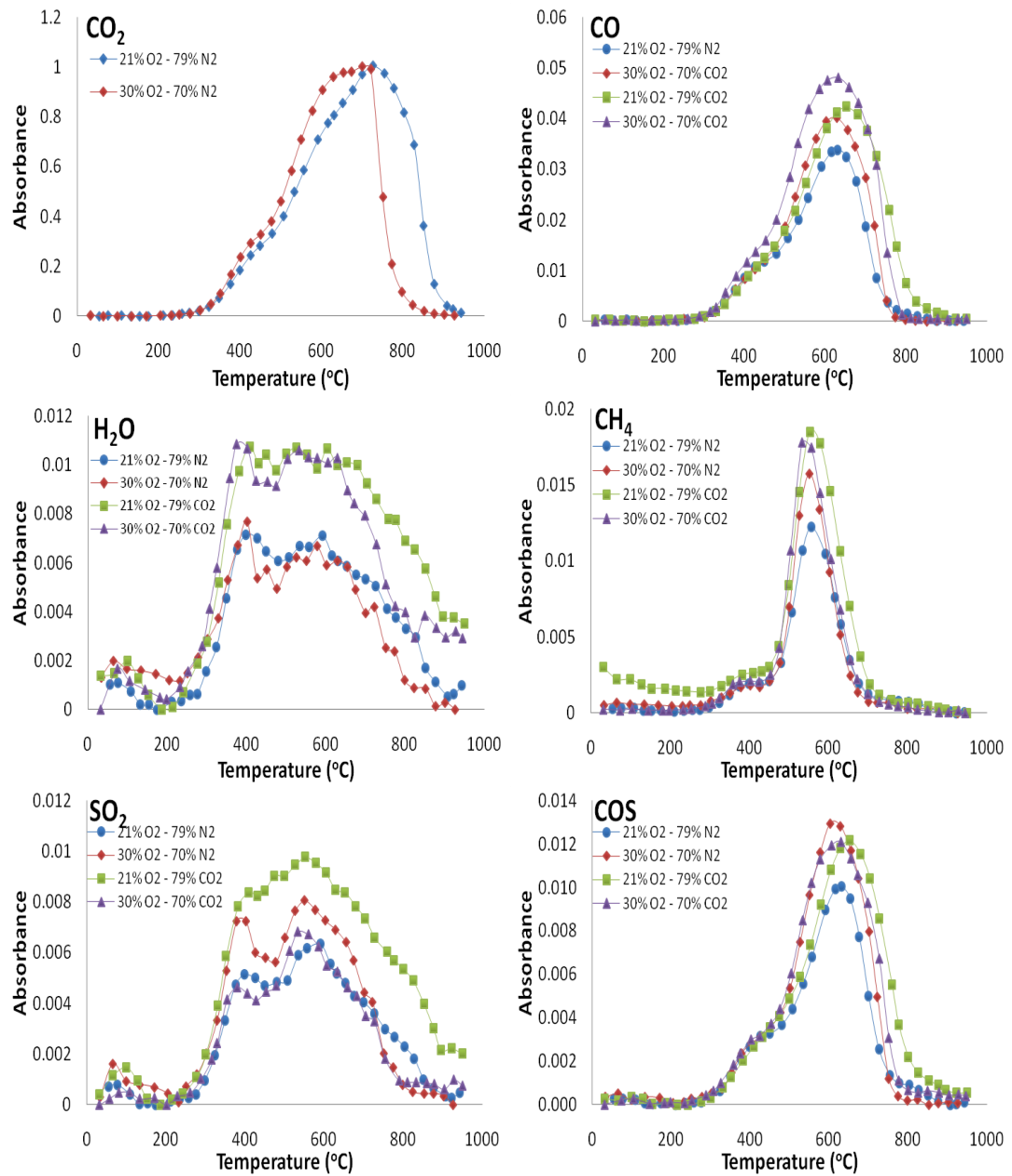


Figure 4.4: Formation profiles of evolved gases during combustion tests of imported coal

### 4.3 Petcoke

Petcoke is a by-product of oil refining process. Petcoke is typically a carbon-rich fuel that contains low volatile matter and high sulphur content with very low ash.

#### 4.3.1 Pyrolysis of Petcoke

TGA and DTG curves of petcoke under nitrogen and carbon dioxide environment are shown in Figure 4.5. Pyrolysis characteristics determined from these profiles are summarized in Table 4.3.

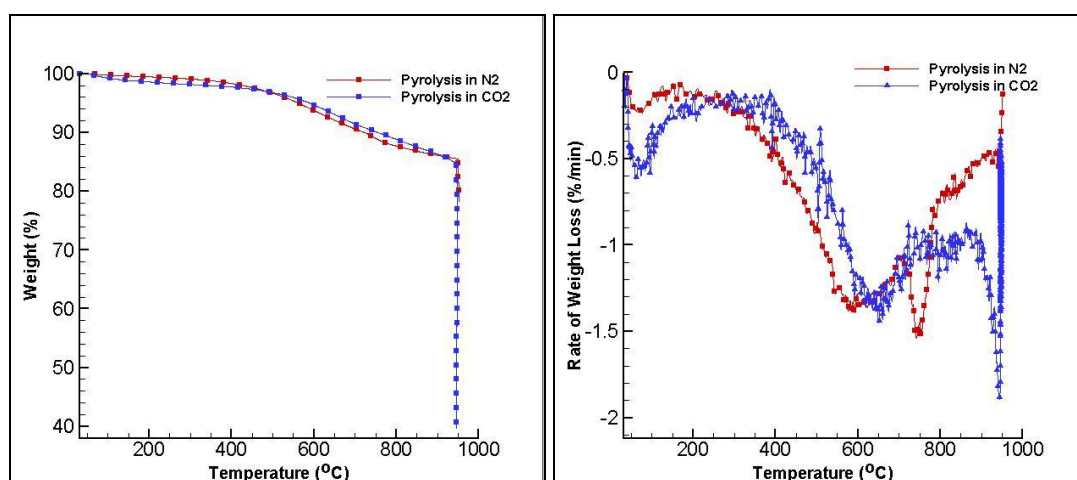


Figure 4.5: TGA and DTG profiles of petcoke during pyrolysis in  $N_2$  and  $CO_2$  atmospheres

As can be seen from TGA curve in Figure 4.5 and Table 4.3 total weight loss of petcoke under  $CO_2$  atmosphere is significantly higher than that in  $N_2$  atmosphere. DTG curves of the petcoke samples show that moisture release takes place with relatively lower weight loss rate due to its lower moisture content in the first 200°C

temperature zone. After moisture release, two main weight loss steps appear in DTG profiles of the fuel samples. First weight loss step within 200-700°C temperature range is attributed to release of volatile matter content. Higher heat capacity of CO<sub>2</sub> gas leads to delay in weight loss profiles, higher initial decomposition and peak temperatures under CO<sub>2</sub> atmosphere. Second weight loss step is represented with additional peaks after 700°C in both atmospheres. In N<sub>2</sub> atmosphere, second peak is attributed to calcite decomposition in N<sub>2</sub> atmosphere. This point can also be confirmed by high CaO content in petcoke ash (Table 3.1) and related studies in the literature [34, 48, 54]. However, the sharp peak observed in CO<sub>2</sub> environment is considered to be due to char-CO<sub>2</sub> gasification reaction.

Table 4.3: Pyrolysis Characteristics of Petcoke

	Pyrolysis in N <sub>2</sub>	Pyrolysis in CO <sub>2</sub>
<b>T<sub>in</sub> (°C)</b>	514.9	570.9
<b>T<sub>max.-1</sub> (°C)</b>	582.3	638.7
<b>T<sub>max.-2</sub> (°C)</b>	742.9	944.2
<b>(dm/dt)<sub>max.-1</sub> ( %/min)</b>	1.4	1.3
<b>(dm/dt)<sub>max.-2</sub> ( %/min)</b>	1.5	1.6
<b>Weight loss up to 950°C ( %)</b>	14.4	17.0

Formation profiles of the gases released during pyrolysis of petcoke is represented in Figure 4.6. CO<sub>2</sub> formation takes place in three steps in the temperature range of 200 – 950°C. First two steps are considered to be due to release of volatilities while last step represents the CO<sub>2</sub> release as a result of calcite decomposition reactions. CO formation profile reveals that significant amount of CO is evolved due to char – CO<sub>2</sub> gasification after 800°C. In CO<sub>2</sub> atmosphere water vapour formation is significantly higher than that in N<sub>2</sub> atmosphere in high temperature zone because of

gasification reactions. Methane formation is observed in the temperature range of 500 – 900°C in both pyrolysis conditions. In pyrolysis of high sulphur content petcoke samples, SO<sub>2</sub> formation is identified after 500°C and relatively higher absorbance intensity is observed in CO<sub>2</sub> atmosphere. COS evolution appears at high temperature zone related to CO formation.



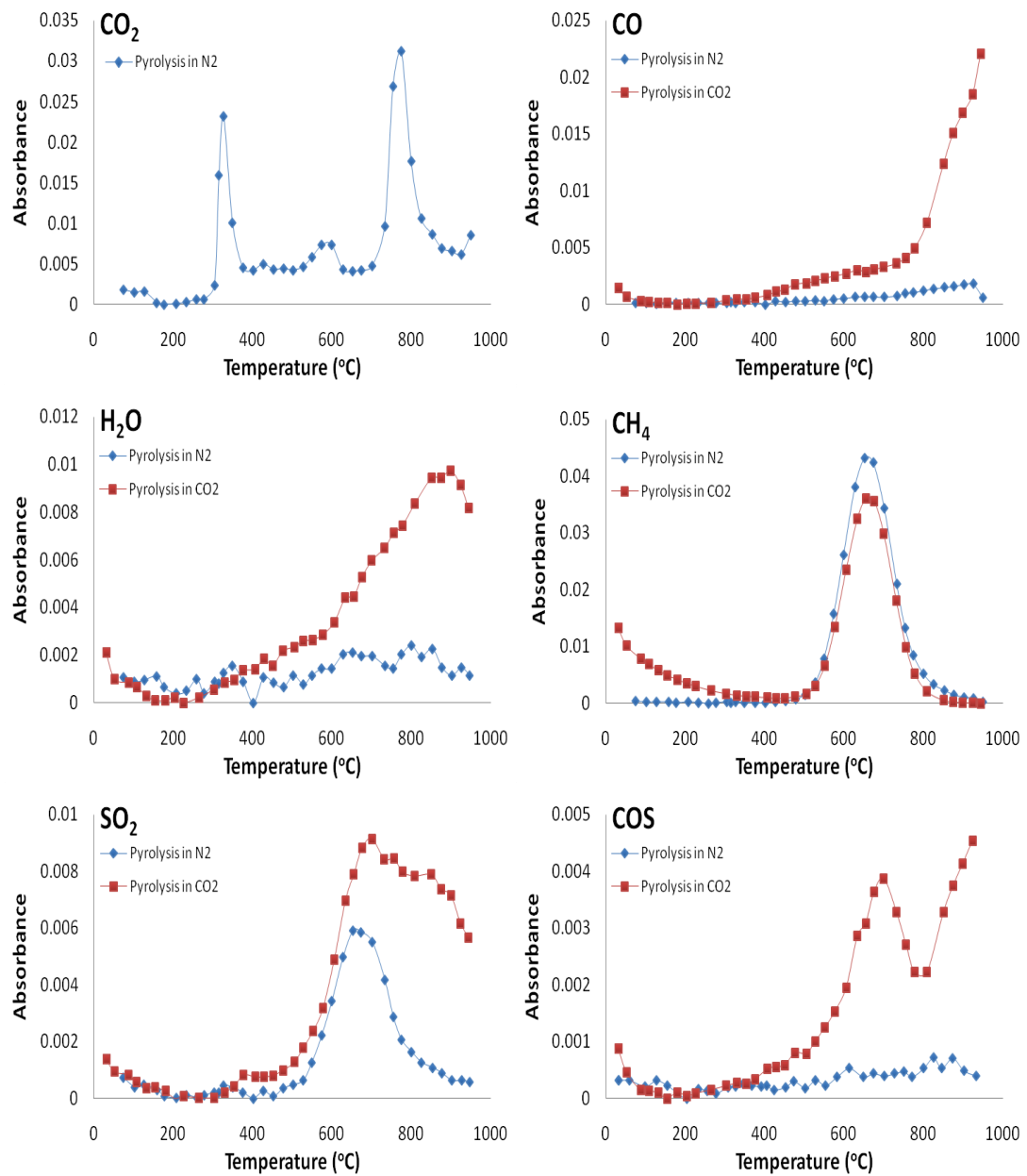


Figure 4.6: Formation profiles of evolved gases during pyrolysis tests of petcoke

### 4.3.2 Combustion of Petcoke

TGA and DTG profiles evaluated in combustion tests of petcoke are represented in Figure 4.7.

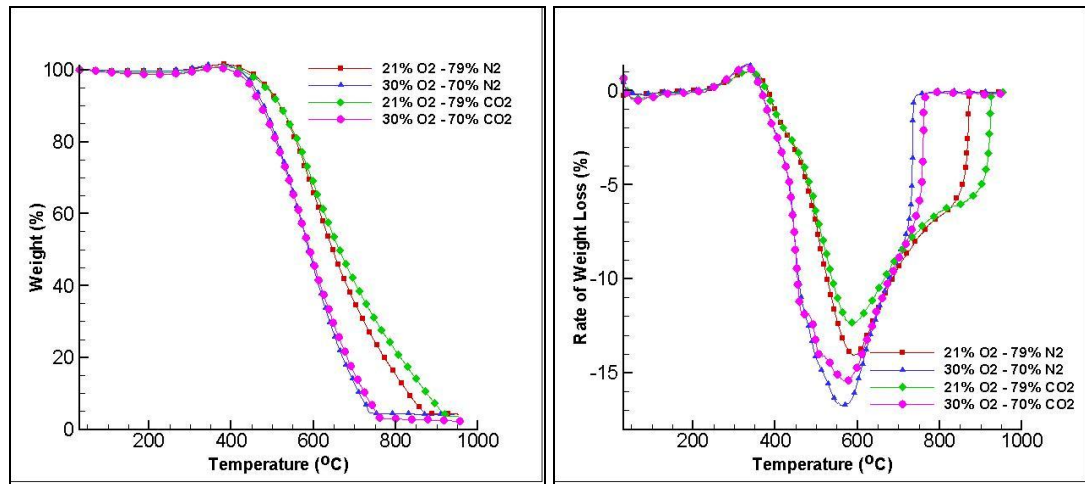


Figure 4.7: TGA and DTG profiles of petcoke in different combustion atmospheres

Different combustion behaviours of petcoke are observed in all combustion conditions. Effects of oxygen concentration and diluting gas ( $N_2$  and  $CO_2$ ) on combustion are clearly displayed in TGA curves of Figure 4.7. Weight loss profiles reveal that elevated oxygen levels lead to shift in combustion curves to lower temperatures. Moreover,  $CO_2$ , as a diluting gas in the combustion environment, causes delay in combustion and results in combustion of petcoke samples at slightly higher temperatures.

Overall comparison of DTG curves in Figure 4.7 reveals that weight loss takes place at one main step. Moisture release is not observed in the first 200°C temperature zone due to absence of moisture in petcoke samples in contrast to other fuels. However, after 100°C, weight gain is observed to initiate that is caused by oxygen adsorption before combustion procedure until 350°C as also observed in

combustion of imported coal. After weight gain, initial decomposition starts at around 400°C and weight loss reaches to its maximum value at around 590°C in air and oxy-fuel environments. After 800°C, distinctive shoulders are observed in DTG profiles in both conditions, which is attributed to thermal decomposition of carbonates. In oxy-fuel case, the calculated characteristic temperatures such as  $T_{in}$ ,  $T_{max}$  and  $T_{ig}$  are found almost the same with air case as reported in Table 4.4. Replacing nitrogen with carbon dioxide in combustion environment results in delayed combustion; lower weight loss rate, higher peak and burnout temperatures.

Table 4.4: Combustion Characteristics of Petcoke

	21 % O <sub>2</sub> -79 % N <sub>2</sub>	30 % O <sub>2</sub> -70 % N <sub>2</sub>	21 % O <sub>2</sub> -79 % CO <sub>2</sub>	30 % O <sub>2</sub> -70 % CO <sub>2</sub>
$T_{in}$ (°C)	400.1	381.6	398.7	379.5
$T_{max}$ (°C)	589.0	562.2	587.6	572.6
$T_b$ (°C)	867.0	735.6	923.7	761.8
$(dm/dt)_{max}$ . (%/min)	14.0	16.8	12.4	15.5
$T_{ig}$ (°C)	469.5	439.7	465.4	434.7
Weight loss up to 950°C ( %)	96.8	95.9	96.7	97.9

In oxygen-enriched conditions, main peak is observed in a narrower temperature interval between 350 – 750°C. In oxygen-enriched conditions, calcite decomposition is not observed as complete combustion is achieved before the temperature interval of thermal decomposition reactions. All characteristic temperatures such as  $T_{max}$ ,  $T_{in}$ ,  $T_{ig}$  and  $T_b$  are lower and weight loss rate is higher in elevated oxygen levels.

Highest relevant temperatures are observed in combustion of petcoke compared to other fuels. These findings are in agreement with the studies reported in the literature about petcoke studies [41, 42, 53, 61]. Petcoke has the highest initial decomposition temperature and is the hardest fuel to ignite and reach to total burnout with its highest ignition and burnout temperatures, respectively.

Formation profiles of the gases evolved in combustion tests of petcoke are demonstrated in Figure 4.8. CO<sub>2</sub> formation is observed to initiate at around 300°C and end with the completion of combustion. The formation profile of CO<sub>2</sub> in oxygen-enriched air atmosphere shifts to lower temperature zone due to the effect of elevated oxygen levels. The major contributor to the evolved gases is found to be CO<sub>2</sub> with its higher absorbance intensity. CO formation takes place in the temperature range of 300 – 800°C and similar trends are observed in formation profiles when oxygen concentrations are identical in combustion environment. Water vapour is evolved between 300-900°C with similar formation trends in all combustion cases. Methane gas is identified mainly between 500-750°C. Combustion of high sulphur content petcoke samples reveal that SO<sub>2</sub> gas is evolved in two steps at around 600°C and 900°C in air and oxy-fuel cases while SO<sub>2</sub> release takes place in one-step at around 500°C in oxygen-enriched conditions. COS formation is detected between 350 – 800°C in all combustion cases.

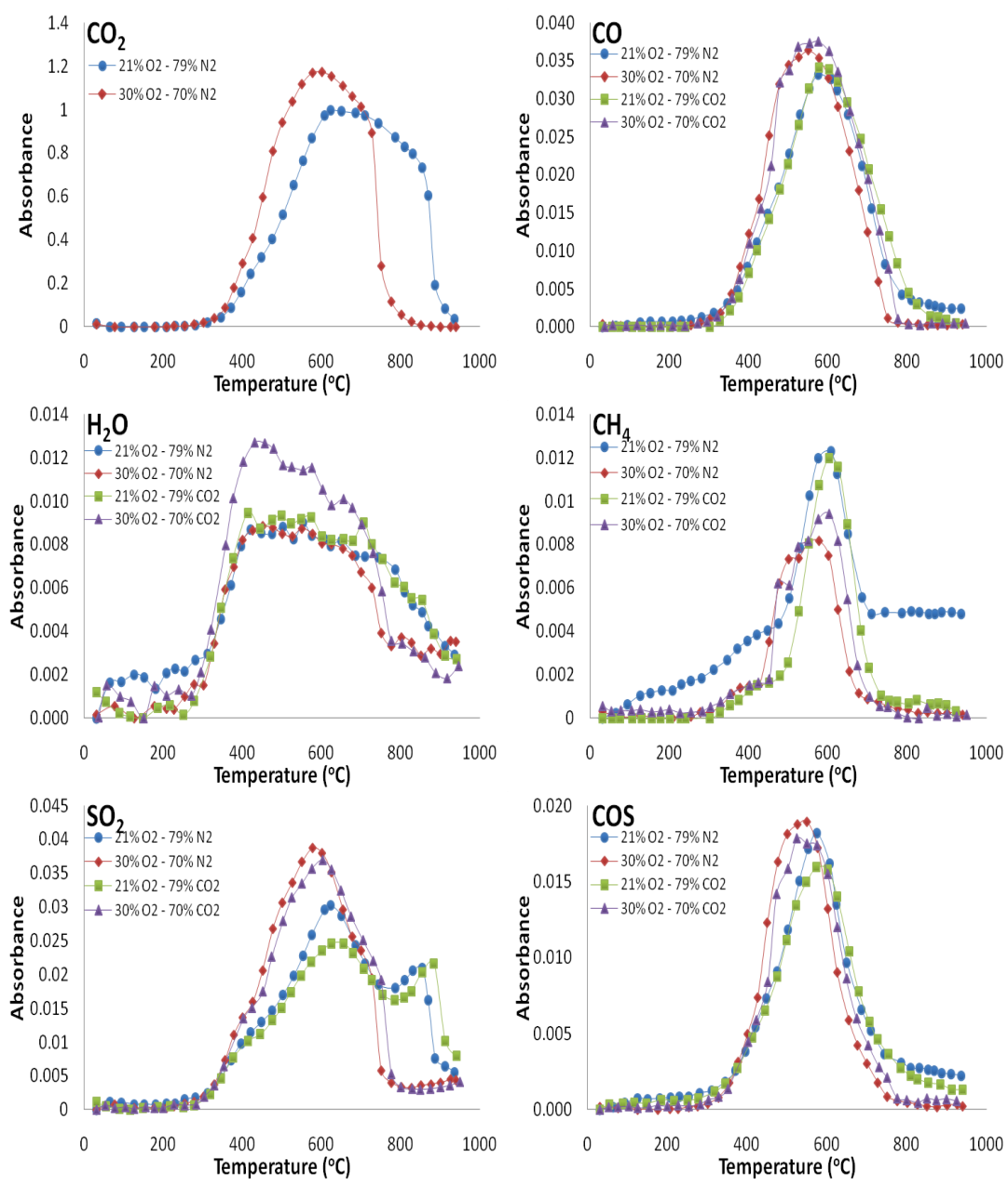


Figure 4.8: Formation profiles of evolved gases during combustion tests of petcoke

#### 4.4 Lignite I

Lignite I is characterized by its low calorific value, high ash content and high total sulphur content.

##### 4.4.1 Pyrolysis of Lignite I

TGA and DTG profiles of pyrolysis tests of lignite I are shown in Figure 4.9.

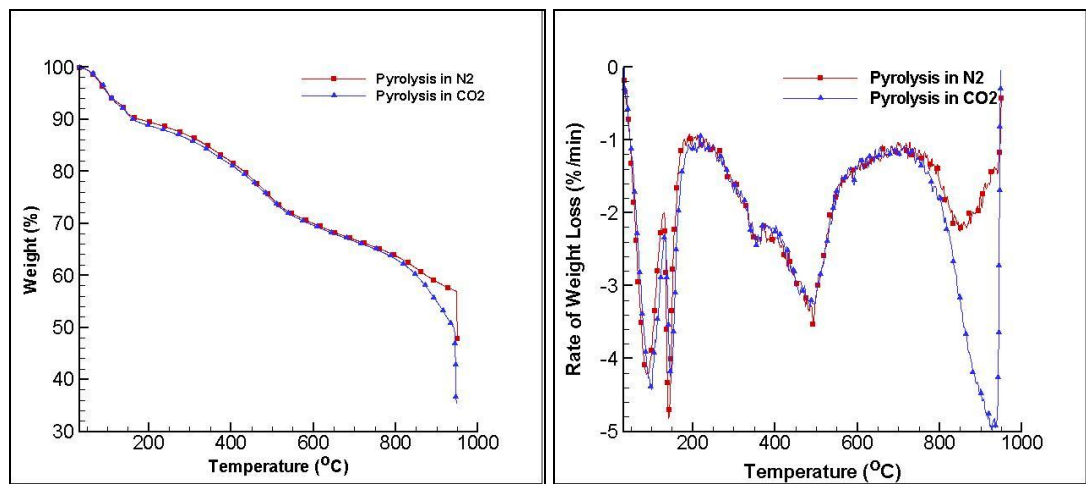


Figure 4.9: TGA and DTG profiles of lignite I in N<sub>2</sub> and CO<sub>2</sub> atmospheres

As can be seen from figures, pyrolysis behaviour of lignite samples in N<sub>2</sub> and CO<sub>2</sub> atmosphere is observed to be very similar up to around 720°C, which indicates that CO<sub>2</sub> behaves as an inert atmosphere until a certain temperature. After moisture release in the first 200°C temperature zone, pyrolysis continues with the release of volatile matter content in the range of 200-750°C. In CO<sub>2</sub> atmosphere, the maximum weight loss rate is found to be slightly lower with higher corresponding temperature ( $T_{max}$ ) than the ones in nitrogen atmosphere, which could be due to

the effect of higher heat capacity of CO<sub>2</sub>. The major difference in pyrolysis of lignite I samples in these two different atmospheres is observed after 720°C with the separation of TGA profiles. In 700-950°C temperature range, additional peaks are displayed in both DTG profiles. In nitrogen atmosphere, a small peak appearing after 700°C is attributed to partial burning of combustible matter at high temperatures by using inherent oxygen (almost 10 % in lignite I) in lignite sample. This is also confirmed with the FTIR results, which show a significant increase in CO<sub>2</sub> formation after 700°C. On the other hand, the sharp peak observed in DTG profile of pyrolysis in CO<sub>2</sub> environment can be attributed to char-CO<sub>2</sub> gasification reaction as also confirmed by higher total weight loss in CO<sub>2</sub> atmosphere as shown in Table 4.5.

Table 4.5: Pyrolysis Characteristics of Lignite I

	Pyrolysis in N <sub>2</sub>	Pyrolysis in CO <sub>2</sub>
<b>T<sub>in</sub> (°C)</b>	230.8	216.7
<b>T<sub>max.-1</sub> (°C)</b>	482.9	481.0
<b>T<sub>max.-2</sub> (°C)</b>	859.8	924.0
<b>T<sub>b</sub> (°C)</b>	-	-
<b>(dm/dt)<sub>max.-1</sub> ( %/min)</b>	3.6	3.16
<b>(dm/dt)<sub>max.-2</sub> ( %/min)</b>	1.9	4.8
<b>T<sub>ig</sub> (°C)</b>	-	-
<b>Weight loss up to 950°C ( %)</b>	41.0	50.3

Formation profiles of evolved gases including CO<sub>2</sub>, CO, H<sub>2</sub>O, CH<sub>4</sub>, SO<sub>2</sub> and COS during pyrolysis in N<sub>2</sub> and CO<sub>2</sub> environments are shown in Figure 4.10. In nitrogen environment, CO<sub>2</sub> release starts after 150°C and continues up to 550°C. Additional peak appears in CO<sub>2</sub> and CO formation curves due to burning of combustible matter

in  $N_2$  environment after  $750^{\circ}C$  as explained in previous section. In the case of pyrolysis in  $CO_2$  environment, significant amount of CO is evolved from char –  $CO_2$  gasification reaction. Formation of CO in  $CO_2$  environment is found to be the major contributor to the evolved gases with its highest absorbance intensity at high temperature zone. Evolution of CO continues with a distinctive increase after  $600^{\circ}C$  in  $CO_2$  environment. On the other hand, in  $N_2$  environment, negligible amount of CO is formed due to partial burning of combustible matter. In both environments,  $H_2O$  is identified in the first  $200^{\circ}C$  due to moisture release and in the temperature range of  $400$ - $600^{\circ}C$  as a consequence of coal oxidation reactions. Methane release starts at  $300^{\circ}C$  and continues up to the end of the pyrolysis tests with a maximum release around  $500^{\circ}C$ , in both environments. Similar trends are observed in evolution of  $CH_4$  during devolatilization. In pyrolysis of high sulphur content lignite,  $SO_2$  and COS release are noted. Similar  $SO_2$  formation profiles are obtained in both environments in the temperature range of  $250$  –  $625^{\circ}C$ , with two main peaks. Similar trends indicate that  $SO_2$  formation does not depend on the pyrolysis environment. COS formation is observed to increase significantly with the initiation of gasification reaction in  $CO_2$  environment. Higher CO concentration in pyrolysis environment leads to the formation of COS in  $CO_2$  atmosphere, in contrast to  $N_2$  atmosphere.



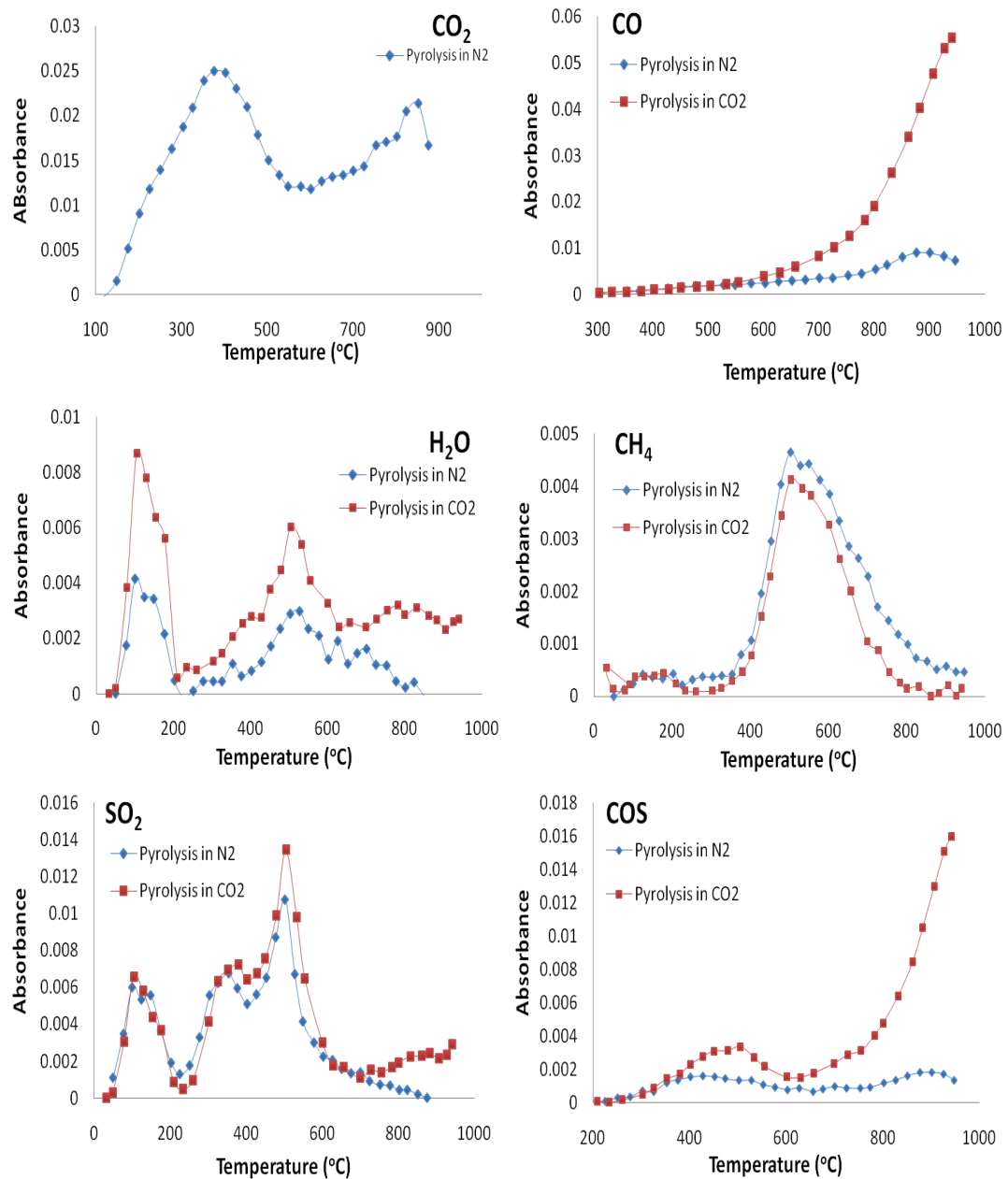


Figure 4.10: Formation profiles of evolved gases during pyrolysis tests of lignite I

#### 4.4.2 Combustion of Lignite I

Figure 4.11 compares TGA and DTG profiles of lignite I under different combustion environments.

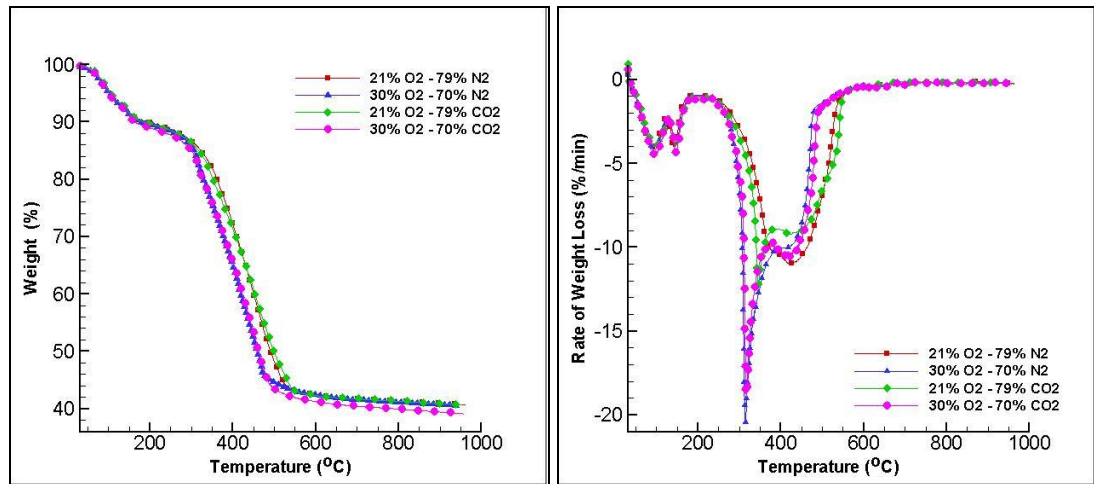


Figure 4.11: TGA and DTG profiles of lignite I in different combustion atmospheres

Comparison of TGA curves in Figure 4.11 indicates that the effect of oxygen concentration is more significant than that of the diluting gas ( $N_2$  or  $CO_2$ ) on the combustion profiles. While combustion in  $O_2/N_2$  and  $O_2/CO_2$  mixtures with identical oxygen concentrations results in only slight differences in combustion characteristics of lignite, elevated oxygen levels in combustion environment leads to shift in weight loss curves to lower temperatures. First step of the weight loss accounts for the moisture release in the first  $200^\circ C$  temperature range and the corresponding weight loss due to moisture release is found approximately 10 % for all cases. The second step represents the weight loss due to devolatilization and char burning. Total weight loss of samples is found to be almost the same in all combustion cases.

First peak within 200°C and the second peak within the temperature range 225-600°C represent moisture release and devolatilization and char burning, respectively in the DTG profiles of the lignite I samples. In air firing case, devolatilization and char burning steps are not discretely separated; however, the shoulder around 370°C can be attributed to volatile release. In oxy-fuel case the DTG profile of the lignite sample differs from the air-firing case with a small peak indicating the volatile matter release and a shoulder in 370-570°C temperature interval indicating char burning which takes place within the same temperature interval in both cases. In oxygen-enriched conditions (30 % O<sub>2</sub> – 70 % N<sub>2</sub> and 30 % O<sub>2</sub> – 70 % CO<sub>2</sub>) the DTG profiles are similar with distinct volatile release peaks and characteristic temperatures as shown in Table 4.6.

Table 4.6: Combustion Characteristics of Lignite I

	<b>21 % O<sub>2</sub>-79 % N<sub>2</sub></b>	<b>30 % O<sub>2</sub>-70 % N<sub>2</sub></b>	<b>21 % O<sub>2</sub>-79 % CO<sub>2</sub></b>	<b>30 % O<sub>2</sub>-70 % CO<sub>2</sub></b>
<b>T<sub>in</sub> (°C)</b>	224.0	226.1	225.8	202.8
<b>T<sub>max.-1</sub> (°C)</b>	-	314.5	347.1	317.2
<b>T<sub>max.-2</sub> (°C)</b>	426.2	-	-	-
<b>T<sub>b</sub> (°C)</b>	546.8	530.0	550.0	535.6
<b>(dm/dt)<sub>max.-1</sub> (%/min)</b>	-	20.5	12.3	19.0
<b>(dm/dt)<sub>max.-2</sub> (%/min)</b>	11.0	-	-	-
<b>T<sub>ig</sub> (°C)</b>	297.1	265.3	308.8	264.1
<b>Weight loss up to 950°C ( %)</b>	59.2	59.3	59.6	61.2

The similarity in DTG profiles obtained at the same oxygen concentration levels but with different diluting gas environments is an expected result. In TGA technique

combustion temperature of the sample is controlled by electrical heating and sample temperature is not affected by combustion environment. Therefore, different heat capacities of diluting gases in combustion environment has no significant effect on combustion in contrast to practical tests as also confirmed in other studies [29, 33, 36]. Slightly higher burnout temperature in the CO<sub>2</sub> environment is indicative of slightly delayed combustion. Effect of higher oxygen concentration on the combustion process is investigated with the tests under 30 % O<sub>2</sub> – 70 % N<sub>2</sub> and 30 % O<sub>2</sub> – 70 % CO<sub>2</sub> environments. Similar trends in the early stage of the process (up to 250°C) in both environments reveal that initiation of the combustion process is not affected by oxygen concentration level. However, at higher temperatures, more significant differences are displayed in DTG curves. In oxygen-enriched conditions, weight loss steps including volatile matter release and char burning are separately displayed in the DTG profile. In oxygen-enriched conditions, a sharper peak that is observed in 250 – 400°C temperature interval with a weight loss of 24 %, is attributed to volatile matter release since weight loss value is in accordance with the one determined in pyrolysis conditions. Sharper peak is observed to continue with a distinctive shoulder up to 500°C as represented in Figure 4.11. In some studies, it was demonstrated that the force of the fusion layer around solid particles is reduced by the presence of oxygen [60, 62]. This situation also results in faster release of volatiles depending on the nature of solid particles and experimental conditions. High volatile matter content of lignite and the ease with which it is released, result in the formation of a sharper preliminary peak previously observed in low rank coals [14]. The shoulder following the peak is considered to account for weight loss due to burning of char in the sample. Increase in the oxygen concentration causes a shift of the burning profile to the lower temperature zone. Effect of oxygen concentration on characteristic temperatures is very clear. Characteristic temperatures including T<sub>ig</sub>, T<sub>max</sub> and T<sub>b</sub> are found to be lower in oxygen-enriched conditions. Moreover, at higher O<sub>2</sub> concentrations complete combustion is achieved at lower temperatures and shorter times.

Figure 4.12 displays formation profiles of gases evolved in different combustion environments. The major contributor to the evolved gases is found to be CO<sub>2</sub> with its higher absorbance intensity as also observed in combustion of other fuels. The formation profile of CO<sub>2</sub> in oxygen-enriched air atmosphere shifts to lower temperature zone as elevated oxygen levels lead to faster burning and earlier release of CO<sub>2</sub>. CO formation profiles display similar trends in identical oxygen concentration levels while increase in oxygen level results in lower peak temperature. H<sub>2</sub>O formation profiles show that moisture is released first in all combustion environments with further release in the temperature range of 200°C to 550°C. Methane evolution mainly takes place in the temperature range of 250-550°C. In oxygen-enriched conditions, maximum release is observed around 350°C, which corresponds to the peak in DTG profile of volatile matter. In the case of sulphur containing gases, SO<sub>2</sub> and COS appear in the FTIR spectra. Trend of SO<sub>2</sub> evolution in FTIR spectra are found to be in accordance with the DTG curves. SO<sub>2</sub> release starts around 200°C and displays different formation profiles depending on the combustion environment. Maximum release takes place at about 500°C in air- and oxy-firing cases and 350°C in oxygen-enriched firing conditions. COS formation is observed in all combustion tests in the temperature range of 200-550°C with sharper peaks in oxygen-enriched conditions.

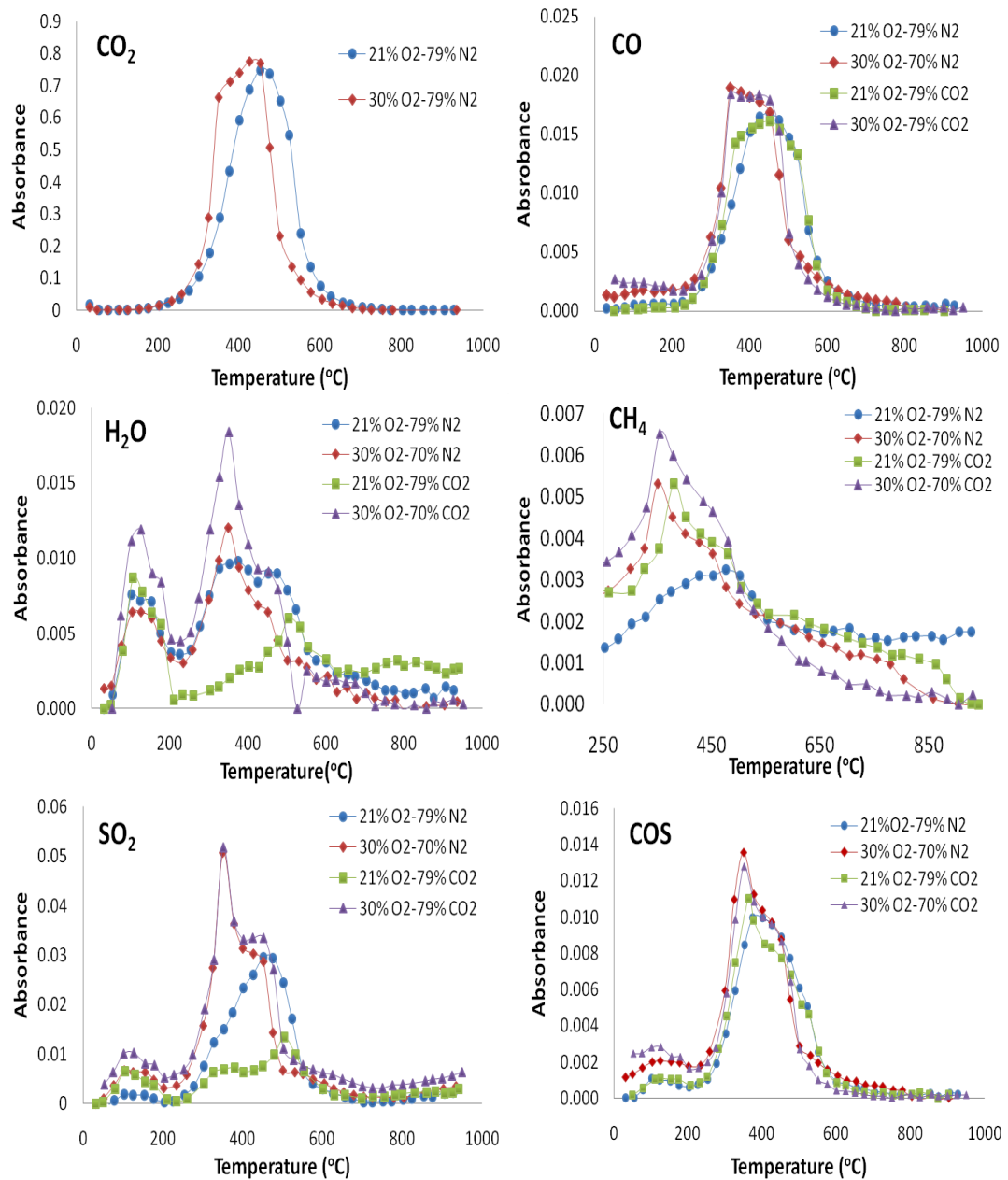


Figure 4.12: Formation profiles of evolved gases during combustion tests of lignite I

## 4.5 Lignite II

Lignite II is mainly characterized by its high moisture content, low calorific value and high CaO content in its ash.

### 4.5.1 Pyrolysis of Lignite II

TGA and DTG profiles of pyrolysis tests under  $N_2$  and  $CO_2$  atmospheres are shown in Figure 4.13. The pyrolysis characteristics of lignite II determined from these profiles are summarized in Table 4.7.

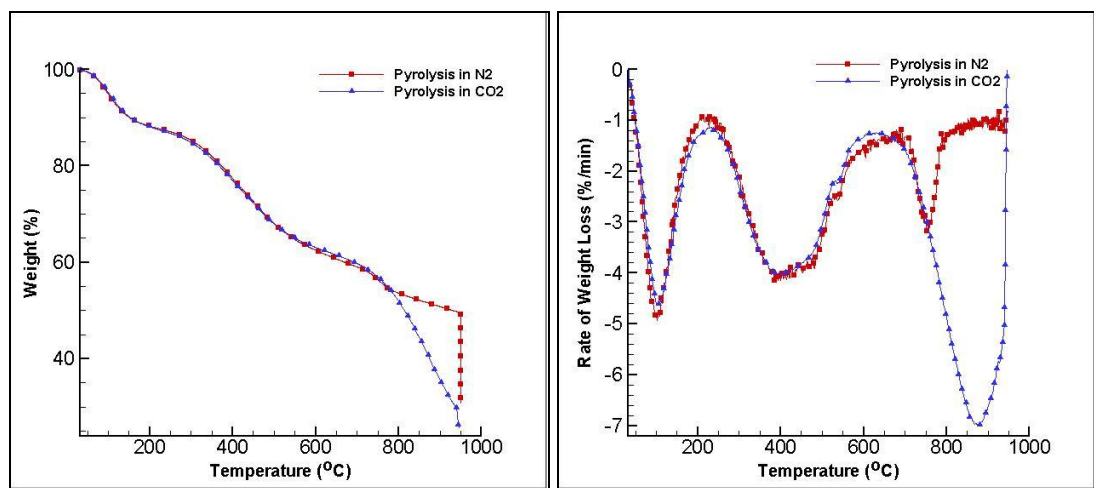


Figure 4.13: TGA and DTG profiles of lignite II in  $N_2$  and  $CO_2$  atmospheres

Pyrolysis results of lignite II samples show that weight loss profiles are almost the same up to a temperature of  $720^{\circ}C$  in  $N_2$  and  $CO_2$  environments, indicating that  $CO_2$  behaves as an inert gas in this temperature range as also observed in pyrolysis of other fuels. After moisture release in the first  $200^{\circ}C$  temperature zone, pyrolysis continues with the release of volatile matter content in the range of  $200-750^{\circ}C$ . In

700-950°C temperature range, additional peaks are displayed in pyrolysis profiles. A small peak appears after 700°C which is attributed to calcite decomposition in N<sub>2</sub> atmosphere. The sharp peak observed in CO<sub>2</sub> environment is considered to be due to char-CO<sub>2</sub> gasification reaction.

Table 4.7: Pyrolysis Characteristics of Lignite II

	Pyrolysis in N <sub>2</sub>	Pyrolysis in CO <sub>2</sub>
<b>T<sub>in</sub> (°C)</b>	241.6	232.6
<b>T<sub>max.-1</sub> (°C)</b>	400.0	398.3
<b>T<sub>max.-2</sub> (°C)</b>	757.0	878.6
<b>(dm/dt)<sub>max.-1</sub> (%/min)</b>	4.1	4.0
<b>(dm/dt)<sub>max.-2</sub> (%/min)</b>	3.1	7.0
<b>Weight loss up to 950°C (%)</b>	50.2	70.2

Formation profiles of the evolved gases during pyrolysis tests are represented in Figure 4.14. CO formation initiates at around 200°C and takes place during the entire devolatilization process with two main peaks at 400°C and 800°C in N<sub>2</sub> environment. The peak displayed at 800°C demonstrates the release of CO<sub>2</sub> due to calcite decomposition reactions. Significant increase is observed in CO and COS formation after 700°C in CO<sub>2</sub> environment because of char-CO<sub>2</sub> gasification reactions. Sharp peaks in the first 200°C temperature zone in H<sub>2</sub>O formation profiles represent water vapour release from high moisture content lignite II. Similar trends are displayed in methane evolution which takes place between 300-800°C in both environments. SO<sub>2</sub> formation is observed to reach its maximum value at 600°C and takes place during the entire devolatilization process.



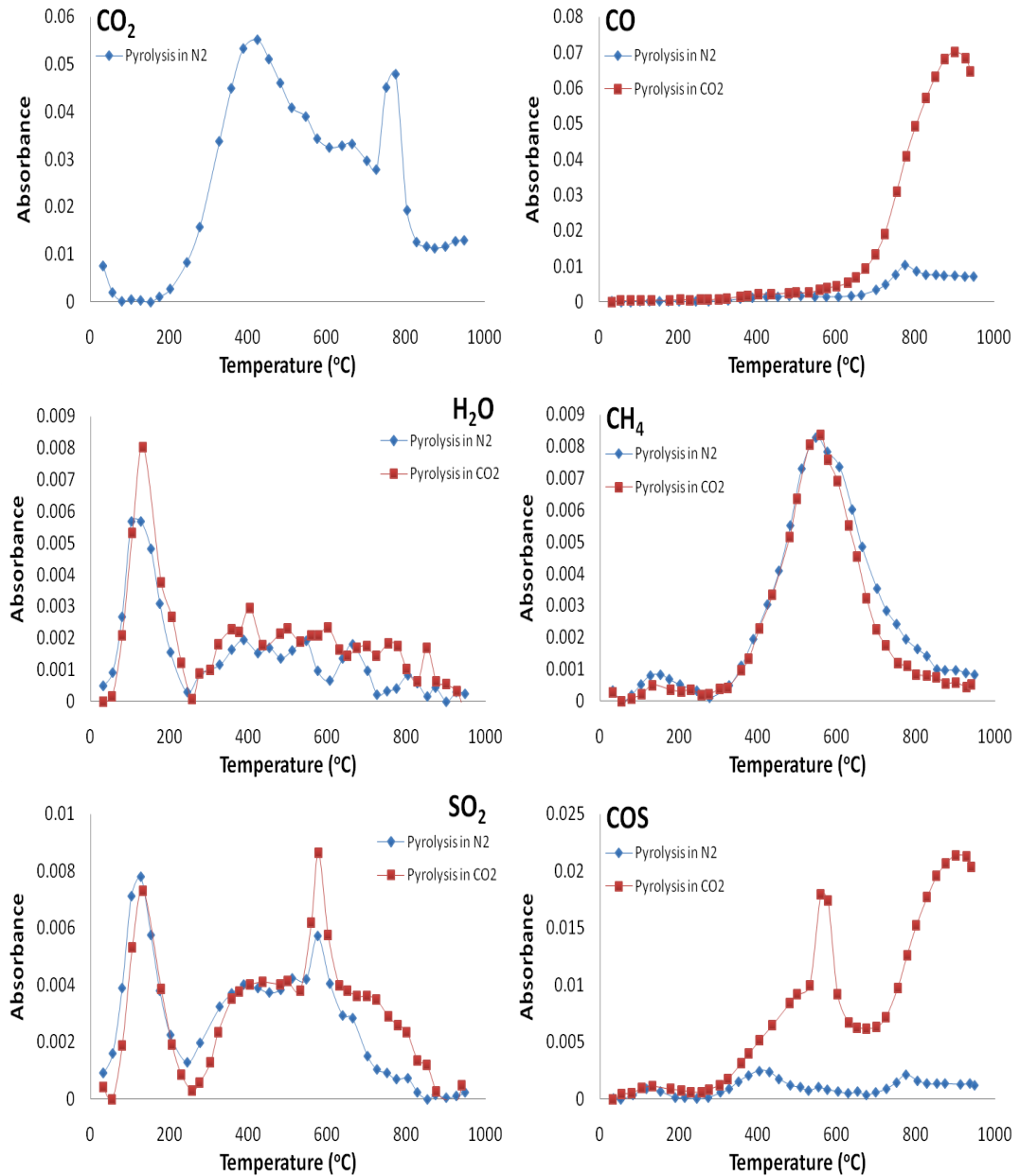


Figure 4.14: Formation profiles of evolved gases during pyrolysis tests of lignite II

#### 4.5.2 Combustion of Lignite II

Figure 4.15 compares TGA and DTG profiles of lignite II in different combustion atmospheres. Combustion characteristics of lignite II is represented in Table 4.8.

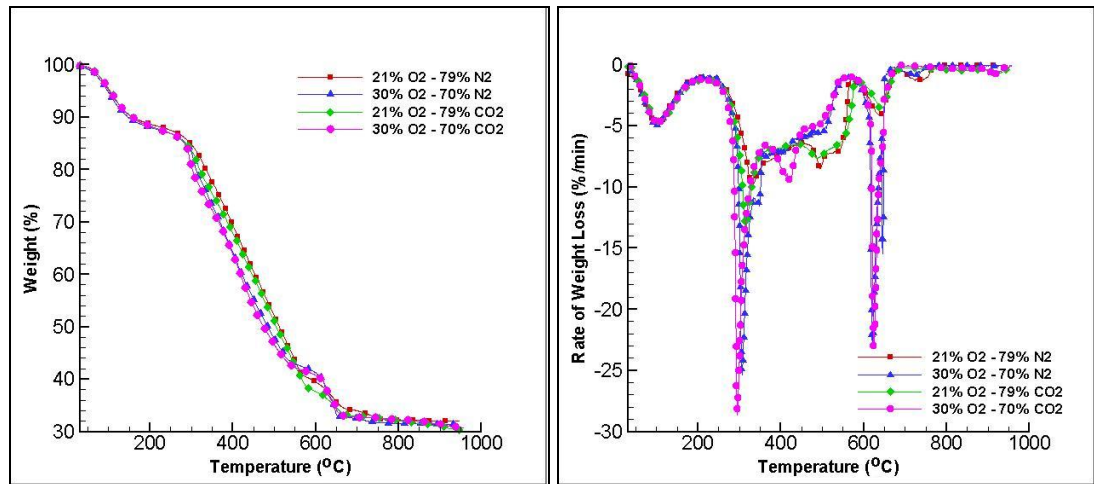


Figure 4.15: TGA and DTG profiles of lignite II in different combustion atmospheres

Comparison of TGA curves reveals that similar behaviours are observed in weight loss profiles in identical oxygen concentration conditions. In oxygen-enriched conditions TGA profiles shift to slightly lower temperatures as higher oxygen levels leads to easier and faster burning. Effect of oxygen concentration on combustion is more clearly displayed in DTG curves in Figure 4.15. Four different peaks are represented in the DTG profiles of lignite II samples. First peaks within 200°C represent moisture release whereas other peaks within the temperature range 225-600°C show devolatilization and char burning steps respectively, for all cases. High volatile matter content of lignite and the ease with its release result in the formation of two distinctive peaks in DTG profiles, representing devolatilization and char burning steps, which is widely observed in low rank coals.

The last peak is considered to account for calcite decomposition. Replacing N<sub>2</sub> by CO<sub>2</sub> in combustion environment causes slight delay, lower maximum rate of weight loss in char combustion zone and higher burnout temperature (Table 4.8) in combustion of lignite II. As O<sub>2</sub> concentration increases, profiles shift to lower temperatures, peak and burnout temperatures decrease, weight loss rate increases and complete combustion is achieved at lower temperatures and shorter times.

Table 4.8: Combustion Characteristics of Lignite II

	21 % O <sub>2</sub> -79 % N <sub>2</sub>	30 % O <sub>2</sub> - 70 % N <sub>2</sub>	21 % O <sub>2</sub> -79 % CO <sub>2</sub>	30 % O <sub>2</sub> -70 % CO <sub>2</sub>
<b>T<sub>in</sub> (°C)</b>	217.3	218.2	219.8	223.7
<b>T<sub>max.-1</sub> (°C)</b>	330.9	306.2	315.3	294.8
<b>T<sub>max.- 2</sub> (°C)</b>	495.5	374.6	488.0	424.0
<b>T<sub>max.- 3</sub> (°C)</b>	639.6	621.5	644.0	623.6
<b>T<sub>b</sub> (°C)</b>	668.9	652.7	671.0	664.0
<b>(dm/dt)<sub>max.-1</sub> (%/min)</b>	9.8	25.5	13.4	28.7
<b>(dm/dt)<sub>max.- 2</sub> (%/min)</b>	8.6	11.5	7.7	9.4
<b>(dm/dt)<sub>max.- 3</sub> (%/min)</b>	4.2	22.9	3.5	23.0
<b>T<sub>ig</sub> (°C)</b>	284.5	256.6	262.7	263.3
<b>Weight loss up to 950°C ( %)</b>	67.9	68.5	69.8	69.2

Figure 4.16 compares evolution trends of the gases identified in combustion tests of lignite II. Three main steps are displayed in CO<sub>2</sub> formation profiles in O<sub>2</sub>/N<sub>2</sub> mixtures, which correspond to CO<sub>2</sub> release due to volatile matter release, char burning and calcite decomposition. Different CO evolution profiles are observed in

all combustion cases. CO evolution takes place between 200-600°C and 600-800°C in two stages. Methane gas is identified in the temperature range of 300-600°C and similar trends are obtained in its formation profiles when oxygen concentration is identical in combustion environment. Two peaks are represented in SO<sub>2</sub> profiles in all conditions. However, additional peaks are observed at around 650°C in oxygen-enriched conditions. Certain amount of COS is evolved between 300-600°C in all combustion conditions.

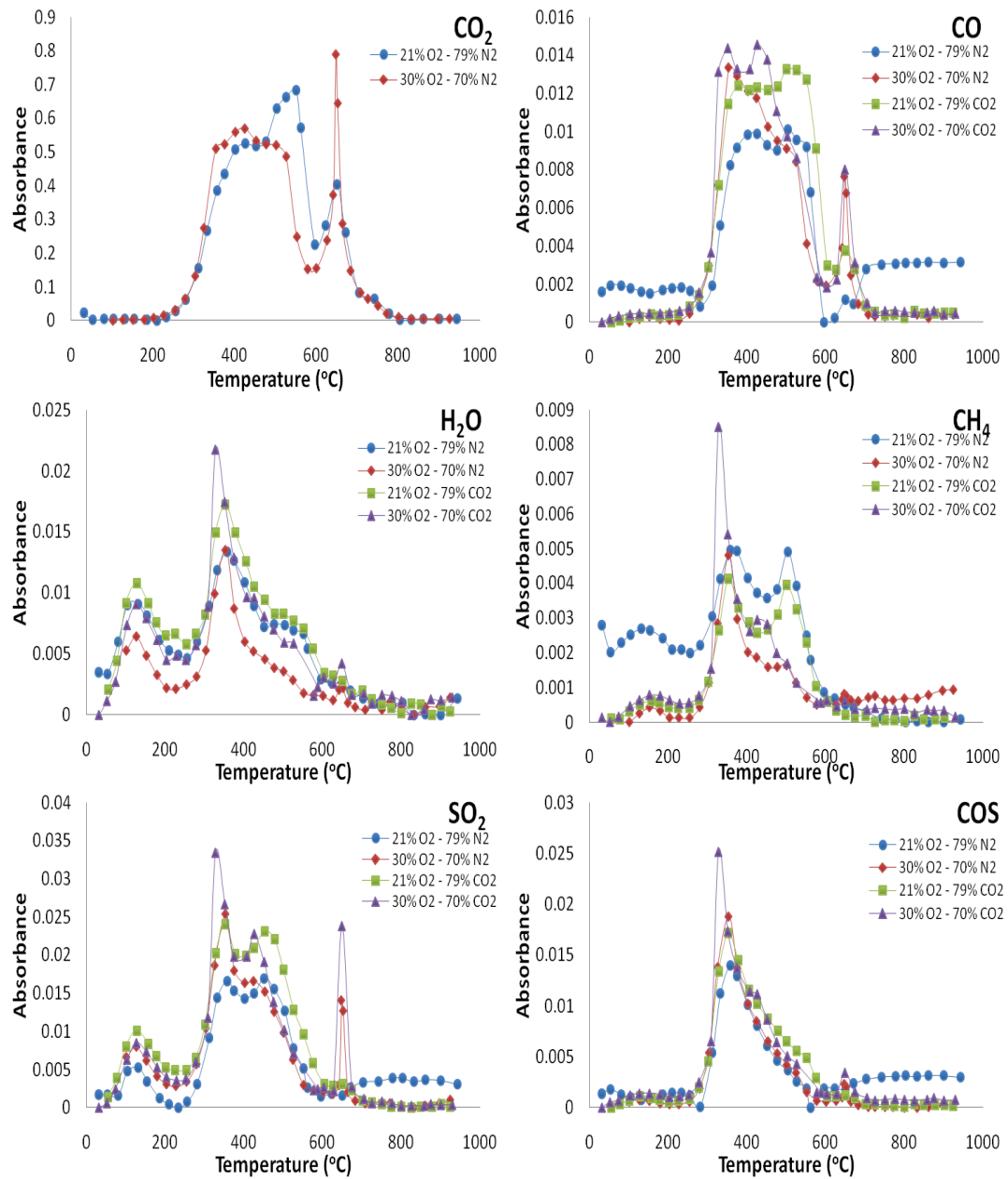


Figure 4.16: Formation profiles of evolved gases during combustion tests of lignite II

## 4.6 Olive Residue

Olive residue is the remaining part of olive after milling and extraction of the olive oil, which is a specific type of biomass from olive oil production process. It contains significant amount of oxygen and volatile matter, low moisture and ash content.

### 4.6.1 Pyrolysis of Olive Residue

TGA and DTG curves obtained in pyrolysis tests of olive residue are shown in Figure 4.17.

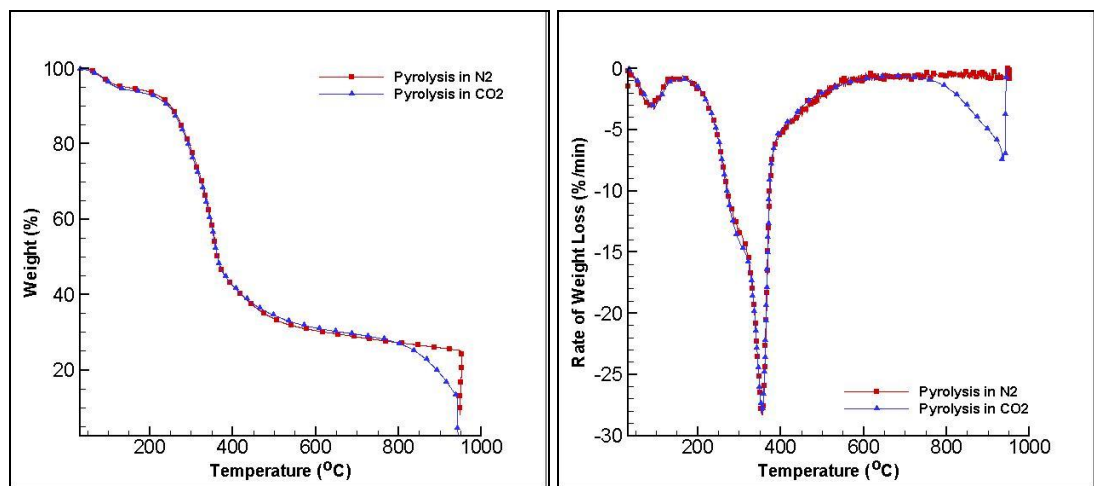


Figure 4.17: TGA and DTG profiles of olive residue in N<sub>2</sub> and CO<sub>2</sub> atmospheres

As can also be seen from Figure 4.17 and Table 4.9, pyrolysis of olive residue starts at around 180°C and continues with a shoulder at around 250°C representing decomposition of hemicellulose and a peak at around 350°C accounting for the decomposition of cellulose. Above 400°C, the weight loss continues at a slower rate, which corresponds to the slow degradation of lignin. Lignite, on the other hand, starts devolatilization at a slightly higher temperature (220°C) and weight loss

continues with a peak around 500°C. Two main weight loss steps are displayed in DTG profiles in nitrogen atmosphere while an additional weight loss step appears after 700°C in CO<sub>2</sub> environment. First weight loss step within 25-200°C temperature range demonstrates moisture release and the second weight loss step within 200-600°C is due to volatile matter release in both atmospheres. Additional peak after 700°C seen in DTG curve under CO<sub>2</sub> atmosphere is considered to be due to CO<sub>2</sub> – char gasification reaction.

Table 4.9: Pyrolysis Characteristics of Olive Residue

	Pyrolysis in N <sub>2</sub>	Pyrolysis in CO <sub>2</sub>
<b>T<sub>in</sub> (°C)</b>	183.1	175.6
<b>T<sub>max.-1</sub> (°C)</b>	355.5	354.9
<b>T<sub>max.-2</sub> (°C)</b>	-	934.4
<b>(dm/dt)<sub>max.-1</sub> ( %/min)</b>	28.4	28.3
<b>(dm/dt)<sub>max.-2</sub> ( %/min)</b>	-	7.5
<b>Total weight loss up to 950°C ( %)</b>	75.0	87.0

Formation profiles of the evolved gases during pyrolysis tests of olive residue are reported in Figure 4.18 . CO<sub>2</sub> formation initiates at around 200°C and continues up to 600°C. CO formation primarily identified at 400°C; however, significant increase is observed in high temperature zone due to gasification reaction in CO<sub>2</sub> environment. Water vapour is evolved between mainly at around 400°C in the temperature range of 200-600°C after moisture release. Two main peaks are displayed in the formation profile of methane at around 300°C and 600°C. SO<sub>2</sub> formation reaches to its maximum value at 400°C and similar evolution trends are observed in both pyrolysis environments. COS formation takes place in a relation with CO formation and is observed to increase after 800°C in CO<sub>2</sub> environment due to the effect of gasification.

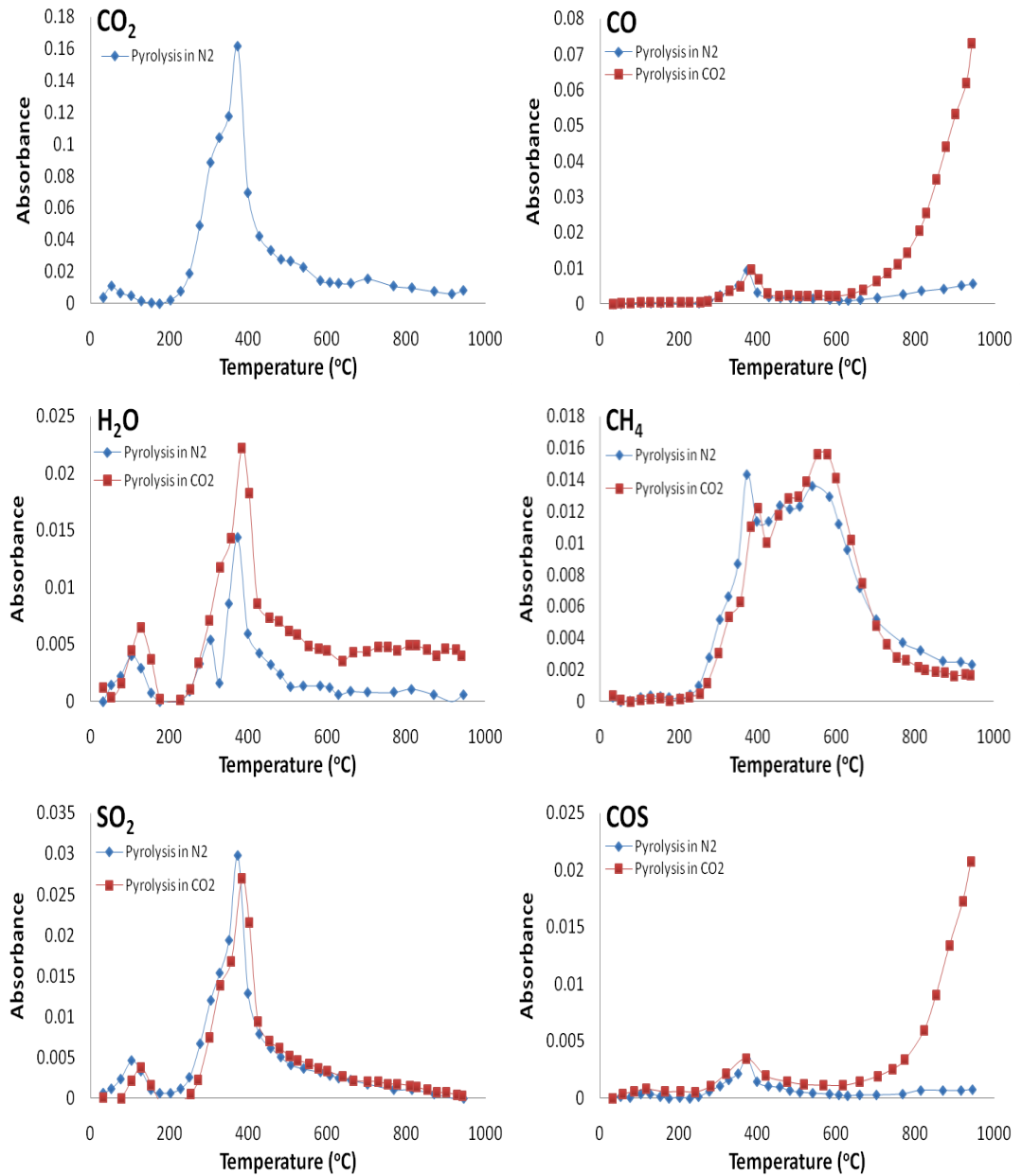


Figure 4.18: Formation profiles of evolved gases during pyrolysis tests of olive residue



#### 4.6.2 Combustion of Olive Residue

Figure 4.19 compares TGA and DTG profiles of olive residue under different combustion environments.

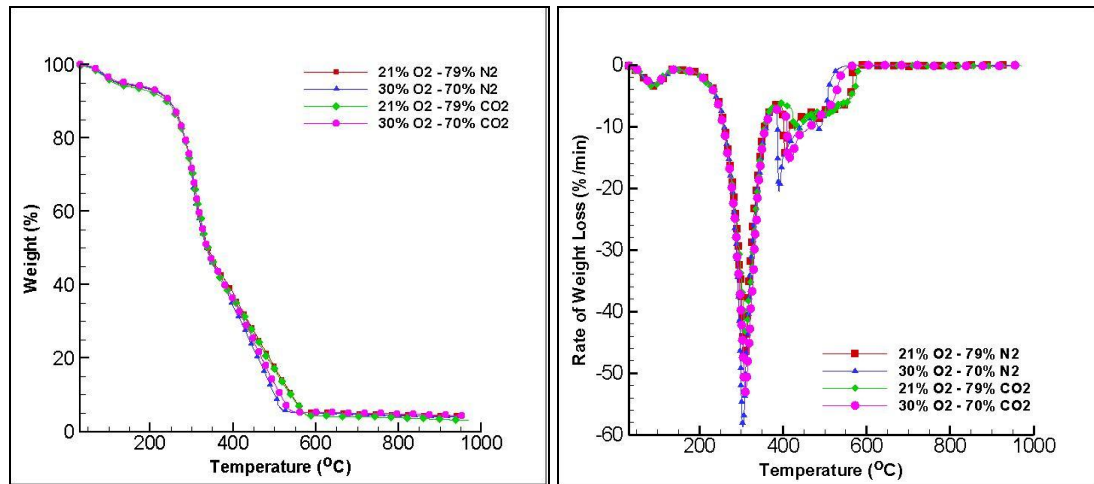


Figure 4.19: TGA and DTG profiles of olive residue in different combustion atmospheres

In the case of olive residue, thermal and oxidative degradation takes place in two stages in all combustion environments. In the first stage the main weight loss occurs within the temperature range 180-360°C. This region corresponds to devolatilization of hemicellulose and cellulose components and their subsequent ignition. The second stage weight loss is associated with char combustion within the temperature range 360-600°C. These findings are in agreement with those in the open literature [11, 63-65]

Table 4.10 displays combustion characteristics of olive residue. As can be seen from the table initial temperature of olive residue is not affected by combustion environment and is around 180°C in all combustion environments. Moreover, similar to initial decomposition temperature, main peak of volatile matter release

appears at around 310°C in all combustion environments. Rate of weight loss, on the other hand, is observed to vary with combustion environment. Increase in oxygen concentration results in higher maximum weight loss rates irrespective of the combustion environment while presence of CO<sub>2</sub> as diluting gas in combustion environment leads to decrease in peak height due to its higher heat capacity. Elevated oxygen level leads to a shift in char combustion peak to lower temperature zone with increase in its weight loss rate. However, higher char combustion peak and burnout temperatures in oxy-fuel conditions are indicative of delayed combustion due to the existence of CO<sub>2</sub> in the combustion environment.

Table 4.10: Combustion Characteristics of Olive Residue

	21 % O <sub>2</sub> -79 % N <sub>2</sub>	30 % O <sub>2</sub> -70 % N <sub>2</sub>	21 % O <sub>2</sub> -79 % CO <sub>2</sub>	30 % O <sub>2</sub> -70 % CO <sub>2</sub>
<b>T<sub>in</sub> (°C)</b>	183.9	186.9	174.6	179.8
<b>T<sub>max.-1</sub> (°C)</b>	308.9	304.3	309.7	311.2
<b>T<sub>max.-2</sub> (°C)</b>	405.3	390.9	435.8	413.2
<b>T<sub>b</sub> (°C)</b>	567.7	526.6	579.9	544.3
<b>(dm/dt)<sub>max.-1</sub> (%/min)</b>	48.4	58.9	43.7	53.2
<b>(dm/dt)<sub>max.-2</sub> (%/min)</b>	14.4	20.5	10.6	15.9
<b>T<sub>ig</sub> (°C)</b>	258.8	258.5	229.5	264.1
<b>Weight loss up to 950 ( %)</b>	95.6	95.8	96.9	95.7

FTIR analysis results of the combustion tests are shown in Figure 4.20. Two main steps are displayed in the formation profiles of CO<sub>2</sub> gas, representing the volatile matter and char combustion steps, respectively. CO and H<sub>2</sub>O formation take place in the temperature range of 200-600°C. Similar trends are observed in the formation

of these gases in all combustion environments. Methane evolution profile displays two stages; one around 300°C and the other 450°C, under all combustion conditions. SO<sub>2</sub> and COS formation take place during entire combustion process with a maximum release at around 300°C and their formation profile display similar trends in all cases.

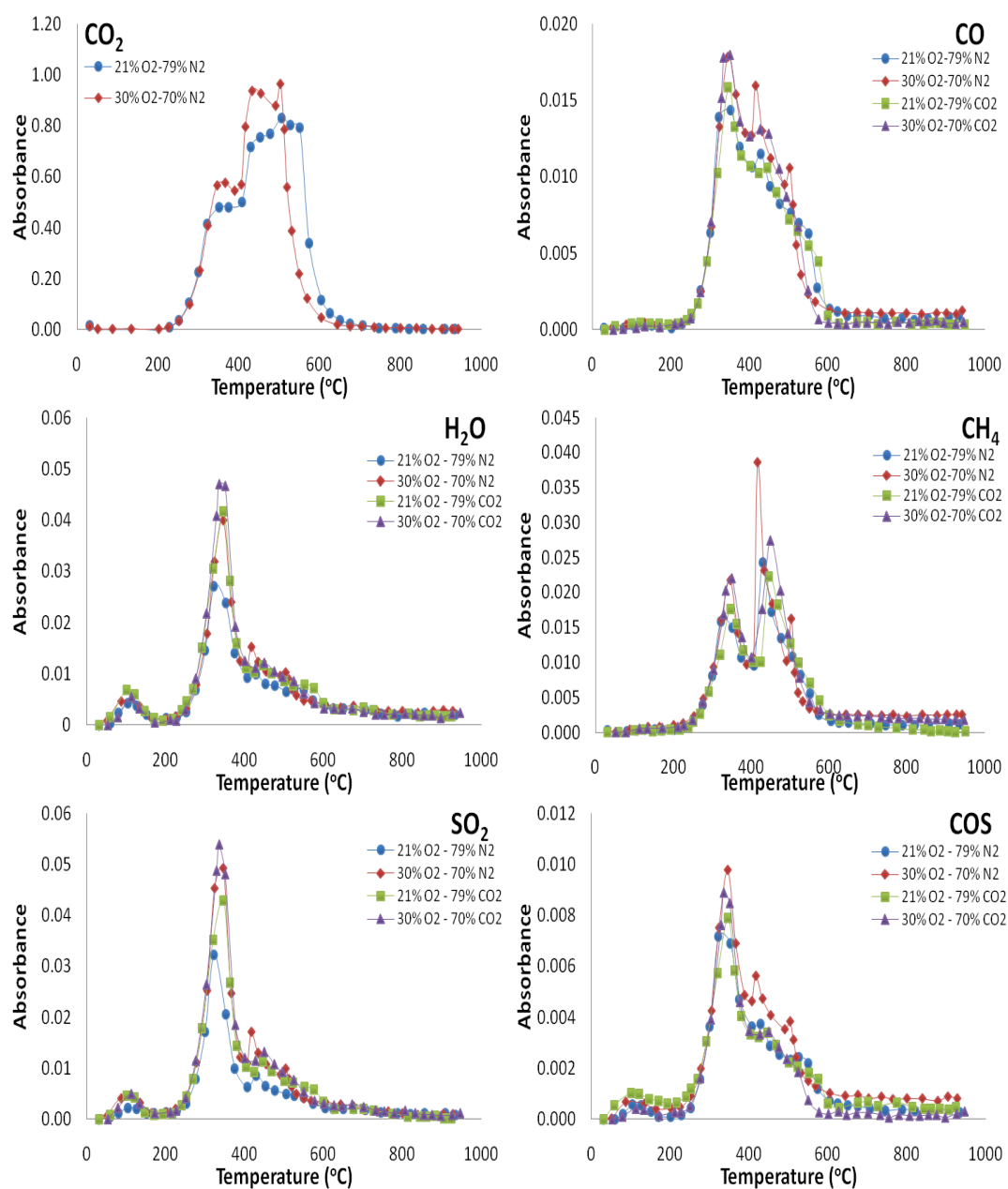


Figure 4.20: Formation profiles of evolved gases during combustion tests of olive residue

#### 4.7 Imported Coal – Petroleum Coke – Lignite I Blend (Blend I)

Blend I was prepared by mixing high rank imported coal, low rank lignite I and petcoke in the proportion of 60:30:10.

##### 4.7.1 Pyrolysis of Blend I

Pyrolysis profiles of the blend samples in N<sub>2</sub> and CO<sub>2</sub> conditions are shown in Figure 4.21. The pyrolysis characteristics of the blend and its parent fuels are summarized in Table 4.11.

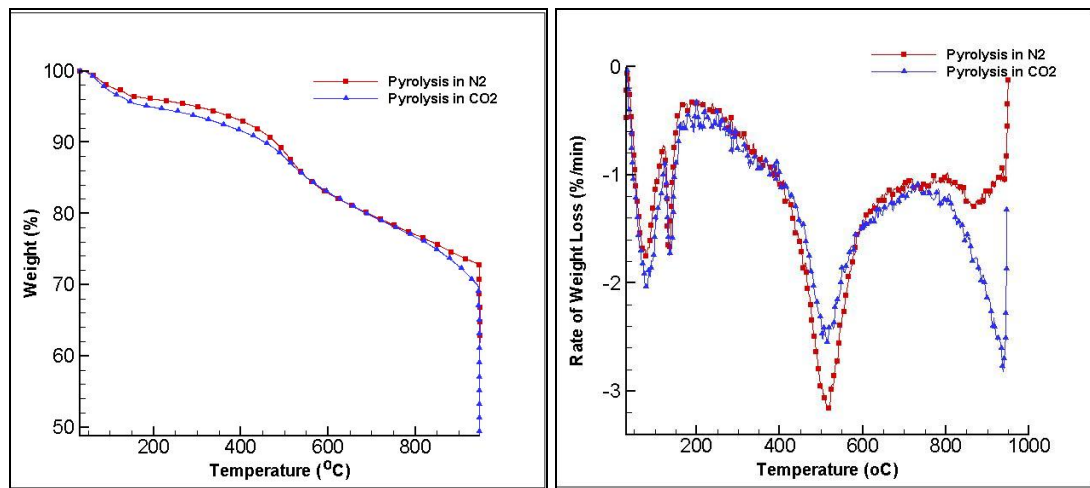


Figure 4.21: TGA and DTG profiles of Blend I in N<sub>2</sub> and CO<sub>2</sub> atmospheres

Two main weight loss steps are displayed in weight loss profiles of blend I in nitrogen atmosphere while further weight loss step appears after 700°C in CO<sub>2</sub> environment. Moisture is released within 25-200°C temperature range in both conditions. Second weight loss step represents devolatilization within 200-600°C. Similar trends are obtained in both pyrolysis tests, however, in CO<sub>2</sub> atmosphere, the weight loss rate is found to be lower than the one in N<sub>2</sub> atmosphere which is due to the effect of higher heat capacity of CO<sub>2</sub> (Table 4.11). Additional peak after 700°C

seen in DTG curve under CO<sub>2</sub> atmosphere is considered to be due to CO<sub>2</sub> – char gasification reaction.

Table 4.11: Pyrolysis characteristics of blend I and its parent fuels

		$T_{in}$	$T_{max}$	$(dm/dt)_{max}$	Weight loss up to 950°C
Imported Coal	Pyrolysis in N <sub>2</sub>	465.2	517.0	2.0	21.1
	Pyrolysis in CO <sub>2</sub>	463.9	528.4	2.0	23.2
Petcoke	Pyrolysis in N <sub>2</sub>	514.9	582.3	1.4	14.4
	Pyrolysis in CO <sub>2</sub>	570.9	638.7	1.3	17.0
Lignite I	Pyrolysis in N <sub>2</sub>	230.8	482.9	3.6	41.0
	Pyrolysis in CO <sub>2</sub>	216.7	481.0	3.16	50.3
Blend Exp.	Pyrolysis in N <sub>2</sub>	389.6	512.5	3.1	27.1
	Pyrolysis in CO <sub>2</sub>	392.3	512.1	2.4	30.0
Blend Theo.	Pyrolysis in N <sub>2</sub>	405.4	500.1	2.1	26.5
	Pyrolysis in CO <sub>2</sub>	409.2	532.2	2.0	30.3

Pyrolysis behaviours of blend I and its parent fuels under N<sub>2</sub> and CO<sub>2</sub> environments and the theoretical pyrolysis behaviour of the blend calculated by using additive rule are compared in Figure 4.22.

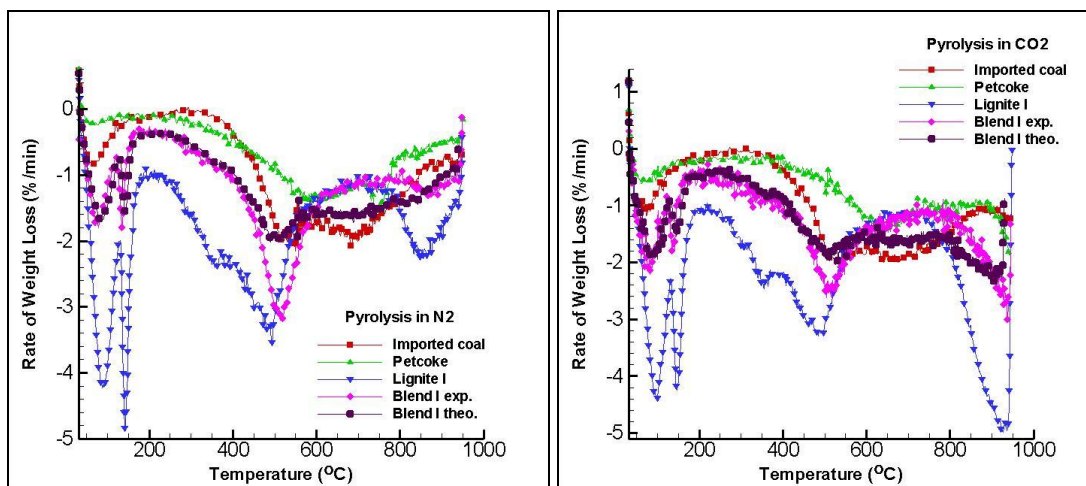


Figure 4.22: Pyrolysis profiles of blend I and its parent fuels in  $N_2$  and  $CO_2$  environments

As can be seen in Figure 4.22 lignite I devolatilizes at lower temperatures with higher weight loss rate due to its high volatile matter content compared to imported coal and petcoke. Overall comparison of DTG curves reveals that experimental curve of blend I reveals close resemblance with lignite I as lignite dominates pyrolysis behaviour of the blend with its significantly higher volatile matter content. Pyrolysis behaviour of blend I shows that peak height decreases and the peak position shifts to higher temperatures with the addition of imported coal and petcoke. Theoretical blend I curve displays some deviations from experimental behaviour. Each devolatilization steps of imported coal, petcoke and lignite appears in theoretical curve of blend with lower weight loss rate in both pyrolysis conditions. This is considered to be due to interactions (synergy) between parent fuels during pyrolysis process [49, 54, 66].

The evolution profiles of the gaseous species including  $CO_2$ ,  $CO$ ,  $H_2O$ ,  $CH_4$ ,  $SO_2$  and  $COS$ , from the pyrolysis of blend I in nitrogen and carbon dioxide are shown in

Figure 4.23. In the formation profile of  $CO_2$ , three peaks are displayed at around 400, 550 and 750°C during pyrolysis in  $N_2$  atmosphere. The first peak represents  $CO_2$  release due to devolatilization of lignite component while second one may account

for volatile matter release of imported coal and petcoke together. The last peak shows  $\text{CO}_2$  release as a consequence of calcite decomposition of petcoke component at high temperature zone. In both environments,  $\text{H}_2\text{O}$  is identified in the first  $200^\circ\text{C}$  due to moisture release. Methane formation takes place between  $400\text{--}800^\circ\text{C}$ . Certain amount of  $\text{SO}_2$  is also formed as a result of the high sulphur content of lignite and petcoke in the blend at around  $350^\circ\text{C}$  and  $500^\circ\text{C}$  with similar trends in both pyrolysis conditions. After  $700^\circ\text{C}$ , distinctive increase is observed in CO and COS formation profiles in  $\text{CO}_2$  atmosphere due to  $\text{CO}_2$  – char gasification reaction.



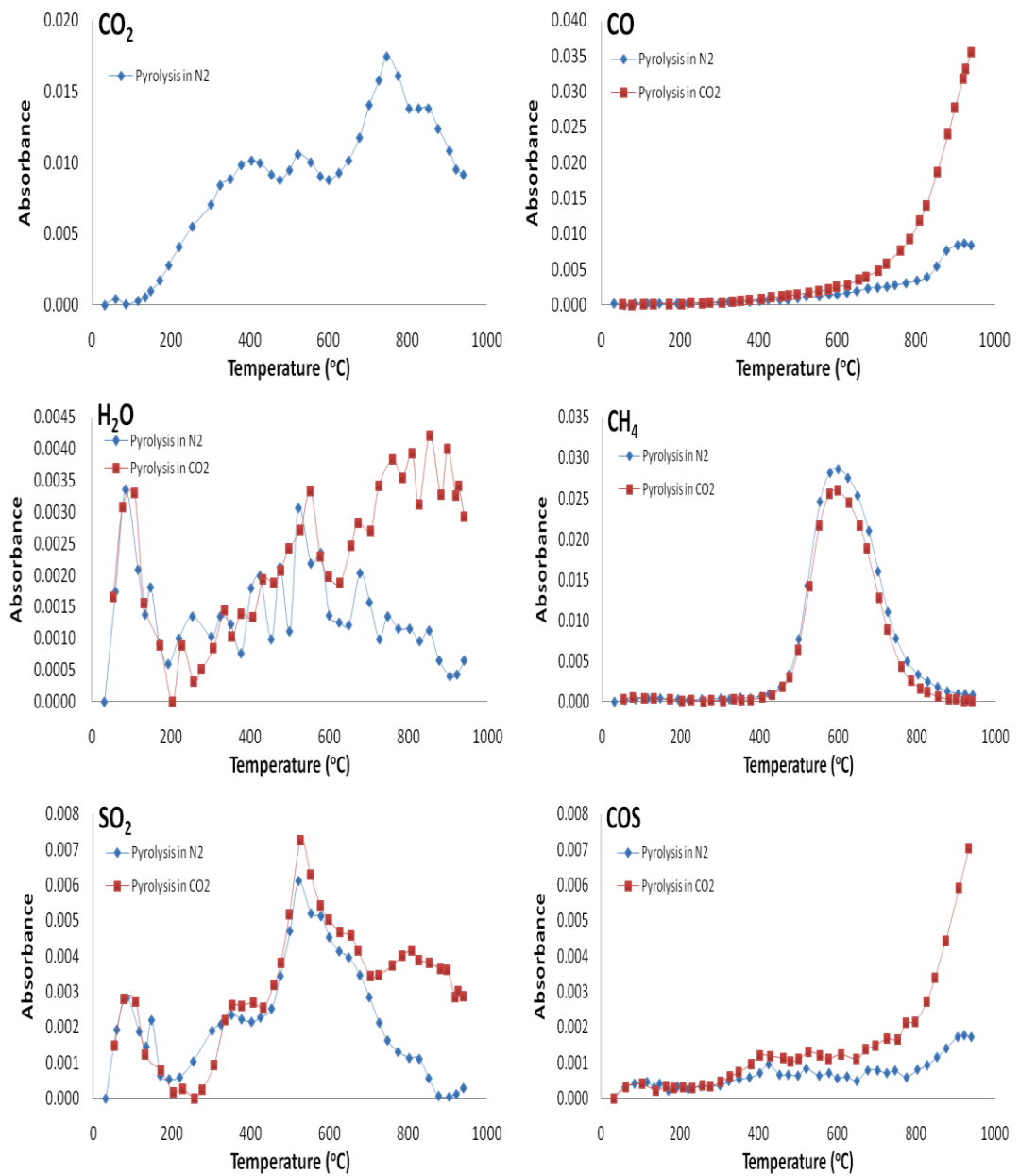


Figure 4.23: Formation profiles of evolved gases during pyrolysis tests of blend I

#### 4.7.2 Combustion of Blend I

Combustion profiles of the imported coal-petcoke-lignite I blend in different combustion environments are given in Figure 4.24. Combustion characteristics of the fuel samples are summarized in Table 4.12.

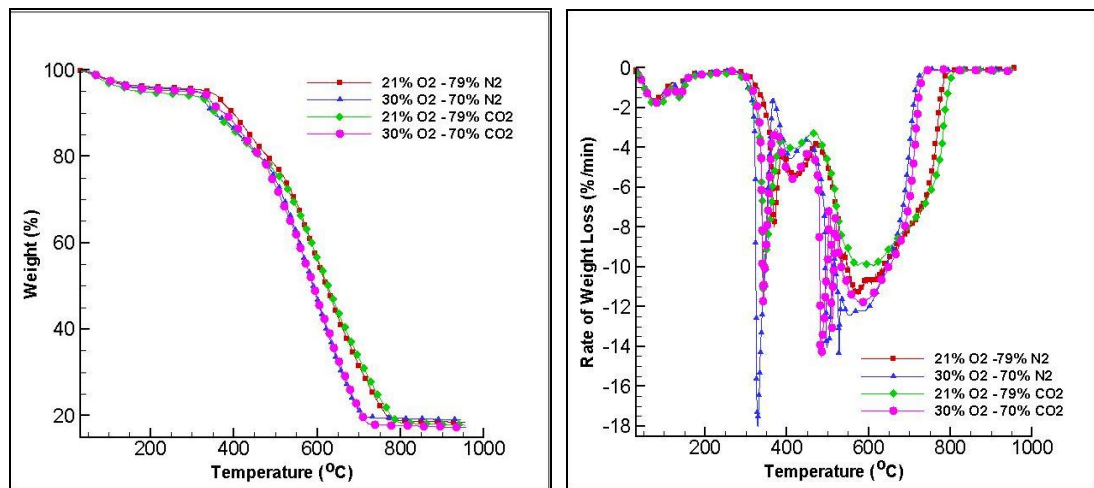


Figure 4.24: TGA and DTG profiles of blend I in different combustion atmospheres

In air and oxy-fuel cases, after moisture release in the first 200°C temperature zone, three weight loss steps are displayed in weight loss curves. The first two steps account for combustion of highly reactive lignite component in the temperature range of 300-450°C. In this interval, volatile matter and char combustion steps of lignite I are discretely separated. The main peak between 450-700°C is attributed to combustion of imported coal and petcoke in both conditions. In this temperature interval, rate of weight loss is lower, peak and burnout temperatures are higher in oxy-fuel conditions as higher heat capacity CO<sub>2</sub> leads to delay in combustion. The effect of oxygen concentration is found to be more significant than that of the diluting gas (N<sub>2</sub> or CO<sub>2</sub>) on the combustion profiles. At elevated oxygen levels, weight loss rates increases and characteristic temperatures including  $T_{ig}$ ,  $T_{max}$  and  $T_b$

decrease. In oxygen-enriched conditions, additional peaks appear in the main combustion peak of imported coal and lignite between 400-700°C. These additional peaks demonstrate burning of volatiles in imported coal and petcoke as volatile matter and char burning steps are separated due to the effect of oxygen concentration.

Table 4.12: Combustion characteristics of blend I and its parent fuels

		$T_{in}$	$T_{max}$			$(dm/dt)_{max}$			$T_{ig}$	$T_b$	Total weight loss up to 950°C
Imported Coal	21 % O <sub>2</sub> - 79 % N <sub>2</sub>	387.4	618.3	-	-	13.3	-	-	446.6	848.4	89.1
	30 % O <sub>2</sub> - 70 % N <sub>2</sub>	376.7	594.9	-	-	16.1	-	-	422.0	745.0	89.2
	21 % O <sub>2</sub> - 79 % CO <sub>2</sub>	387.0	629.2	-	-	11.8	-	-	393.0	885.1	93.3
	30 % O <sub>2</sub> - 70 % CO <sub>2</sub>	371.4	591.1	-	-	15.0	-	-	420.3	752.0	90.3
Petcoke	21 % O <sub>2</sub> - 79 % N <sub>2</sub>	400.1	589.0	-	-	14.0	-	-	469.5	867.0	96.8
	30 % O <sub>2</sub> - 70 % N <sub>2</sub>	381.6	562.2	-	-	16.8	-	-	439.7	735.6	95.9
	21 % O <sub>2</sub> - 79 % CO <sub>2</sub>	398.7	587.6	-	-	12.4	-	-	465.4	923.7	96.7
	30 % O <sub>2</sub> - 70 % CO <sub>2</sub>	379.5	572.6	-	-	15.5	-	-	434.7	761.8	97.9
Lignite I	21 % O <sub>2</sub> - 79 % N <sub>2</sub>	224.0	-	426.2	-	-	11.0	-	297.1	546.7	59.2
	30 % O <sub>2</sub> - 70 % N <sub>2</sub>	226.1	314.5	-	-	20.5	-	-	265.3	530.0	59.3
	21 % O <sub>2</sub> - 79 % CO <sub>2</sub>	225.8	347.1	-	-	12.3	-	-	308.8	550.0	59.6
	30 % O <sub>2</sub> - 70 % CO <sub>2</sub>	202.8	317.2	-	-	19.0	-	-	264.1	535.6	61.2
Blend Exp.	21 % O <sub>2</sub> - 79 % N <sub>2</sub>	329.6	368.8	424.1	573.7	7.8	5.4	11.4	363.4	780.2	81.5
	30 % O <sub>2</sub> - 70 % N <sub>2</sub>	306.9	328.3	403.9	551.2	18.0	4.5	12.4	324.3	715.6	80.8
	21 % O <sub>2</sub> - 79 % CO <sub>2</sub>	308.1	343.1	410.0	609.9	11.5	4.0	10.0	338.7	795.23	82.3
	30 % O <sub>2</sub> - 70 % CO <sub>2</sub>	315.3	343.2	411.0	583.5	11.8	5.6	11.8	346.3	725.9	82.9
Blend Theo.	21 % O <sub>2</sub> - 79 % N <sub>2</sub>	332.8	-	637.8	-	-	10.8	-	360.7	852.8	80.9
	30 % O <sub>2</sub> - 70 % N <sub>2</sub>	295.7	314.7	595.7	-	5.5	11.5	-	298.1	740.7	81.1
	21 % O <sub>2</sub> - 79 % CO <sub>2</sub>	316.4	-	630.4	-	-	8.3	-	334.7	887.4	83.2
	30 % O <sub>2</sub> - 70 % CO <sub>2</sub>	300.5	316.4	591.5	-	4.9	10.7	-	308.4	754.5	82.3

Combustion profiles of imported coal, petcoke and lignite I and their blend with its theoretical behaviour under different combustion environments are shown in Figure 4.25.

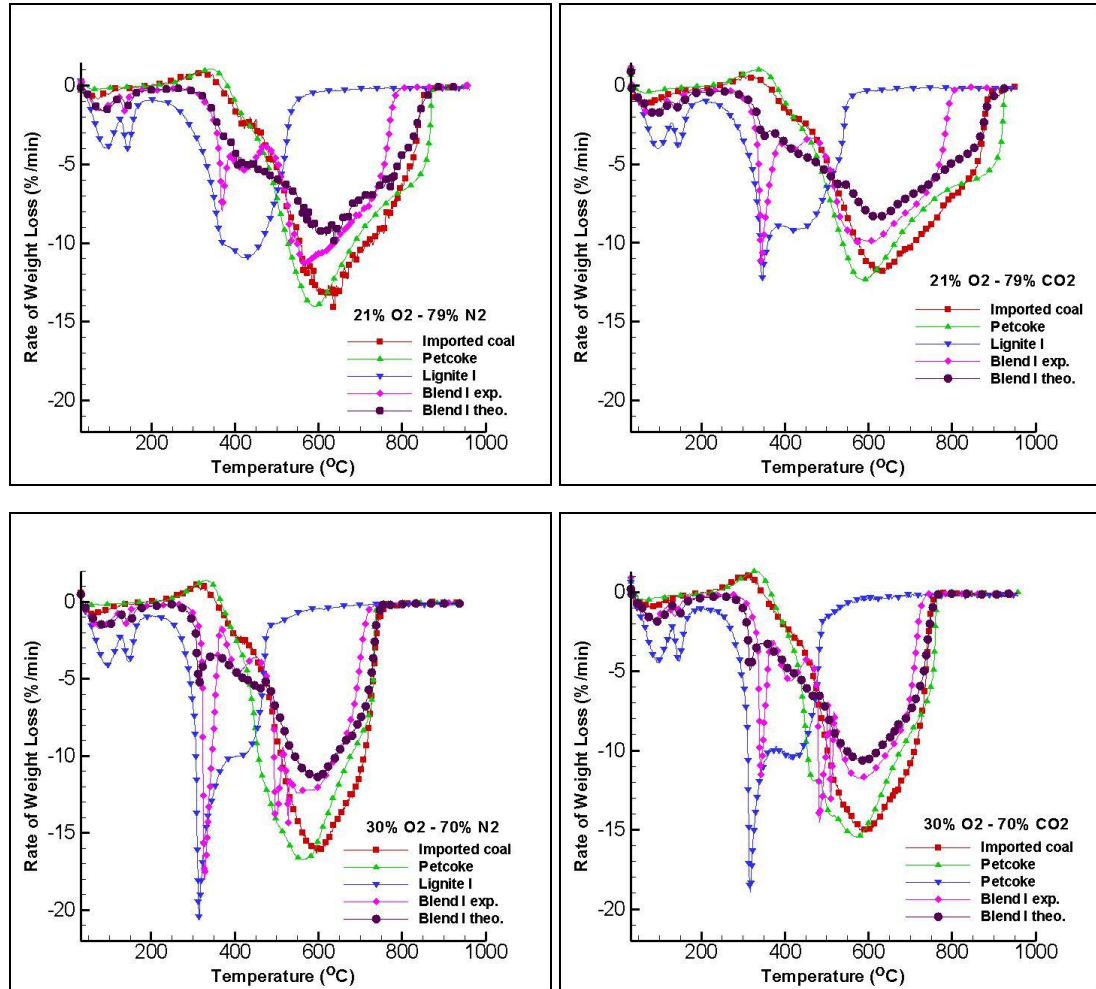


Figure 4.25: Combustion profiles of blend I and its parent fuels in different combustion environments

Theoretical and experimental combustion profiles of the blend mainly display different trends, which may be due to synergistic interactions between parent fuels in all combustion environments. In theoretical DTG curves of the blend samples, lignite combustion is not distinguished due to its lower proportion in the blend. However, as lignite burns separately from imported coal and petcoke, its

combustion peak is clearly demonstrated in DTG curves in contrast to the expected behaviour. The positive effect of blending is observed at high temperatures. In this temperature zone, the main combustion peaks of imported coal and petcoke have higher weight loss rates and lower corresponding peak temperatures than those in theoretical conditions. All these results are the indicative of interaction behaviour of the component coals during combustion in all cases.

The formation profiles of evolved gases during combustion of the blend I in different atmospheres are shown in Figure 4.26. The formation profile of  $\text{CO}_2$  in oxygen-enriched air atmosphere shifts to lower temperature zone as elevated oxygen levels lead to faster burning and earlier release of  $\text{CO}_2$ . Two steps are observed in formation profiles of  $\text{CO}_2$  gas due to burning of lignite and imported coal-petcoke, consecutively. CO formation takes place between 300-800°C with a shoulder at around 375°C.  $\text{H}_2\text{O}$  formation profiles show that moisture is released first in all combustion environments with further release in the temperature range of 200-800°C.  $\text{CH}_4$ ,  $\text{SO}_2$  and COS gases evolve between 250-750°C and reveal two stages in their evolution profiles. Mainly similar formation trends are observed for gases in all combustion cases.

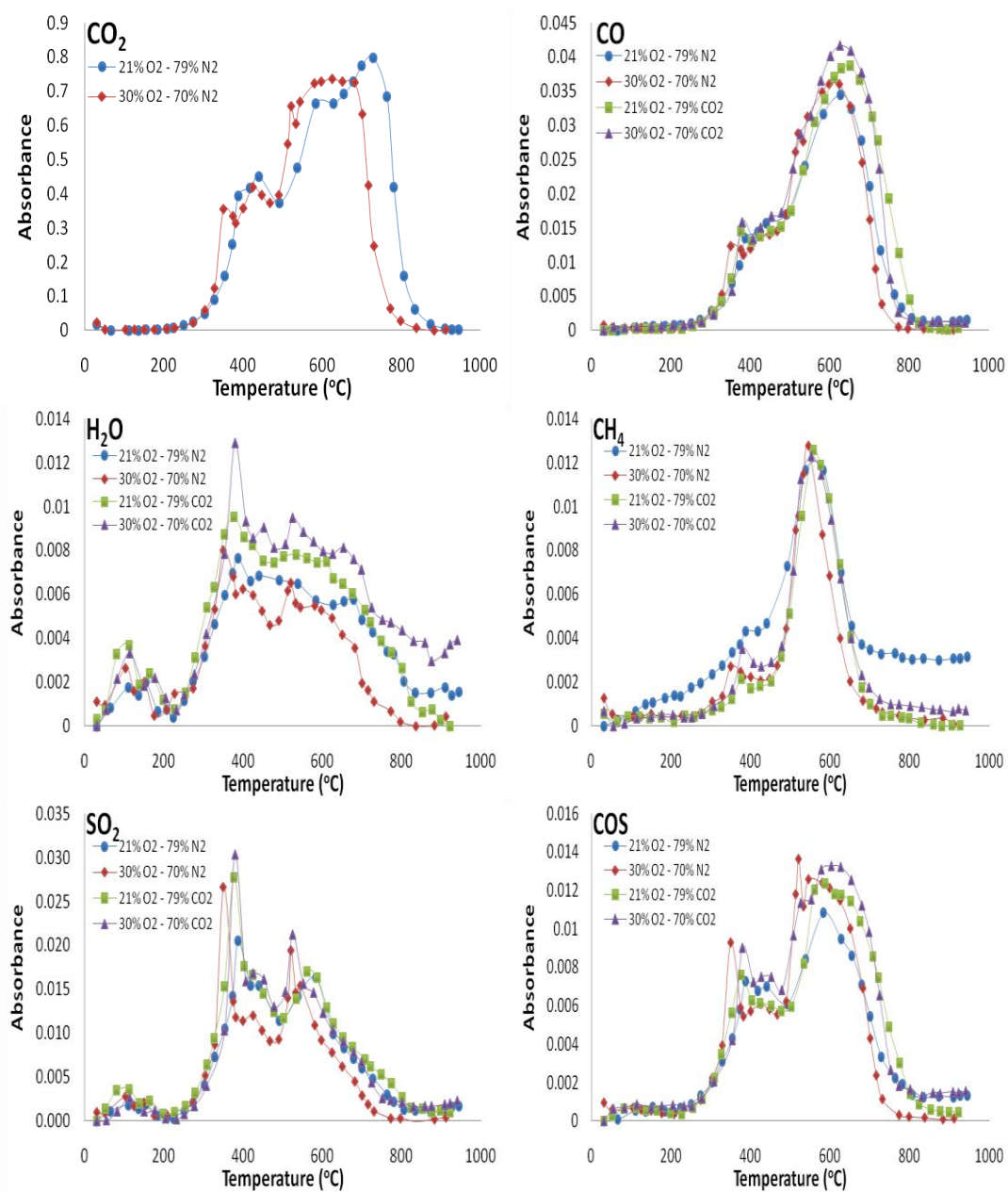


Figure 4.26: Formation profiles of evolved gases during combustion tests of blend I

#### 4.8 Petroleum Coke – Lignite II Blend (Blend II)

Blend II was prepared by mixing lignite II with low calorific value, high ash and moisture contents with high calorific value, low ash and moisture content petcoke in the proportion of 70:30. Their pyrolysis and combustion characteristics in air and oxy-fuel conditions are described in the following sections.

##### 4.8.1 Pyrolysis of Blend II

TGA and DTG profiles of pyrolysis tests are shown in Figure 4.27. The pyrolysis characteristics of the blend and its parent fuels are summarized in Table 4.13.

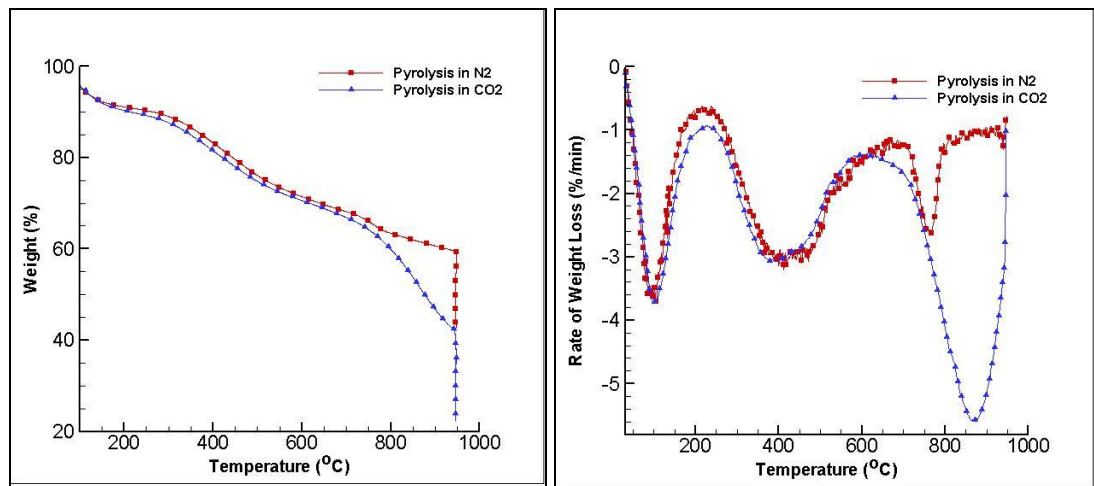


Figure 4.27: TGA and DTG profiles of blend II in N<sub>2</sub> and CO<sub>2</sub> atmospheres

Three main weight loss steps appear in weight loss profiles in both pyrolysis atmospheres. In DTG profiles of Figure 4.27, peaks appearing in the first 200°C temperature zone are attributed to moisture release while second main peak accounts for volatile matter release up to 650°C. Identical DTG trends up to 650°C indicates that CO<sub>2</sub> behaves as an inert atmosphere before high temperature zone.



However, at high temperature zone, weight loss profiles start to differ and additional weight loss steps are displayed. Additional peak after 700°C in N<sub>2</sub> atmosphere is considered to be due to calcite decomposition of the parent fuels in the blend while in CO<sub>2</sub> atmosphere CO<sub>2</sub> – char gasification reaction leads to further weight loss.

Table 4.13: Pyrolysis characteristics of blend II and its parent fuels

		T <sub>in</sub>	T <sub>max</sub>	(dm/dt) <sub>max</sub>	Weight loss up to 950°C
Lignite II	Pyrolysis in N <sub>2</sub>	241.6	400.0	4.1	50.2
	Pyrolysis in CO <sub>2</sub>	232.6	398.3	4.0	70.2
Petcoke	Pyrolysis in N <sub>2</sub>	514.9	582.3	1.4	14.4
	Pyrolysis in CO <sub>2</sub>	570.9	638.7	1.3	17.0
Blend Exp.	Pyrolysis in N <sub>2</sub>	270.6	393.8	3.0	40.3
	Pyrolysis in CO <sub>2</sub>	246.6	378.1	3.1	59.6
Blend Theo.	Pyrolysis in N <sub>2</sub>	276.0	393.0	3.2	39.6
	Pyrolysis in CO <sub>2</sub>	248.4	399.6	3.1	56.6

Pyrolysis behaviours of blend II and its parent fuels under N<sub>2</sub> and CO<sub>2</sub> environments are compared in Figure 4.28. The theoretical pyrolysis behaviour of the blend calculated by using additive rule is also displayed in the figure.

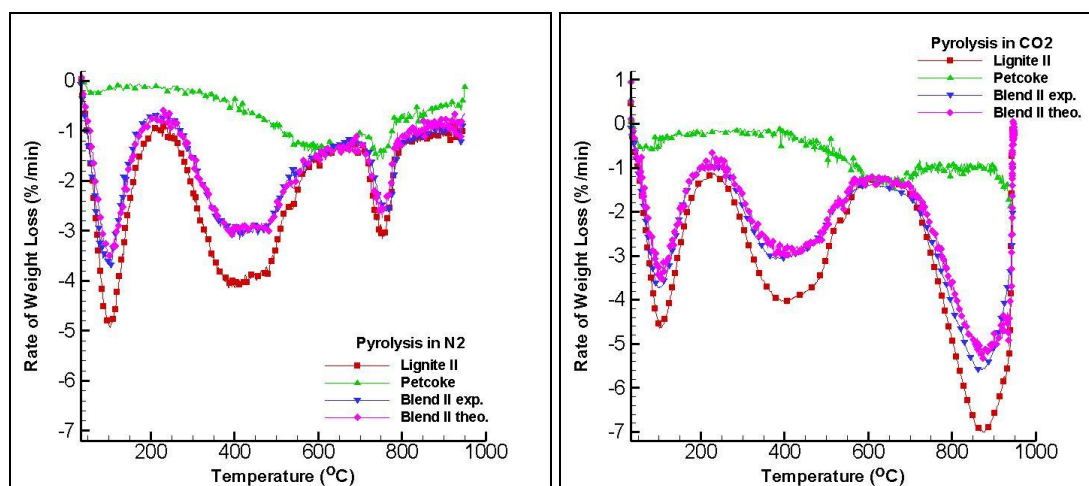


Figure 4.28: Pyrolysis profiles of blend II and its parent fuels in N<sub>2</sub> and CO<sub>2</sub> environments

As can be seen from Figure 4.28, lignite II devolatilizes at lower temperatures with higher weight loss rate due to its significantly high volatile matter content compared to petcoke. Overall comparison of DTG curves clearly indicate that pyrolysis behaviour of the blend II is dominated by lignite II as can also be observed with the similarity in their DTG profiles. Pyrolysis behaviour of blend II shows that peak height decreases and the peak position shifts to higher temperatures with the addition of petcoke.

Identical pyrolysis characteristics (Table 4.13) and overlap between the DTG curve of the blend itself (experimental) and the DTG curve found by additive rule (theoretical) of the two components of the blend (Figure 4.28) shows that there is no interaction (synergy) between lignite II and petcoke during pyrolysis in both conditions.

The evolution profiles of the gaseous species including CO<sub>2</sub>, CO, H<sub>2</sub>O, CH<sub>4</sub>, SO<sub>2</sub> and COS, from the pyrolysis of blend II in nitrogen and carbon dioxide are shown in Figure 4.29. In the formation profile of CO<sub>2</sub>, two peaks at around 400°C and 750°C are displayed between 200°C and 800°C which corresponds to the devolatilization temperature interval as represented in DTG curve of blend. These two peaks

account for  $\text{CO}_2$  release due to devolatilization and calcite decomposition, respectively. Formation of  $\text{CO}_2$  in  $\text{N}_2$  environment is found to be the major contributor to the evolved gases with its highest absorbance intensity. In both environments,  $\text{H}_2\text{O}$  is identified in the first  $200^\circ\text{C}$  due to moisture release.  $\text{CH}_4$  and  $\text{SO}_2$  formation take place during the entire devolatilization process. Certain amount of  $\text{SO}_2$  is also formed as a consequence of the high sulphur content of petcoke in the blend at around  $350^\circ\text{C}$  and  $550^\circ\text{C}$ .  $\text{CO}$  and  $\text{COS}$  display different trends in  $\text{CO}_2$  atmosphere due to  $\text{CO}_2$  – char gasification reaction. After  $700^\circ\text{C}$ , a distinctive increase is observed in the formation profile of  $\text{CO}$  with the initiation of the gasification reaction. Moreover, higher  $\text{CO}$  concentration leads to formation of  $\text{COS}$  which is formed by reaction of pyrite or sulphur formed during pyrite decomposition with  $\text{CO}$ .

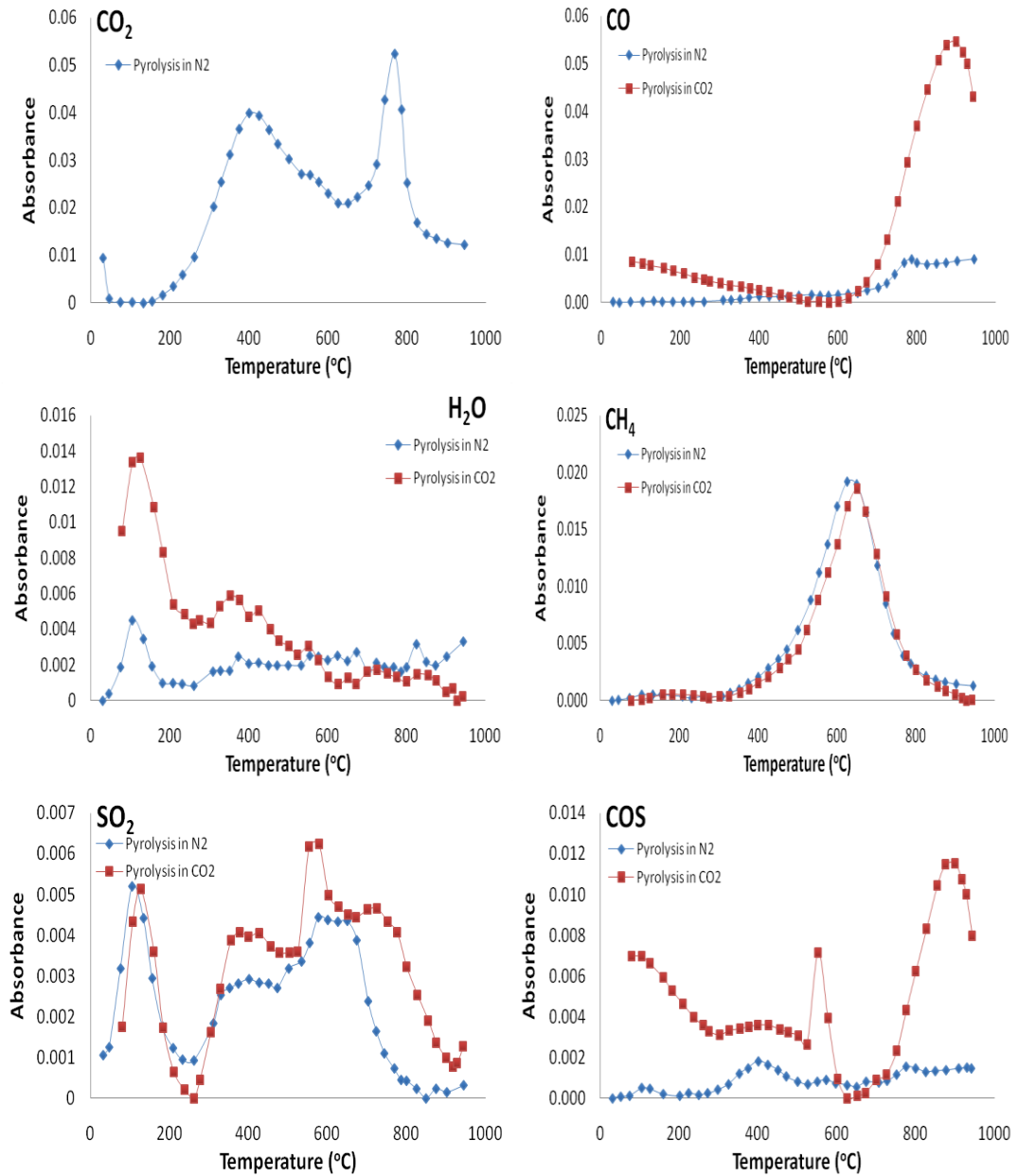


Figure 4.29: Formation profiles of evolved gases during pyrolysis tests of blend II

#### 4.8.2 Combustion of Blend II

Combustion profiles of the lignite II-petcoke blend in different combustion environments are given in Figure 4.30.

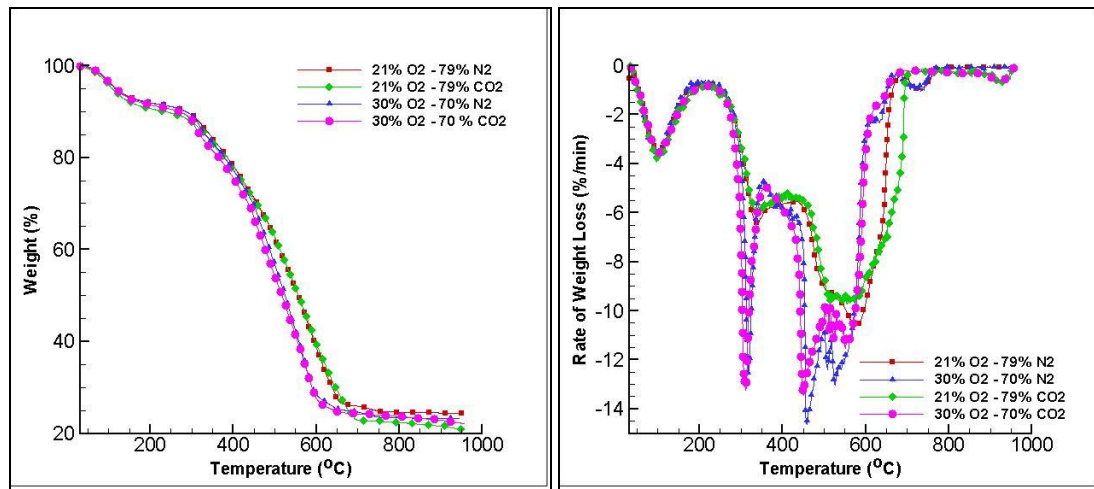


Figure 4.30: TGA and DTG profiles of blend II in different combustion atmospheres

In air and oxy-fuel cases, after moisture release in the first 200°C temperature zone, rate of weight loss curves continue with a shoulder at around 330°C, as also displayed in Table 4.14. The main peak between 400-650°C, is attributed to combustion of petcoke and lignite chars in both conditions. A small peak appears after 650°C in air case due to decomposition of calcite. However, this small peak is not observed in oxy-fuel conditions as calcite decomposition is prevented by CO<sub>2</sub>. Similar trend in burning profiles with air and oxy-firing conditions is observed with less weight loss rate and higher burnout temperature in oxy-fuel conditions, which are indicative of the slight delay in combustion. The effect of oxygen concentration is found to be more significant than that of the diluting gas (N<sub>2</sub> or CO<sub>2</sub>) on the combustion profiles. At elevated oxygen levels, more significant differences are

displayed in the DTG profiles of blend samples. Higher oxygen concentration in combustion environment leads to significant increase in weight loss rates and decrease in characteristic temperatures including  $T_{ig}$ ,  $T_{max}$  and  $T_b$ . Moreover, in oxygen-enriched conditions, burning of lignite II and petcoke are discretely separated as displayed with two different steps in the main combustion peak of DTG profiles.

Table 4.14: Combustion characteristics of blend II and its parent fuels

		$T_{in}$	$T_{max}$			$(dm/dt)_{max}$			$T_{ig}$	$T_b$	Total weight loss up to 950°C
Lignite II	21 % O <sub>2</sub> - 79 % N <sub>2</sub>	217.3	330.9	495.5	639.6	9.8	8.6	4.2	284.5	668.9	67.9
	30 % O <sub>2</sub> - 70 % N <sub>2</sub>	218.2	306.2	374.6	621.5	25.5	11.5	22.9	256.6	652.7	68.5
	21 % O <sub>2</sub> - 79 % CO <sub>2</sub>	219.8	315.3	488.0	644.0	13.4	7.7	3.5	262.7	671.0	69.8
	30 % O <sub>2</sub> - 70 % CO <sub>2</sub>	223.7	294.8	424.0	623.6	28.7	9.4	23.0	263.3	664.0	69.2
Petcoke	21 % O <sub>2</sub> - 79 % N <sub>2</sub>	400.1	589.0	-	-	14.0	-	-	469.5	867.0	96.8
	30 % O <sub>2</sub> - 70 % N <sub>2</sub>	381.6	562.2	-	-	16.8	-	-	439.7	735.6	95.9
	21 % O <sub>2</sub> - 79 % CO <sub>2</sub>	398.7	587.6	-	-	12.4	-	-	465.4	923.7	96.7
	30 % O <sub>2</sub> - 70 % CO <sub>2</sub>	379.5	572.6	-	-	15.5	-	-	434.7	761.8	97.9
Blend Exp.	21 % O <sub>2</sub> - 79 % N <sub>2</sub>	257.3	332.6	581.4	726.6	6.3	10.6	1.0	312.1	663.7	75.5
	30 % O <sub>2</sub> - 70 % N <sub>2</sub>	257.6	317.5	450.5	525.3	12.5	14.6	13.1	303.4	652.7	76.8
	21 % O <sub>2</sub> - 79 % CO <sub>2</sub>	246.1	334.0	575.4	-	5.8	9.6	-	311.9	694	79.3
	30 % O <sub>2</sub> - 70 % CO <sub>2</sub>	248.8	310.9	448.6	551.4	13.3	13.4	11.5	304.7	650.3	77.0
Blend Theo.	21 % O <sub>2</sub> - 79 % N <sub>2</sub>	261.0	332.0	540.0	635	6.6	8.3	6.6	302.2	866.0	76.3
	30 % O <sub>2</sub> - 70 % N <sub>2</sub>	256.7	306.7	485.7	620.3	17.4	8.2	20.1	283.7	734.7	76.8
	21 % O <sub>2</sub> - 79 % CO <sub>2</sub>	247.7	314.7	544.7	641.7	9.1	7.6	5.8	300.5	923.7	77.8
	30 % O <sub>2</sub> - 70 % CO <sub>2</sub>	252.7	294.7	506.7	623.7	19.8	7.4	20.1	281.3	759.7	77.8

Combustion profiles of lignite II, petcoke and their blend with its theoretical behaviour under different combustion environments are shown in Figure 4.31.

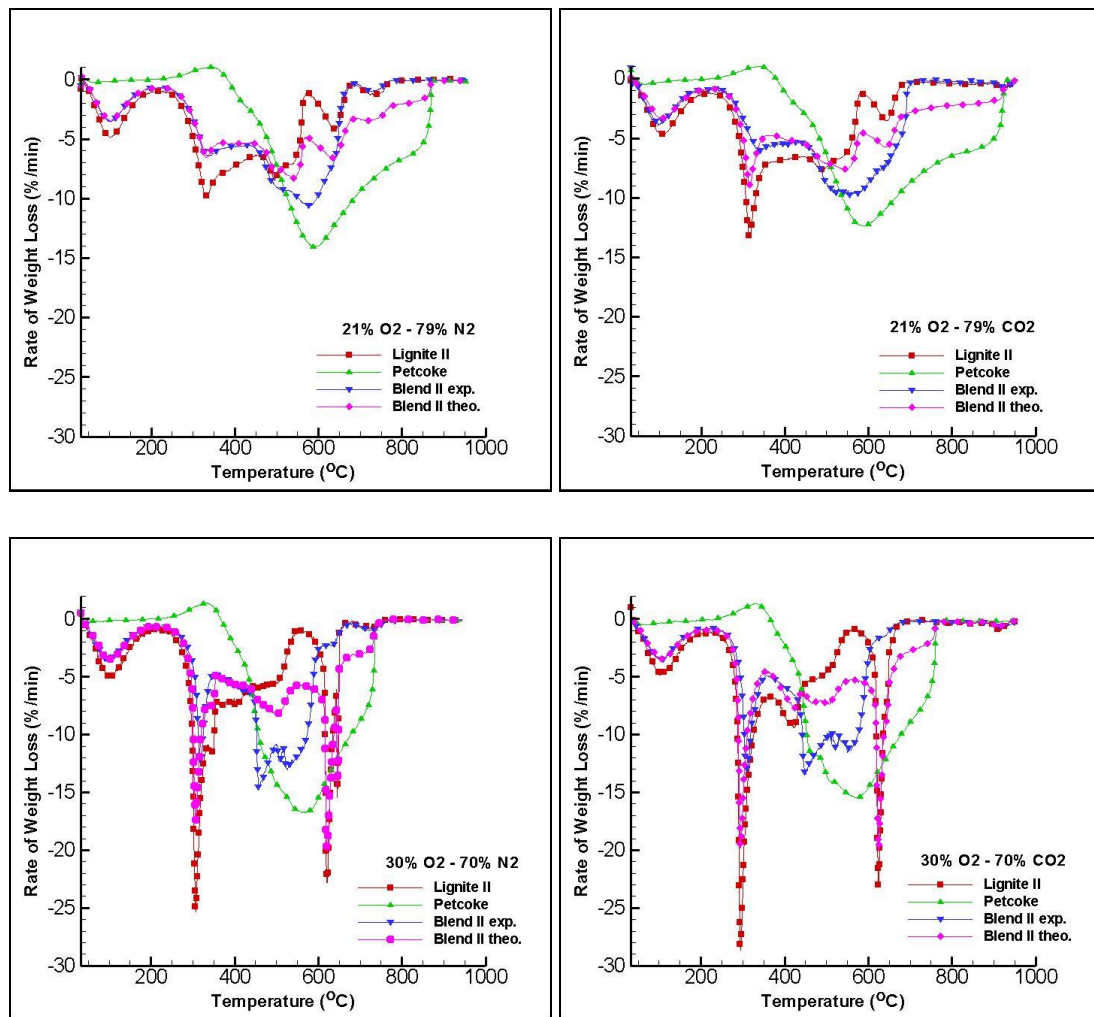


Figure 4.31: Combustion profiles of blend II and its parent fuels in different combustion environments

As can be seen from Figure 4.31, combustion profile of the blend lies between those of parent fuels in all combustion environments. Theoretical and experimental combustion profiles of the blend mainly display different trends, which may be due to synergistic interactions between lignite and petcoke in all combustion environments. Some deviations from expected behaviour are observed DTG curves and characteristic temperatures. Theoretical DTG curves of the blend samples



contain each weight loss step observed in individual DTG curves of lignite and petcoke. However, comparison of experimental and theoretical curves reveals that in experimental DTG curves, some peaks are observed to disappear. In all combustion conditions, weight loss rate of main peak in the temperature range of 250-650°C is always higher than the expected behaviour which may indicate the positive effect of the blending. All these results point out that there is an interaction between component coals during combustion in all cases.

The formation profiles of evolved gases during combustion of the blend in different atmospheres are shown in Figure 4.32. The formation profile of CO<sub>2</sub> in oxygen-enriched air atmosphere shifts to lower temperature zone as elevated oxygen levels lead to faster burning and earlier release of CO<sub>2</sub>. CO formation takes place between 300-700°C with a shoulder at around 375°C. H<sub>2</sub>O formation profiles show that moisture is released first in all combustion environments with further release in the temperature range of 300-700°C. CH<sub>4</sub>, SO<sub>2</sub> and COS reveal two stages in their evolution profiles. Similar trends are observed for all gases in identical oxygen conditions.

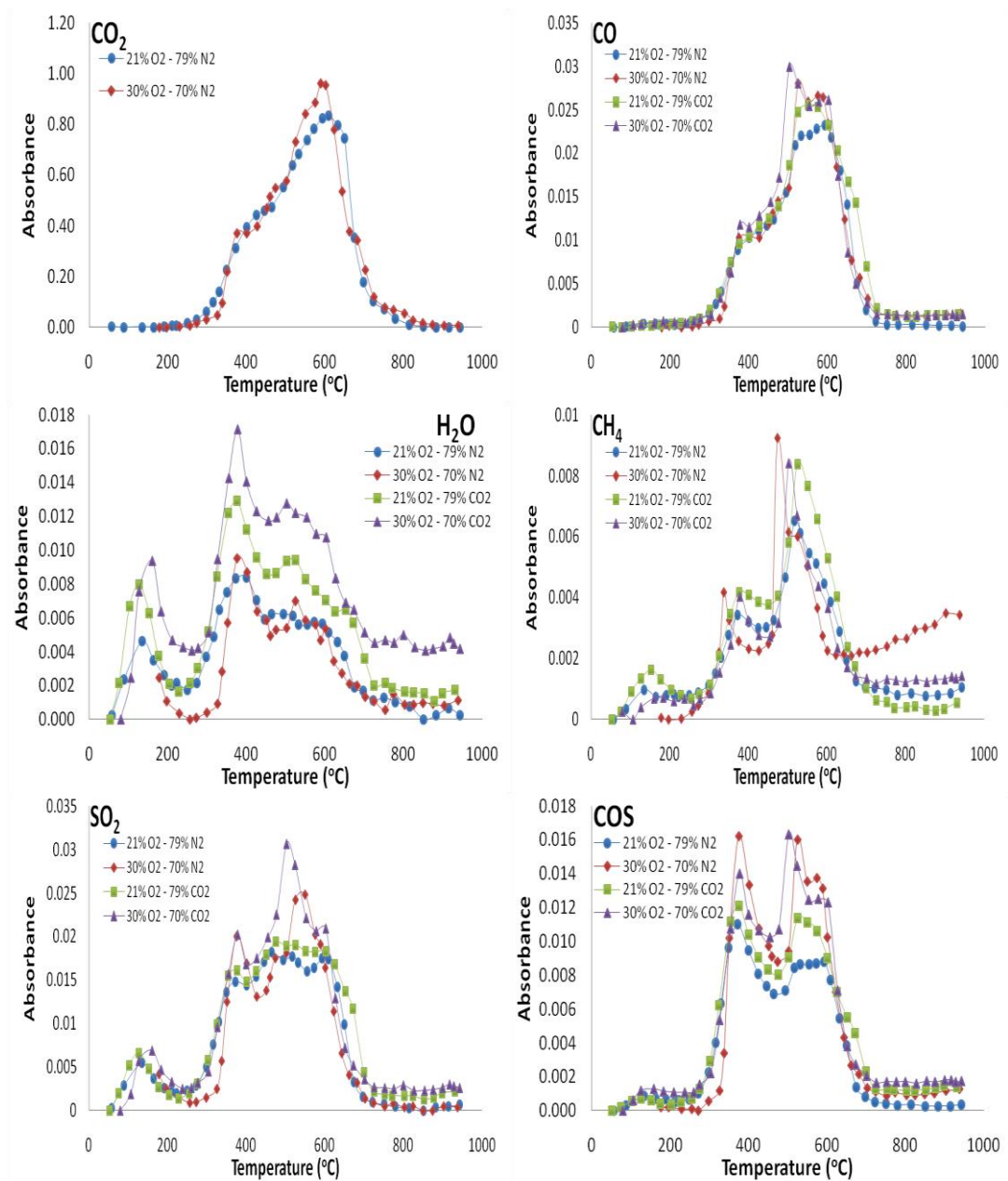


Figure 4.32: Formation profiles of evolved gases during combustion tests of blend II

#### 4.9 Lignite I - Olive Residue Blend (Blend III)

In this section, pyrolysis and combustion behaviour of indigenous lignite, olive residue and their 50/50 wt % blend in air and oxy-fuel conditions is described.

#### 4.9.1 Pyrolysis of Blend III

Pyrolysis tests are carried out under  $N_2$  and  $CO_2$  atmosphere which are the main diluting gases of air and oxy-fuel environments. TGA and DTG curves of lignite-olive residue blend are shown in Figure 4.33. The pyrolysis characteristics of the blend and its parent fuels for comparison are summarized in Table 4.15.

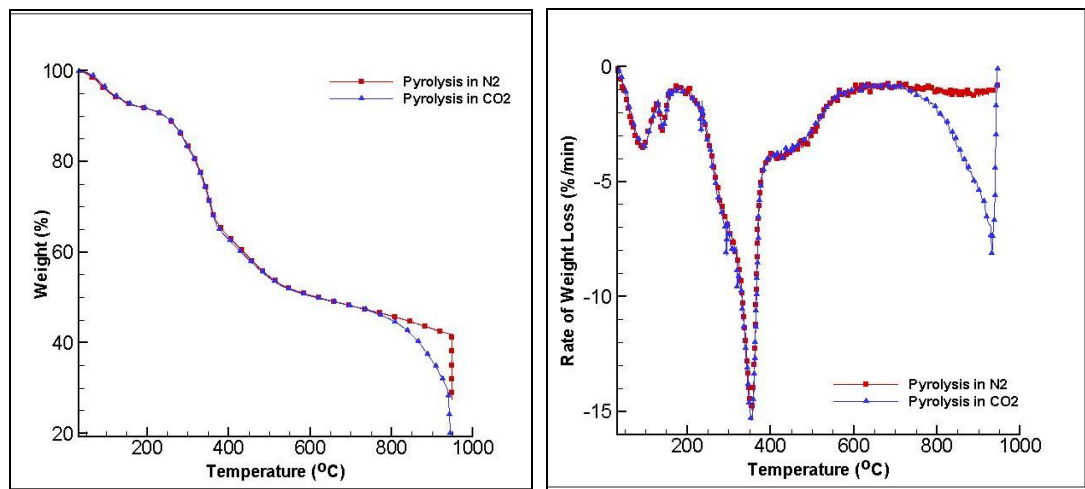


Figure 4.33: TGA and DTG profiles of blend III in  $N_2$  and  $CO_2$  atmospheres

Two main weight loss steps appear in weight loss profiles in nitrogen atmosphere while an additional weight loss step is observed after  $700^\circ C$  in  $CO_2$  environment. First weight loss step within  $25-200^\circ C$  temperature range accounts for moisture release and the second weight loss step within  $200-600^\circ C$  corresponds to volatile matter release in both atmospheres. Identical DTG trends up to  $700^\circ C$  are obtained in both atmospheres in pyrolysis tests. This indicates that  $CO_2$  behaves as an inert atmosphere before high temperature zone [34]. Additional peak after  $700^\circ C$  seen in DTG curve under  $CO_2$  atmosphere is considered to be due to  $CO_2$  – char gasification reaction.

Table 4.15: Pyrolysis characteristics of blend III and its parent fuels

		$T_{in}$	$T_{max}$	$(dm/dt)_{max}$	Weight loss up to 950°C
Lignite I	Pyrolysis in N <sub>2</sub>	230.8	482.9	3.6	41.0
	Pyrolysis in CO <sub>2</sub>	216.7	481.0	3.2	50.3
Olive Res.	Pyrolysis in N <sub>2</sub>	183.1	355.5	28.4	75.0
	Pyrolysis in CO <sub>2</sub>	175.6	354.9	28.3	87.0
Blend Exp.	Pyrolysis in N <sub>2</sub>	196.0	355.6	15.0	57.9
	Pyrolysis in CO <sub>2</sub>	187.8	354.4	15.5	74.1
Blend Theo.	Pyrolysis in N <sub>2</sub>	184.7	355.3	15.4	58.9
	Pyrolysis in CO <sub>2</sub>	189.9	354.9	15.4	68.9

Pyrolysis behaviours of lignite I and olive residue samples and their blend under N<sub>2</sub> and CO<sub>2</sub> environments are compared in Figure 4.34. The theoretical pyrolysis behaviour of blend is also included in DTG profiles of fuel samples in the figure.

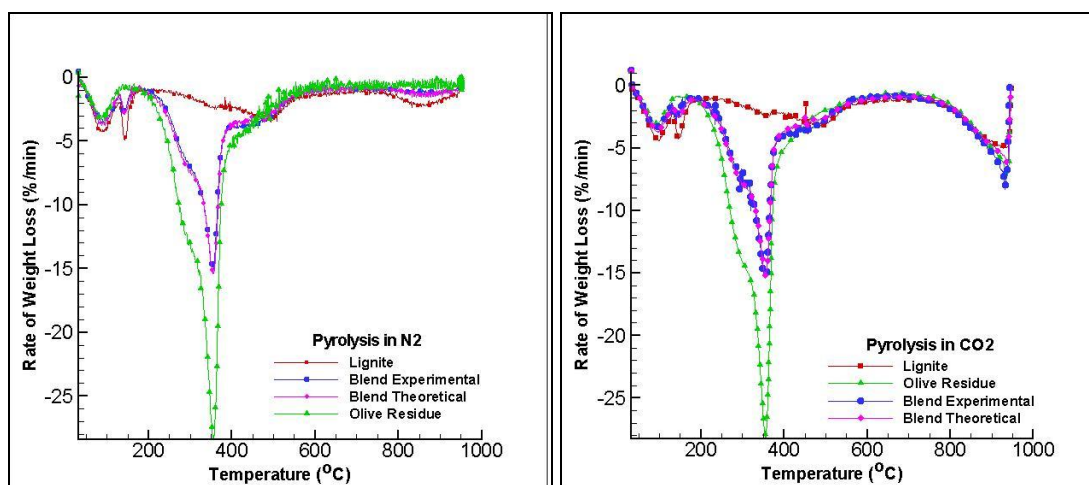


Figure 4.34: Pyrolysis profiles of blend III and its parent fuels in  $N_2$  and  $CO_2$  environments

Comparison between the DTG profiles of olive residue and lignite clearly shows that olive residue devolatilizes at lower temperatures than lignite. Lower resistance to heat even at lower temperatures displayed by olive residue is considered to be due to the weaker bonds between the macromolecular constituents of this biomass. Pyrolysis behaviour of lignite/olive residue (50/50 wt. %) blend shows that peak height increases and the peak position shifts to lower temperature with the addition of olive residue.

The overlap between the DTG curve of the blend itself (experimental) and the DTG curve found by additive rule (theoretical) of the two components of the blend reveals the absence of synergy between lignite and olive residue during pyrolysis.

The evolution profiles of the gaseous species including  $CO_2$ ,  $CO$ ,  $H_2O$ ,  $CH_4$ ,  $SO_2$  and  $COS$ , from the pyrolysis of olive residue-lignite blend in nitrogen and carbon dioxide are shown in Figure 4.35. In the formation profile of  $CO_2$ , a peak at around  $350^\circ C$  is displayed between  $200^\circ C$  and  $600^\circ C$  which corresponds to the devolatilization temperature interval as represented in DTG curve of blend. Formation of  $CO_2$  in  $N_2$  environment is found to be the major contributor to the evolved gases with its highest absorbance intensity. The high yield of  $CO_2$  during the pyrolysis of blend is

considered to be due to high oxygen contents of olive residue and lignite [49]. In both environments,  $\text{H}_2\text{O}$  is identified in the first  $200^\circ\text{C}$  due to moisture release. In the temperature range of  $200\text{--}700^\circ\text{C}$ , further  $\text{H}_2\text{O}$  release is observed probably from condensation of phenols as also confirmed in the literature. Methane formation takes place during the entire devolatilization process. Certain amount of  $\text{SO}_2$  is also formed as a consequence of the high sulphur content of lignite in the blend at around  $350^\circ\text{C}$  and  $500^\circ\text{C}$ . Formation profiles of  $\text{H}_2\text{O}$ ,  $\text{CH}_4$  and  $\text{SO}_2$  are not affected by pyrolysis environment and display identical evolution trends in both  $\text{N}_2$  and  $\text{CO}_2$  environments. However,  $\text{CO}$  and  $\text{COS}$  display different trends in  $\text{CO}_2$  atmosphere due to  $\text{CO}_2$  – char gasification reaction. After  $700^\circ\text{C}$ , a distinctive increase is observed in the formation profile of  $\text{CO}$  with the initiation of the gasification reaction. Moreover, higher  $\text{CO}$  concentration leads to formation of  $\text{COS}$  which may be caused by pyrite ( $\text{FeS}_2$ ) –  $\text{CO}$  gas solid reaction.

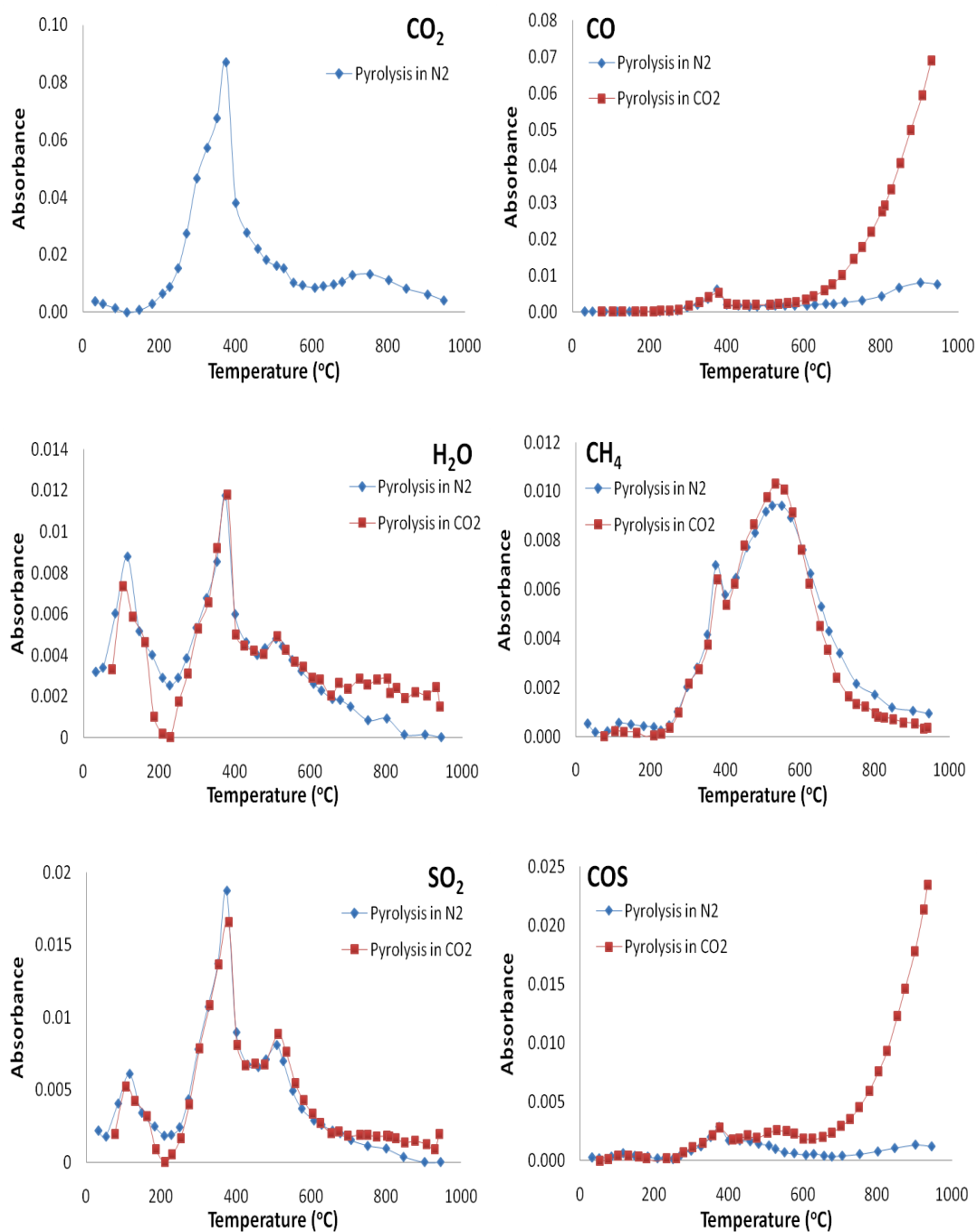


Figure 4.35: Formation profiles of evolved gases during pyrolysis tests of blend III

#### 4.9.2 Combustion of Blend III

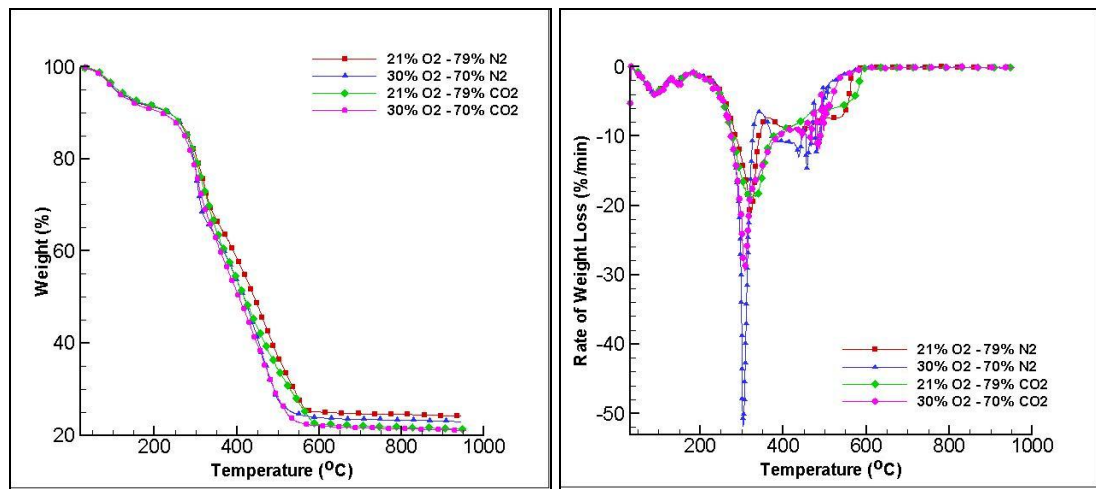


Figure 4.36: TGA and DTG profiles of blend III in different combustion environments

Combustion profiles of the olive residue/lignite blend in different combustion environments are compared in Figure 4.36. In air-firing case three weight loss steps are displayed in the DTG curve of the blend. The main peak between 200-360°C is attributed to release of volatiles in olive residue and their burning. The second step represented with a shoulder at around 430°C is considered to be due to burning of biomass char and volatile matter of lignite whereas the last stage is mostly due to combustion of lignite char after 500°C. Similar trend in burning profiles with air- and oxy-firing conditions is observed with less loss rate and higher burnout temperature in oxy-fuel conditions which are indicative of the delay in combustion. The effect of oxygen concentration is found to be more significant than that of the diluting gas ( $N_2$  or  $CO_2$ ) on the combustion profiles. As can be seen from Table 4.16, at elevated oxygen levels characteristic temperatures including  $T_{ig}$ ,  $T_{max}$  and  $T_b$  are found to be lower, complete combustion is achieved at lower temperatures and shorter times.



Table 4.16: Combustion characteristics of blend III and its parent fuels

		$T_{in}$	$T_{max}$		$(dm/dt)_{max}$		$T_{ig}$	$T_b$	Total weight loss up to 950°C
Lignite I	21 % O <sub>2</sub> - 79 % N <sub>2</sub>	224.0	-	426.2	-	11.0	297.1	546.7	59.2
	30 % O <sub>2</sub> - 70 % N <sub>2</sub>	226.1	314.5	-	20.5	-	265.3	530.0	59.3
	21 % O <sub>2</sub> - 79 % CO <sub>2</sub>	225.8	347.1	-	12.3	-	308.8	550.0	59.6
	30 % O <sub>2</sub> - 70 % CO <sub>2</sub>	202.8	317.2	-	19.0	-	264.1	535.6	61.2
Olive Res.	21 % O <sub>2</sub> - 79 % N <sub>2</sub>	183.9	308.9	405.3	48.4	14.4	258.8	567.7	95.6
	30 % O <sub>2</sub> - 70 % N <sub>2</sub>	186.9	304.3	390.9	58.9	20.5	258.5	526.6	95.8
	21 % O <sub>2</sub> - 79 % CO <sub>2</sub>	174.6	309.7	435.8	43.7	10.5	229.5	579.9	96.9
	30 % O <sub>2</sub> - 70 % CO <sub>2</sub>	179.8	311.2	413.2	53.2	15.9	264.1	544.3	95.7
Blend Exp.	21 % O <sub>2</sub> - 79 % N <sub>2</sub>	188.8	321.3	-	21.2	-	267.4	567.8	75.7
	30 % O <sub>2</sub> - 70 % N <sub>2</sub>	187.7	303.5	-	52.0	-	263.5	544.2	77.0
	21 % O <sub>2</sub> - 79 % CO <sub>2</sub>	183.0	323.5	-	18.8	-	239.2	587.2	79.0
	30 % O <sub>2</sub> - 70 % CO <sub>2</sub>	180.8	306.7	-	29.4	-	264.0	553.7	79.2
Blend Theo.	21 % O <sub>2</sub> - 79 % N <sub>2</sub>	186.9	309.7	405.9	25.8	12.5	260.8	567.0	77.5
	30 % O <sub>2</sub> - 70 % N <sub>2</sub>	185.2	311.2	391.2	34.1	15.3	256.2	527.2	77.7
	21 % O <sub>2</sub> - 79 % CO <sub>2</sub>	188.8	309.8	438.8	23.9	10.2	231.9	576.8	78.1
	30 % O <sub>2</sub> - 70 % CO <sub>2</sub>	188.5	315.5	413.5	33.9	13.2	235.9	543.5	78.3

Combustion behaviours of lignite I and olive residue samples and their blend including theoretical curves under different combustion environments are compared in Figure 4.37.

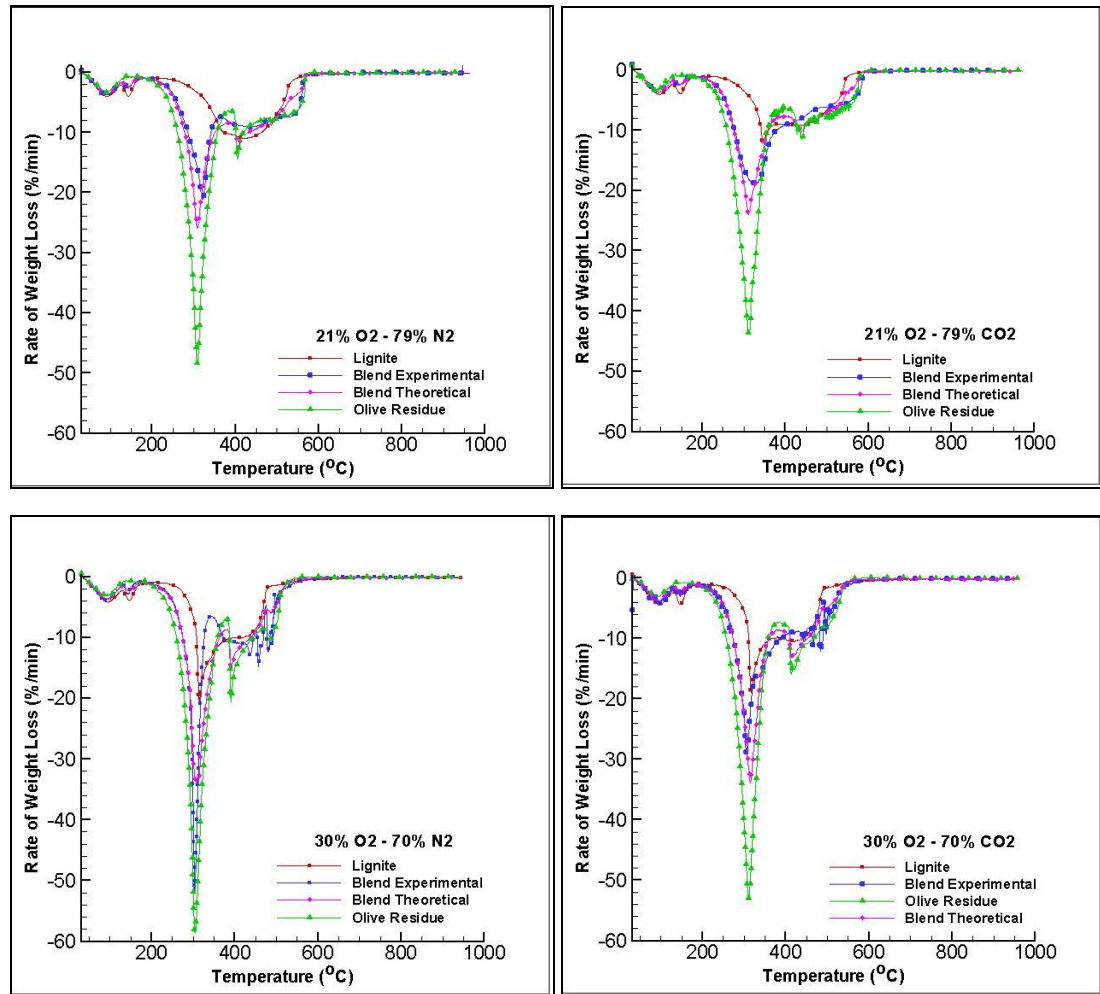


Figure 4.37: Combustion profiles of blend III and its parent fuels in different combustion environments

As can be seen from Figure 4.37, combustion profile of the blend lies between those of parent fuels in all combustion environments. Theoretical and experimental combustion profiles of the blend mainly display similar trend with slight deviations, which may be due to synergistic interactions between olive residue – lignite. Some

deviations from expected behaviour are observed in  $T_{\max}$  and  $(dm/dt)_{\max}$  values in volatile matter decomposition stage. In air, oxy-fuel and oxygen-enriched conditions maximum weight loss rate is found lower in experimental conditions than the calculated ones. In oxygen-enriched air combustion conditions, on the other hand, weight loss is observed faster than expected which may indicate the positive effect of the blending. Another point that indicates the synergistic behaviours is the disappearance of the peak at around 400°C in the experimental profile. Moreover, theoretical and experimental results differ in characteristic temperatures such as ignition and burnout temperatures, which reflect the interaction behaviour of component fuels.

The formation profiles of evolved gases during combustion of the blend in different atmospheres are shown in Figure 4.38. The formation profile of CO<sub>2</sub> in oxygen-enriched air atmosphere shifts to lower temperature zone as elevated oxygen levels lead to faster burning and earlier release of CO<sub>2</sub>. H<sub>2</sub>O formation profiles show that moisture is released first in all combustion environments with further release in the temperature range of 200-500°C. Also sulphur containing gases, SO<sub>2</sub> and COS reveal two stages in their evolution profiles in air firing conditions, whereas one stage formation is observed in oxy-fuel conditions. This can be due to effect of high CO<sub>2</sub> concentration under oxy-fuel conditions.

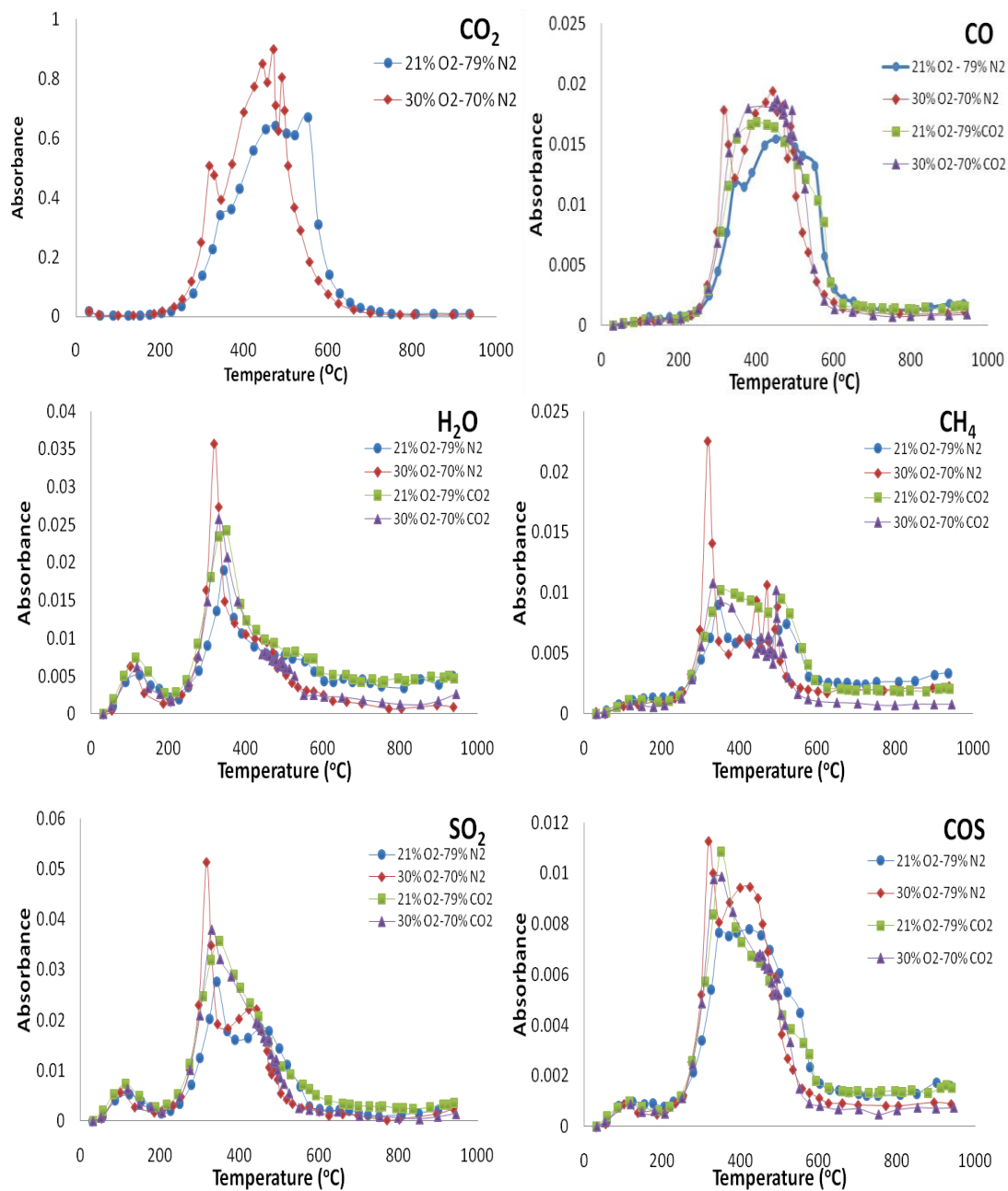


Figure 4.38: Formation profiles of evolved gases during combustion tests of blend III

## CHAPTER 5

### CONCLUSIONS

#### 5.1 General

Pyrolysis and combustion characteristics of different fuels; imported coal, petroleum coke, two kinds of indigenous lignite, olive residue and their blends with various proportions is investigated in air and oxy-fuel conditions by using a combined TGA-FTIR system. The following conclusions were reached under the observations of this study:

- Pyrolysis tests were carried out in nitrogen and carbon dioxide environments which are the main diluting gases of air and oxy-fuel environment, respectively. Pyrolysis tests under  $N_2$  and  $CO_2$  environments reveal that fuel samples display similar behaviour up to  $700^\circ C$  regardless of the diluting gas. However, DTG profiles are observed to differ in high temperature zone due to char- $CO_2$  gasification reaction in  $CO_2$  atmosphere. Moreover, distinctive increase in CO and COS is identified from FTIR formation profiles due to gasification reaction.
- Combustion experiments were carried out in four different atmospheres; air, oxygen-enriched air environment (30 %  $O_2$  – 70 %  $N_2$ ), oxy-fuel environment (21 %  $O_2$  – 79 %  $CO_2$ ) and oxygen-enriched oxy-fuel environment (30 %  $O_2$  – 70 %  $CO_2$ ). Combustion behaviour of fuels and their blends in air and oxy-

fuel conditions show that burning process is slightly delayed in oxy-fuel conditions compared to air conditions at the same oxygen levels. However, as oxygen concentration increases, weight loss profiles shift to lower temperatures, rate of weight loss increases and complete combustion is achieved at lower temperatures.

- Pyrolysis and combustion behaviour of three different fuel blends were investigated. Pyrolysis tests reveal that there is no interaction between parent fuels during pyrolysis of petcoke-lignite and lignite-olive residue blend under both  $N_2$  and  $CO_2$  environments as theoretical and experimental behaviours of the samples overlap. However in pyrolysis of imported coal-petcoke-lignite blend and all combustion tests of these three blends deviations from expected behavior which are indicative of synergistic interactions are observed. Therefore it can be concluded that it is not possible to predict blends behaviour from that of the parent fuels.
- During pyrolysis and combustion tests gaseous products  $CO_2$ ,  $CO$ ,  $H_2O$ ,  $CH_4$ ,  $SO_2$  and  $COS$  in flue gas were identified and analyzed by using FTIR. In pyrolysis tests, significant amount of  $CO$  due to char –  $CO_2$  gasification reaction and consecutively  $COS$  is evolved in  $CO_2$  atmosphere in all fuels. No general consensus has been obtained in combustion tests as formation profiles displayed different trends in each case.

In conclusion, the current results add to previous literature data on pyrolysis and combustion behaviour of different rank fuels and their blends in air and oxy-fuel conditions, some of which such as; petcoke, indigenous lignite, olive residue have not been studied to date. Moreover, these results provide basic information about retrofit applications to existing coal-fired power plants or alternatively be used in designs of new coal-fired power plants with near zero emissions.

## **5.2 Suggestions for Future Work**

Based on the experience gained in the present study, the following recommendations for future extension of the work are suggested:

- Pyrolysis and combustion behaviour of different types of energy sources including various coals, biomass or municipal solid wastes can be investigated in similar conditions.
- Pilot scale combustion tests of the fuels investigated in the present study can be carried out in fluidized bed combustion systems under oxygen enriched air and oxy-fuel conditions.
- Mathematical models of fluidized bed combustion systems under oxygen enriched air and oxy-firing conditions can be developed.

## REFERENCES

- [1] *BP Statistical Review of World Energy, 2010* [http://www.bp.com/liveassets/bp\\_internet/globalbp/globalbp\\_uk\\_english/reports\\_and\\_publications/statistical\\_energy\\_review\\_2008/STAGING/local\\_assets/2010\\_downloads/statistical\\_review\\_of\\_world\\_energy\\_full\\_report\\_2010.pdf](http://www.bp.com/liveassets/bp_internet/globalbp/globalbp_uk_english/reports_and_publications/statistical_energy_review_2008/STAGING/local_assets/2010_downloads/statistical_review_of_world_energy_full_report_2010.pdf) Last access: 25.12.2010.
- [2] *Atmospheric CO2 emissions*. <http://co2now.org/> Last access: 16.01.2011.
- [3] *IEA, 2010 Key world energy statics* [http://www.iea.org/textbase/nppdf/free/2010/key\\_stats\\_2010.pdf](http://www.iea.org/textbase/nppdf/free/2010/key_stats_2010.pdf) Last access: 16.01.2011.
- [4] *CO2 emissions from fuel combustion highlights*. <http://www.iea.org/co2highlights/CO2highlights.pdf> Last access: 16.01.2011.
- [5] L. Y. Wall T., Spero C., Elliotta L., Kharea S., Rathnama R. , Zeenathala F., Moghtaderia B., Buhred B., Shenge C. , Gupta R., Yamadac T. , Makinoc K. , Yua J., "An overview on oxyfuel coal combustion—State of the art research and technology development," *Chemical Engineering Research and Design*, **87**, (2009), 1003-1016.
- [6] B. J. P. Buhre, L. K. Elliott, C. D. Sheng, R. P. Gupta, and T. F. Wall, "Oxy-fuel combustion technology for coal-fired power generation," *Progress in Energy and Combustion Science*, **31**, (2005), 283-307.
- [7] T. F. Wall, "Combustion processes for carbon capture," *Proceedings of the Combustion Institute* **31**, (2007), 31-47.
- [8] B. J. Toftegaard M. B., Jensen P. A., P. Glarborg, Jensen A. D., "Oxy-fuel combustion of solid fuels," *Progress in Energy and Combustion Science*, **36** (2010), 581-625.



- [9] E. Croiset, K. Thambimuthu, and A. Palmer, "Coal combustion in O<sub>2</sub>/CO<sub>2</sub> mixtures compared with air," *The Canadian Journal of Chemical Engineering*, **78**, (2000), 402-407.
- [10] A. H. B. Anthony, "Overview of Oxy-combustion technologies with pure oxygen and chemical looping combustion," in *Handbook of Combustion*. vol. 5, F. W. M. Lackner, A. K. Agarwal, Ed., ed Weinheim: Wiley-VCH, 2010, pp. 517-541.
- [11] M. V. Gil, D. Casal, C. Pevida, J. J. Pis, and F. Rubiera, "Thermal behaviour and kineticsof coal/biomass blends during co-combustion," *Bioresource Technology*, **101**, (2010), 5601-5608.
- [12] S. Su, J. H. Pohl, D. Holcombe, and J. A. Hart, "Techniques to determine ignition, flame stability and burnout of blended coals in p.f. power station boilers," *Progress in Energy and Combustion Science*, **27**, (2001), 75-98.
- [13] P. A. Morgan, S. D. Robertson, and J. F. Unsworth, "Combustion studies by thermogravimetric analysis: 1. Coal oxidation," *Fuel*, **65**, (1986), 1546-1551.
- [14] J. W. Cumming, "A DTG combustion study on anthracitic and other coal chars," *Thermochimica Acta*, **155**, (1989), 151-161.
- [15] W.-P. Pan, Y. Gan, and M. A. Serageldin, "A study of thermal analytical values for coal blends burned in an air atmosphere," *Thermochimica Acta*, **180**, (1991), 203-217.
- [16] G. A. Norton, "A review of the derivative thermogravimetric technique (burning profile) for fuel combustion studies," *Thermochimica Acta*, **214**, (1993), 171-182.
- [17] D. Vamvuka, E. Kakaras, E. Kastanaki, and P. Grammelis, "Pyrolysis characteristics and kinetics of biomass residuals mixtures with lignite," *Fuel*, **82**, 1949-1960.
- [18] M. B. Toftegaard, J. Brix, P. A. Jensen, P. Glarborg, and A. D. Jensen, "Oxy-fuel combustion of solid fuels," *Progress in Energy and Combustion Science*, **36**, (2010), 581-625.

- [19] D. Singh, E. Croiset, P. L. Douglas, and M. A. Douglas, "Techno-economic study of CO<sub>2</sub> capture from an existing coal-fired power plant: MEA scrubbing vs. O<sub>2</sub>/CO<sub>2</sub> recycle combustion," *Energy Conversion and Management*, **44**, (2003), 3073-3091.
- [20] T. F. Wall, "Combustion processes for carbon capture," *Proceedings of the Combustion Institute*, **31**, (2007), 31-47.
- [21] T. Kiga, S. Takano, N. Kimura, K. Omata, M. Okawa, T. Mori, and M. Kato, "Characteristics of pulverized-coal combustion in the system of oxygen/recycled flue gas combustion," *Energy Conversion and Management*, **38**, (1997), S129-S134.
- [22] T. Wall, Y. Liu, C. Spero, L. Elliott, S. Khare, R. Rathnam, F. Zeenathal, B. Moghtaderi, B. Buhre, C. Sheng, R. Gupta, T. Yamada, K. Makino, and J. Yu, "An overview on oxyfuel coal combustion--State of the art research and technology development," *Chemical Engineering Research and Design*, **87**, (2009), 1003-1016.
- [23] Y. Tan, E. Croiset, M. A. Douglas, and K. V. Thambimuthu, "Combustion characteristics of coal in a mixture of oxygen and recycled flue gas," *Fuel*, **85**, (2006), 507-512.
- [24] B. M. Abraham, "Coal-oxygen process provides CO<sub>2</sub> for enhanced recovery," *Oil Gas J.*, **80:11**, (1982), 68-70.
- [25] Q. Li, C. Zhao, X. Chen, W. Wu, and Y. Li, "Comparison of pulverized coal combustion in air and in O<sub>2</sub>/CO<sub>2</sub> mixtures by thermo-gravimetric analysis," *Journal of Analytical and Applied Pyrolysis*, **85**, (2009), 521-528.
- [26] J. J. Murphy and C. R. Shaddix, "Combustion kinetics of coal chars in oxygen-enriched environments," *Combustion and Flame*, **144**, (2006), 710-729.
- [27] P. A. Bejarano and Y. A. Levendis, "Single-coal-particle combustion in O<sub>2</sub>/N<sub>2</sub> and O<sub>2</sub>/CO<sub>2</sub> environments," *Combustion and Flame*, **153**, (2008), 270-287.
- [28] E. Croiset and K. V. Thambimuthu, "NO<sub>x</sub> and SO<sub>2</sub> emissions from O<sub>2</sub>/CO<sub>2</sub> recycle coal combustion," *Fuel*, **80**, (2001), 2117-2121.

- [29] R. K. Rathnam, L. K. Elliott, T. F. Wall, Y. Liu, and B. Moghtaderi, "Differences in reactivity of pulverised coal in air (O<sub>2</sub>/N<sub>2</sub>) and oxy-fuel (O<sub>2</sub>/CO<sub>2</sub>) conditions," *Fuel Processing Technology*, **90**, (2009), 797-802.
- [30] H. Liu, R. Zailani, and B. M. Gibbs, "Comparisons of pulverized coal combustion in air and in mixtures of O<sub>2</sub>/CO<sub>2</sub>," *Fuel*, **84**, (2005), 833-840.
- [31] P. Glarborg and L. L. B. Bentzen, "Chemical Effects of a High CO<sub>2</sub> Concentration in Oxy-Fuel Combustion of Methane," *Energy & Fuels*, **22**, (2007), 291-296.
- [32] H. Liu, R. Zailani, and B. M. Gibbs, "Pulverized coal combustion in air and in O<sub>2</sub>/CO<sub>2</sub> mixtures with NO<sub>x</sub> recycle," *Fuel*, **84**, (2005), 2109-2115.
- [33] H. Liu, "Combustion of Coal Chars in O<sub>2</sub>/CO<sub>2</sub> and O<sub>2</sub>/N<sub>2</sub> Mixtures: A Comparative Study with Non-isothermal Thermogravimetric Analyzer (TGA) Tests," *Energy & Fuels*, **23**, (2009), 4278-4285.
- [34] L. Duan, C. Zhao, W. Zhou, C. Qu, and X. Chen, "Investigation on Coal Pyrolysis in CO<sub>2</sub> Atmosphere," *Energy & Fuels*, **23**, (2009), 3826-3830.
- [35] L. Duan, C. Zhao, W. Zhou, C. Liang, and X. Chen, "Sulfur evolution from coal combustion in O<sub>2</sub>/CO<sub>2</sub> mixture," *Journal of Analytical and Applied Pyrolysis*, **86**, (2009), 269-273.
- [36] N. N. Y. Bozzuto C. R. , Sloan D. G. ,MacWhinnie R. , Marion J. L., "Engineering Feasibility and Economics of CO<sub>2</sub> Capture on an Existing Coal Fired Power Plant Report," Alstom Power Inc2001.
- [37] V. Saravanan, A. Aravind, S. Jayanti, and Ramakrishna, "Burning Profile of High Ash Indian Coals in Oxy-Fuel Environment," *ASME Conference Proceedings*, **2008**, (2008), 119-131.
- [38] H. Haykiri-Acma, A. Z. Turan, S. Yaman, and S. Kucukbayrak, "Controlling the excess heat from oxy-combustion of coal by blending with biomass," *Fuel Processing Technology*, **91**, (2010), 1569-1575.
- [39] R. K. W. Borman G. L., *Combustion Engineering*: McGraw Hill, 1998.

- [40] J. Chen and X. Lu, "Progress of petroleum coke combustng in circulating fluidized bed boilers--A review and future perspectives," *Resources, Conservation and Recycling*, **49**, (2007), 203-216.
- [41] B.-X. Shen, D.-C. Liu, and H.-P. Chen, "A Study of the Mechanism of Petroleum Coke Pyrolysis," *Developments in Chemical Engineering and Mineral Processing*, **8**, (2000), 351-358.
- [42] C. Zhao, C. Chen, X. Chen, F. Wang, W. Wang, A. Zhu, and X. Wu, "Experimental Study on Characteristics of Pyrolysis, Ignition and Combustion of Blends of Petroleum Coke and Coal in CFB," *ASME Conference Proceedings*, **2005**, (2005), 617-622.
- [43] [http://www.enerji.gov.tr/index.php?dil=en&sf=webpages&b=kotur\\_EN&bn=511&hn=&nm=40717&id=4072924.12.2010](http://www.enerji.gov.tr/index.php?dil=en&sf=webpages&b=kotur_EN&bn=511&hn=&nm=40717&id=4072924.12.2010)).
- [44] S. N. Gogebakan Z. , "Co-firing Biomass with Coal in Fluidized Bed Combustion Systems," in *Handbook of Combustion*. vol. 4, W. F. Lackner M., Agarwal A. K. , Ed., ed Weinheim: Wiley-VCH, 2010, pp. 557-584.
- [45] "Statistical Year Book of Turkey 2009," Turkish Statistical Institute Prime Ministry Republic of Turkey, Ankara2010
- [46] A. Arenillas, F. Rubiera, B. Arias, J. Pis, J. Faúndez, A. Gordon, and X. García, "A TG/DTA study on the effect of coal blending on ignition behaviour," *Journal of Thermal Analysis and Calorimetry*, **76**, (2004), 603-614.
- [47] B. Arias, C. Pevida, F. Rubiera, and J. J. Pis, "Effect of biomass blending on coal ignition and burnout during oxy-fuel combustion," *Fuel*, **87**, (2008), 2753-2759.
- [48] J. P. Charland, J. A. MacPhee, L. Giroux, J. T. Price, and M. A. Khan, "Application of TG-FTIR to the determination of oxygen content of coals," *Fuel Processing Technology*, **81**, (2003), 211-221.
- [49] G. Di Nola, W. de Jong, and H. Spliethoff, "TG-FTIR characterization of coal and biomass single fuels and blends under slow heating rate conditions:

- Partitioning of the fuel-bound nitrogen," *Fuel Processing Technology*, **91**, (2010), 103-115.
- [50] T. Kaljuvee, J. Pelt, and M. Radin, "TG-FTIR study of gaseous compounds evolved at thermooxidation of oil shale," *Journal of Thermal Analysis and Calorimetry*, **78**, (2004), 399-414.
- [51] I. Pitkänen, J. Huttunen, H. Halttunen, and R. Vesterinen, "Evolved Gas Analysis of Some Solid Fuels by TG-FTIR," *Journal of Thermal Analysis and Calorimetry*, **56**, (1999), 1253-1259.
- [52] W. M. Groenewoud and W. de Jong, "The thermogravimetric analyser - coupled - Fourier transform infrared/mass spectrometry technique," *Thermochimica Acta*, **286**, (1996), 341-354.
- [53] L. Jia, E. J. Anthony, I. Lau, and J. Wang, "Study of coal and coke ignition in fluidized beds," *Fuel*, **85**, (2006), 635-642.
- [54] D. Vamvuka, E. Kastanaki, and M. Lasithiotakis, "Devolatilization and Combustion Kinetics of Low-Rank Coal Blends from Dynamic Measurements," *Industrial & Engineering Chemistry Research*, **42**, (2003), 4732-4740.
- [55] H. Haykiri-Acma and S. Yaman, "Interaction between biomass and different rank coals during co-pyrolysis," *Renewable Energy*, **35**, (2010), 288-292.
- [56] E. Osorio, M. L. F. Ghiggi, A. C. F. Vilela, W. D. Kalkreuth, and A. G. Borrego, "Non-isothermal combustion behaviour of coal blends in a thermobalance as seen by optical microscopy," *Thermochimica Acta*, **475**, (2008), 1-7.
- [57] J. Yu, J. A. Lucas, and T. F. Wall, "Formation of the structure of chars during devolatilization of pulverized coal and its thermoproperties: A review," *Progress in Energy and Combustion Science*, **33**, (2007), 135-170.
- [58] R. Bassilakis, Y. Zhao, P. R. Solomon, and M. A. Serio, "Sulfur and nitrogen evolution in the Argonne coals. Experiment and modeling," *Energy & Fuels*, **7**, (1993), 710-720.

- [59] S. Biswas, N. Choudhury, P. Sarkar, A. Mukherjee, S. G. Sahu, P. Boral, and A. Choudhury, "Studies on the combustion behaviour of blends of Indian coals by TGA and Drop Tube Furnace," *Fuel Processing Technology*, **87**, (2006), 191-199.
- [60] M. X. Fang, D. K. Shen, Y. X. Li, C. J. Yu, Z. Y. Luo, and K. F. Cen, "Kinetic study on pyrolysis and combustion of wood under different oxygen concentrations by using TG-FTIR analysis," *Journal of Analytical and Applied Pyrolysis*, **77**, (2006), 22-27.
- [61] T. Mi, Z. S. Wu, B. X. Shen, D. C. Liu, and H. P. Chen, "An Experimental Study of Combustion Characteristics of Petroleum Coke," *Developments in Chemical Engineering and Mineral Processing*, **10**, (2002), 601-614.
- [62] G. H. Liu, X. Q. Ma, and Z. Yu, "Experimental and kinetic modeling of oxygen-enriched air combustion of municipal solid waste," *Waste Management*, **29**, (2009), 792-796.
- [63] A. Chouchene, M. Jeguirim, B. Khiari, F. Zagrouba, and G. Trouvé, "Thermal degradation of olive solid waste: Influence of particle size and oxygen concentration," *Resources, Conservation and Recycling*, **54**, (2010), 271-277.
- [64] S. S. Daood, S. Munir, W. Nimmo, and B. M. Gibbs, "Char oxidation study of sugar cane bagasse, cotton stalk and Pakistani coal under 1% and 3% oxygen concentrations," *Biomass and Bioenergy*, **34**, (2010), 263-271.
- [65] S. Munir, S. S. Daood, W. Nimmo, A. M. Cunliffe, and B. M. Gibbs, "Thermal analysis and devolatilization kinetics of cotton stalk, sugar cane bagasse and shea meal under nitrogen and air atmospheres," *Bioresource Technology*, **100**, (2009), 1413-1418.
- [66] E. Biagini, F. Lippi, L. Petarca, and L. Tognotti, "Devolatilization rate of biomasses and coal-biomass blends: an experimental investigation," *Fuel*, **81**, (2002), 1041-1050.

## **APPENDIX A**

### **Pilot Scale Carbon Capture and Storage Projects**

In this section, Tables A.1 and A.2 shows large and pilot scale carbon capture and storage projects in worldwide, respectively. In these tables, names of projects, leader companies, fuel types, size, capturing type, start up time and location are summarized.

Table A.1: Large-Scale Power Plant Carbon Capture and Storage Projects

Large-scale Power Plant CCS Projects Worldwide							
USA							
Project Name	Leader	Feedstock	Size MW	Capture Process	CO <sub>2</sub> Fate	Start-up	Location
AEP Mountaineer	AEP	Coal	235	Post	Saline	2016	West Virginia
Taylorville	Tenaska	Coal	602	Pre	Saline	2012	Illinois
WA Parish	NRG Energy	Coal	60	Post	EOR	2013	Texas
TCEP	Summit Power	Coal	400	Pre	EOR	2014	Texas
Trailblazer	Tenaska	Coal	600	Post	EOR	2014	Texas
Kemper County	Southern	Coal	582	Pre	EOR	2014	Mississippi
HECA	HEI	Petcoke	390	Post	EOR	2014	California
FutureGen	FutureGen Alliance	Coal	200	Oxy	Saline	TBD	Illinois
Sweeny Gasification	ConocoPhillips	Coal	460	Pre	Saline & EOR	TBD	Texas
Antelope Valley	Basin Electric	Coal	120	Post	EOR	On Hold	North Dakota



Table A.1 Continued

Canada							
Project Name	Leader	Feedstock	Size MW	Capture Process	CO <sub>2</sub> Fate	Start-up	Location
Boundary Dam	SaskPower	Coal	100	Oxy	EOR	2015	Saskatchewan
Project Pioneer	TransAlta	Coal	450	Post	Saline & EOR	2015	Alberta
Bow City	BCPL	Coal	1000	Post	EOR	2014	Alberta
Belle Plaine	TransCanada	Petcoke	500	Pre	Undecided	Undecided	Saskatchewan
European Union							
Project Name	Leader	Feedstock	Size MW	Capture Process	CO <sub>2</sub> Fate	Start-up	Location
Belchatow	PGE	Coal	250-858	Post	Saline	2011-15	Poland
Ferrybridge	SSE	Coal	500	Post	Seq	2011-2012	UK
Longannet	Scottish Power	Coal	300	Post	EOR	2014	UK
Janschwalde	Vattenfall	Coal	250	Oxy	Saline	2015	Germany
Maasvlakte	E.ON	Coal	1100	Post	EGR	2015	Netherlands
Porto Tolle	ENEL	Coal	660	Post	Saline	2015	Italy
Compostilla	ENDESA	Coal	30-500	Oxy	Saline	2015	Spain
Goldenbergwerk	RWE	Coal	450	Pre	Saline	2015	Germany
Magnum	Nuon	Various	1200	Pre	EOR/ EGR	2015	Netherlands
Hatfield	Powerfuel	Coal	900	Pre	EOR	On hold	UK

Table A.1 Continued

Norway							
Project Name	Leader	Feedstock	Size MW	Capture Process	CO <sub>2</sub> Fate	Start-up	Location
Kårstø	Naturkraft	Gas	420	Post	Undecided	2011-2012	Norway
Husnes	Sargas	Coal	400	Post	EOR	2011	Norway
Mongstad	Statoil	Gas	350	Post	Saline	Waiting Funding	Norway
Rest of the World							
Project Name	Leader	Feedstock	Size MW	Capture Process	CO <sub>2</sub> Fate	Start-up	Location
GreenGen	GreenGen	Coal	250/800**	Pre	Saline	2010	China
NZEC	UK&China	Coal	460	Pre	EOR	2015	China
ZeroGen	ZeroGen	Coal	100	Pre	Saline	2012	Australia
UAE Project	Masdar	Gas	420	Pre	EOR	2015	UAE

Table A.2: Pilot Scale Power Plant Carbon Capture and Storage Projects

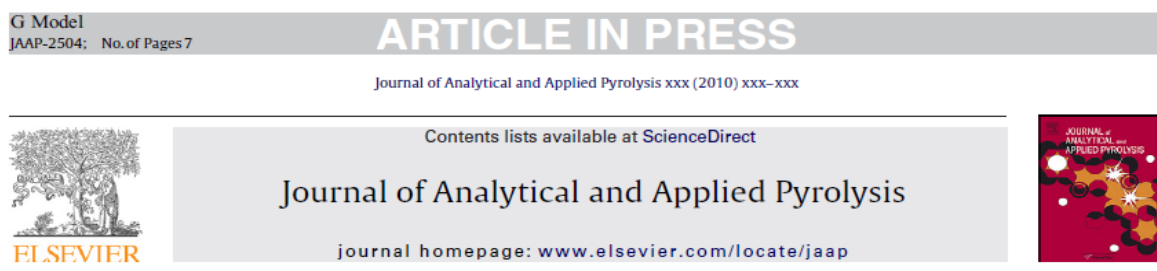
<b>Pilot CCS Projects</b>							
<b>Project Name</b>	<b>Leader</b>	<b>Feedstock</b>	<b>Size MW</b>	<b>Capture Process</b>	<b>CO<sub>2</sub> Fate</b>	<b>Start-up</b>	<b>Location</b>
Schwarze Pumpe	Vattenfall	Coal	30	Oxy	--	2008	Germany
ECO2 Berger	Powerspan	Coal	1	Post	Vented	2008	OH, USA
Pleasant Prarie	Alstom	Coal	5	Post	Vented	2008	WI, USA
AEP Mountaineer	AEP	Coal	30	Post	Saline	2009	WV, USA
Karlshamn	E.ON	Oil	5	Post	Vented	2009	Sweden
Shidongkou	Huaneng	Coal	0.1MT/Yr	Post	Commercial use	2009	China
Lacq	Total	Oil	35	Oxy	Depleted Gas	2010	France
Buggenum	Vattenfall	Coal	20	Post	Vented	2010	Netherlands
Brindisi	Enel &Eni	Coal	48	Post	EOR	2010	Italy
Kimberlina	Clean Energy Systems	Coal	50	Oxy	Saline	2011	CA, USA
Callide-A Oxy Fuel	CS Energy	Coal	30	Oxy	Saline	2011	Australia
Plant Barry	Southern Energy	Coal	25	Post	EOR	2011	AL, USA
Big Bend Station	Siemens	Coal	1	Post	Vented	2013	FL, USA
ZENG Risavika	CO2-Norway	Gas	50-70	Oxy	Undecided	Undecided	Norway
ZENG Worsham-Steed	CO2-Global	Gas	70	Oxy	EOR	Undecided	TX, USA

## **APPENDIX B**

### **Published Paper**

In this section, one of the papers that is published in Journal of Analytical and Applied Pyrolysis with doi:10.1016/j.jaap.2010.11.003, in the scope of this thesis study is given in Figure B.1.

Figure B.1: Published Paper



## Combustion behaviour of Turkish lignite in O<sub>2</sub>/N<sub>2</sub> and O<sub>2</sub>/CO<sub>2</sub> mixtures by using TGA–FTIR

Nevin Selcuk\*, Nur Sena Yuzbasi<sup>1</sup>

Middle East Technical University, Department of Chemical Engineering, Inonu Bulvarı, 06531 Ankara, Turkey

### ARTICLE INFO

#### Article history:

Received 25 September 2010

Accepted 9 November 2010

Available online xxx

#### Keywords:

Oxy-fuel combustion

Lignite

TGA–FTIR

Oxygen-enriched combustion

### ABSTRACT

The pyrolysis and combustion behaviour of a low calorific value Turkish lignite with high sulphur and ash content in air and oxy-fuel conditions were investigated by using non-isothermal thermo-gravimetric method (TGA) coupled with Fourier-transform infrared (FTIR) spectrometer. Pyrolysis tests were carried out in nitrogen and carbon dioxide environments which are the main diluting gases of air and oxy-fuel environment, respectively. Pyrolysis results show that weight loss profiles are almost the same up to a temperature of 720 °C in these two environments, indicating that CO<sub>2</sub> behaves as an inert gas in this temperature range. However, further weight loss takes place in CO<sub>2</sub> atmosphere at higher temperatures due to CO<sub>2</sub>–char gasification reaction. Combustion experiments were carried out in four different atmospheres: air, oxygen-enriched air environment (30% O<sub>2</sub>–70% N<sub>2</sub>), oxy-fuel environment (21% O<sub>2</sub>–79% CO<sub>2</sub>) and oxygen-enriched oxy-fuel environment (30% O<sub>2</sub>–70% CO<sub>2</sub>). Combustion experiments reveal that replacing nitrogen in the gas mixture by the same concentration of CO<sub>2</sub> does not affect the combustion process significantly but only leads to slight delay in combustion. Overall comparison of derivative thermogravimetry (DTG) profiles shows that oxygen content in the combustion environment is the most effective parameter irrespective of the diluting gas. As O<sub>2</sub> concentration increases profiles shift through lower temperature zone, peak and burnout temperatures decrease, weight loss rate increases and complete combustion is achieved at lower temperatures and shorter times. During pyrolysis and combustion tests gaseous products CO<sub>2</sub>, CO, H<sub>2</sub>O, CH<sub>4</sub>, SO<sub>2</sub> and COS in flue gas were identified and analyzed by using FTIR. Results indicate that higher CO and COS formation takes place during pyrolysis due to gasification reaction. Gaseous species evolution trends in combustion tests are found to be almost identical in oxygen enriched conditions independent of the diluting gas.

© 2010 Elsevier B.V. All rights reserved.

### 1. Introduction

Today, demand for electric power continues to increase due to population growth, technological and economical development. With 826 billion tones of proved coal reserves, coal combustion has an important role in energy production worldwide [1]. Growing concern about greenhouse gas emissions and their potential impact on climate change necessitate investigation of alternative technologies for reduction of CO<sub>2</sub> emissions from coal fired power plants. Conventional technologies for removing CO<sub>2</sub> from the stack gas in the existing coal fired power plants are expensive since CO<sub>2</sub> is diluted (typically about 14% by volume on a dry basis) [2]. The cost of gas separation can be reduced by increasing the concentration of CO<sub>2</sub> in the flue gas. Oxy-fuel combustion technology is

suggested as one of the new promising technologies for capturing CO<sub>2</sub> from power plants. This technology is based on burning coal in a mixture of oxygen and recycled flue gas (RFG) leading to CO<sub>2</sub> concentrations greater than 95% in the exhaust gas. Recycled flue gas is used to control flame temperature and supply the volume of missing N<sub>2</sub>. Oxy-fuel combustion technology for coal-fired power generation has been briefly described and reviewed in detail recently [3–5]. Oxy-fuel combustion is found to differ from air combustion in combustion characteristics such as burning stability, char burnout, gas temperature profiles and heat transfer due to differences in gas properties between CO<sub>2</sub> and N<sub>2</sub>, the main diluting gases in oxy-fuel and air, respectively. Previous studies on oxy-fuel combustion mainly revealed that similar temperature profiles with air case are achieved at higher oxygen concentrations, around 30% in the combustion environment, as the higher heat capacity of CO<sub>2</sub> causes delay in combustion process [2–7].

Non-isothermal thermo-gravimetric analysis (TGA) technique is a rapid, inexpensive and simple method that has been widely used in studying the pyrolysis and combustion behaviour of coal and evaluating the relative burning properties of coal samples.

\* Corresponding author. Tel.: +90 312 2102603; fax: +90 312 2102600.  
E-mail addresses: selcuk@metu.edu.tr (N. Selcuk), e168388@metu.edu.tr (N.S. Yuzbasi).

<sup>1</sup> Tel.: +90 312 2104395; fax: +90 312 2102600.

Figure B.1 Continued

There exists a considerable number of studies carried out for the investigation of combustion behaviour high rank coals in oxy-fuel environment by TGA [8–13]. However, an investigation of oxy-fuel combustion characteristics of indigenous lignites by TGA–FTIR technique is not available to date. Therefore, pyrolysis and combustion behaviours of an indigenous lignite with low calorific value, high ash and sulphur contents are studied in air and oxy-fuel conditions by using a TGA–FTIR combined system.

## 2. Experimental

### 2.1. Sample

A typical low quality indigenous lignite from Çan town of Çanakkale province in Turkey was used in pyrolysis and combustion tests. Proximate analysis of the Çan lignite was performed by using LECO TGA-701. Ultimate analysis was carried out with LECO CHNS-932. Calorific values of the fuels are measured by using AC-500 bomb calorimeter. Analyses were performed according to ASTM standards. The Jeol JSM-6400 scanning electron microscope (SEM) configured with a Noran energy dispersive spectrometer (EDS) was utilised for determination of ash composition. Proximate, ultimate and ash analyses of Çan lignite together with its calorific value are briefly summarized in Table 1. As can be seen from the table, Çan lignite can be characterized by its low calorific value, high ash content (~25%) and high total sulphur content (~4%).

### 2.2. Experimental setup and method

In the present work TGA/DTG were used to determine pyrolysis and combustion characteristics of lignite samples. TGA system was coupled with FTIR spectrometer for determination of evolved gases during pyrolysis and combustion experiments. Fig. 1 shows a schematic diagram of the experimental setup consisting of Perkin Elmer Pyris STA 6000 thermo-gravimetric analyzer, Spectrum 1 FTIR spectrometer and a mass flow controller (MFC) for each gaseous species. TGA and FTIR were connected by a heated line with a temperature of 270 °C in order to prevent the condensation of gases. FTIR spectra were collected with 4 cm<sup>-1</sup> resolution, in the range of 4000–700 cm<sup>-1</sup> IR absorption band.

About 12 mg of coal sample with particle size less than 100 µm was held initially at room temperature for 1 min and then heated with a heating rate of 40 °C/min from room temperature up to 950 °C during each experiment. In pyrolysis tests, samples were held at 950 °C for an additional 60 min. The required combustion environments were formed by mixing two gases in the desired ratio by using two different mass flow controllers in order to regulate the flow rates of the gases. The total gas flow was set to 70 ml/min for pyrolysis and 45 ml/min for combustion experiments.

**Table 1**  
Proximate, ultimate and ash analysis of Çan lignite.

Ultimate analysis (as received, % by wt.)		Proximate analysis (as received, % by wt.)	
C	37.31	Moisture	16.35
H	3.3	Ash	28.78
O	10.02	Volatile matter	29.79
N	0.91	Fixed carbon	25.08
S <sub>combustible</sub>	3.33		
Ash	28.78	LHV (MJ/kg)	9.89
Total moisture	16.35		
S <sub>total</sub>	3.49		
Ash analysis (% by wt.)			
SiO <sub>2</sub>	Al <sub>2</sub> O <sub>3</sub>	Fe <sub>2</sub> O <sub>3</sub>	CaO
43.13	18.2	15.78	7.63
			MgO
			0.48
			Na <sub>2</sub> O
			2.0
			K <sub>2</sub> O
			0.63
			SO <sub>3</sub>
			11.08
			TiO <sub>2</sub>
			1.07

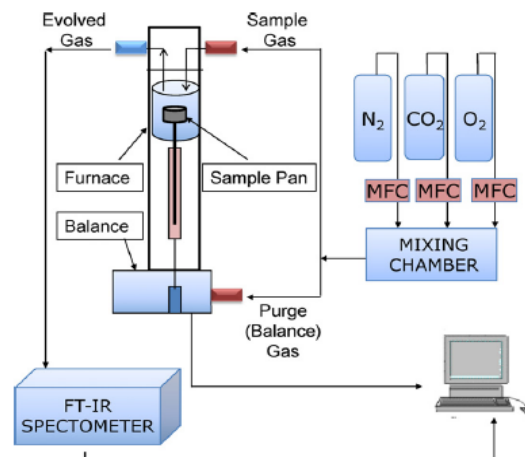


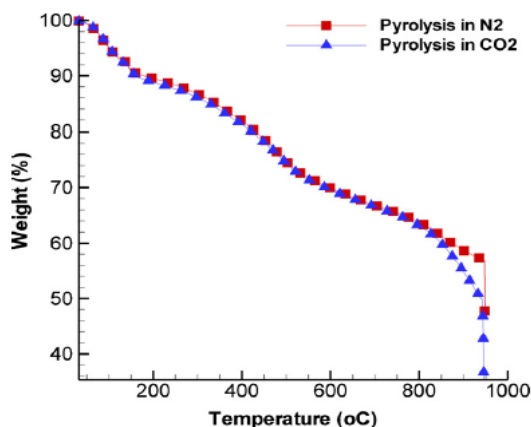
Fig. 1. Schematic diagram of the experimental setup.

Pyrolysis tests were carried out under nitrogen and carbon dioxide atmospheres which are the diluting gases of air and oxy-fuel environments, respectively. Four combustion tests were performed in air environment to investigate the effect of combustion environment on burning process of lignite sample. The base case was considered as lignite combustion in air environment. In oxygen-enriched air case the sample is burned in 30% O<sub>2</sub>–70% N<sub>2</sub> atmosphere. In oxy-fuel combustion tests, the volume of N<sub>2</sub> used in the base case was replaced with an equal volume of CO<sub>2</sub>. In the last case, combustion of lignite sample was investigated in oxygen-enriched oxy-fuel environment, that is, in 30% O<sub>2</sub>–70% CO<sub>2</sub> atmosphere.

TGA and DTG profiles obtained during pyrolysis and combustion experiments were used to determine some characteristic parameters such as initial decomposition temperature ( $T_{in}$ ), peak temperature ( $T_{max}$ ), ignition temperature ( $T_{ig}$ ) and burnout temperature ( $T_b$ ).  $T_{in}$  represents the initiation of weight loss and is defined as the temperature at which the rate of weight loss reaches 1%/min after initial moisture loss peak in DTG profile [22].  $T_{max}$  is the point at which maximum reaction rate occurs. Different from initial decomposition temperature, ignition temperature  $T_{ig}$  is defined as the temperature at which coal starts burning. It is taken as the temperature at which the weight loss curves in the oxidation and pyrolysis experiments diverge [20]. The last characteristic temperature considered is burnout temperature which represents the temperature where sample oxidation is completed. It is taken as the point immediately before reaction ceases when the rate of weight loss is 1%/min [21].

A linear relation between spectral absorbance at a given wavenumber and concentration of gaseous components is given by Beer's Law. In this study, the points of absorbance at a certain wavenumber are plotted against temperature in order to obtain a formation profile for each evolved gas observed in the spectra during experiments. The IR wavenumbers of CO<sub>2</sub>, CO, H<sub>2</sub>O, CH<sub>4</sub>, SO<sub>2</sub> and COS are 2360, 2112, 1540, 3016, 1340 and 2042 cm<sup>-1</sup>, respectively. Formation profiles of NO<sub>x</sub> related species such as NO and NO<sub>2</sub> are not reported due to overlap of their absorption bands with the characteristic absorption bands of water in the range of 3900–3500 and 1900–1350 cm<sup>-1</sup>.

Figure B.1 Continued

Fig. 2. TGA profile of Çan lignite during pyrolysis in N<sub>2</sub> and CO<sub>2</sub> atmospheres.

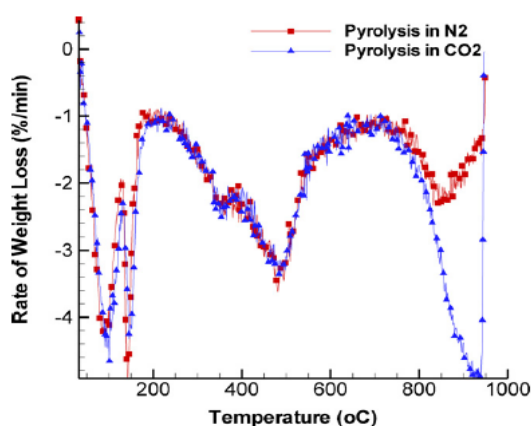
### 3. Results and discussion

#### 3.1. Pyrolysis tests of lignite in CO<sub>2</sub> and N<sub>2</sub> environments

##### 3.1.1. TGA/DTG results of pyrolysis tests

Pyrolysis as the preliminary process of coal combustion plays a crucial role in determining flame stability, ignition, and product distributions [14]. The possible impacts of different gases on pyrolysis process necessitate the investigation of devolatilization behaviour of coal in both N<sub>2</sub> and CO<sub>2</sub> environments. In nitrogen and carbon dioxide atmospheres, devolatilization of coals may differentiate in volatile composition, volatile yield and possible CO<sub>2</sub>–char reaction at high temperature range. TGA and DTG profiles of pyrolysis tests are shown in Figs. 2 and 3, respectively.

As can be seen from figures, pyrolysis behaviour of lignite samples in N<sub>2</sub> and CO<sub>2</sub> atmosphere is observed to be very similar up to around 720 °C which indicates that CO<sub>2</sub> behaves as an inert atmosphere until a certain temperature. After moisture release in the first 200 °C temperature zone, pyrolysis continues with the release

Fig. 3. DTG profile of Çan lignite during pyrolysis in N<sub>2</sub> and CO<sub>2</sub> atmospheres.

**Table 2**  
Pyrolysis characteristics of Çan lignite in N<sub>2</sub> and CO<sub>2</sub>.

	Pyrolysis in N <sub>2</sub>	Pyrolysis in CO <sub>2</sub>
$T_{in}$ (°C)	230.8	216.7
$T_{max}$ (°C)	482.9	481.0
$(dm/dt)_{max}$ (%/min)	3.6	3.2
Total weight loss up to 950 °C	41.0	50.3

of volatile matter content in the range of 200–750 °C. In 250–490 °C temperature interval, it is known that primary pyrolysis takes place which includes the release of larger fraction of volatiles, mainly light species and gases; CO<sub>2</sub>, light aliphatic gases, CH<sub>4</sub> and H<sub>2</sub>O. Tar and hydrocarbons evolve between 490 and 640 °C. During secondary pyrolysis additional gas formation such as CH<sub>4</sub>, CO and H<sub>2</sub> from ring condensation is mainly observed [14,15]. In CO<sub>2</sub> atmosphere, the maximum weight loss rate is found to be slightly lower with higher corresponding temperature ( $T_{max}$ ) than the ones in nitrogen atmosphere which could be due to the effect of higher heat capacity of CO<sub>2</sub>. The major difference in pyrolysis of lignite samples in these two different atmospheres is observed after 720 °C with the separation of TGA profiles. In 700–950 °C temperature range, additional peaks are displayed in both DTG profiles as shown in Fig. 3. In nitrogen atmosphere, a small peak appearing after 700 °C is attributed to partial burning of combustible matter at high temperatures by using inherent oxygen (almost 10% in Çan lignite) in lignite sample. This is also confirmed with the FTIR results which show a significant increase in CO<sub>2</sub> formation after 700 °C as presented in Fig. 4. On the other hand, the sharp peak observed in DTG profile of pyrolysis in CO<sub>2</sub> environment can be attributed to char–CO<sub>2</sub> gasification reaction as also confirmed by higher total weight loss in CO<sub>2</sub> atmosphere as shown in Table 2 and by other studies [8,9,12].

##### 3.1.2. FTIR results of pyrolysis tests

Formation profiles of evolved gases including CO<sub>2</sub>, CO, H<sub>2</sub>O, CH<sub>4</sub>, SO<sub>2</sub> and COS during pyrolysis in N<sub>2</sub> and CO<sub>2</sub> environments are shown in Fig. 4. In both environments, H<sub>2</sub>O is detected in the first 200 °C due to moisture release and also in the temperature range of 400–600 °C. In nitrogen environment, CO<sub>2</sub> release starts after 150 °C and continues up to 550 °C. Additional peak appears in CO<sub>2</sub> and CO formation curves due to burning of combustible matter in N<sub>2</sub> environment after 750 °C as explained in previous section. In the case of pyrolysis in CO<sub>2</sub> environment, significant amount of CO is evolved from char–CO<sub>2</sub> gasification reaction. Formation of CO in CO<sub>2</sub> environment is found to be the major contributor to the evolved gases with its highest absorbance intensity at high temperature zone. Evolution of CO continues with a distinctive increase after 600 °C in CO<sub>2</sub> environment. On the other hand, in N<sub>2</sub> environment, negligible amount of CO is formed due to partial burning of combustible matter. Methane release starts at 300 °C and continues till the end of the pyrolysis tests with a maximum release around 500 °C, in both environments. Similar trends are observed in evolution of CH<sub>4</sub> during devolatilization. In pyrolysis of high sulphur content lignite, SO<sub>2</sub> and COS release is noted. Similar SO<sub>2</sub> formation profiles are obtained in both environments in the temperature range of 250–625 °C, with two main peaks. Similar trends indicate that SO<sub>2</sub> formation does not depend on the pyrolysis environment. The other sulphur containing gas COS is formed by reaction of pyrite or sulphur formed during pyrite decomposition with CO [12,16]. COS formation is observed to increase significantly with the initiation of gasification reaction in CO<sub>2</sub> environment. Higher CO concentration in pyrolysis environment leads to the formation of COS in CO<sub>2</sub> atmosphere, in contrast to N<sub>2</sub> atmosphere.



Figure B.1 Continued

G Model

JAAP-2504; No. of Pages 7

ARTICLE IN PRESS

4

N. Selcuk, N.S. Yuzbasi / Journal of Analytical and Applied Pyrolysis xxx (2010) xxx–xxx

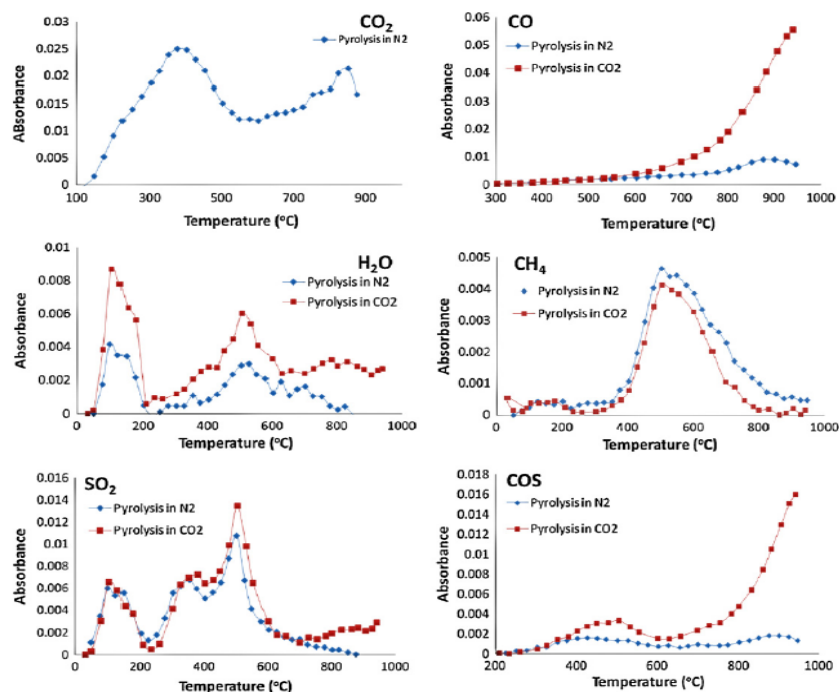


Fig. 4. Formation profiles of evolved gases during pyrolysis tests.

### 3.2. Combustion tests of lignite in O<sub>2</sub>/N<sub>2</sub> and O<sub>2</sub>/CO<sub>2</sub> environments

#### 3.2.1. TGA/DTG results of combustion tests

Combustion tests of lignite were carried out in air, oxygen-enriched air (30% O<sub>2</sub>–70% N<sub>2</sub>), oxy-fuel environment (21% O<sub>2</sub>–79% CO<sub>2</sub>), and oxygen-enriched oxy-fuel environment (30% O<sub>2</sub>–70% CO<sub>2</sub>) and their TGA/DTG curves are shown in Figs. 5 and 6. Results obtained from combustion profiles show clear differences in the combustion characteristics as summarized in Table 3.

Comparison of TGA curves in Fig. 5 indicates that the effect of oxygen concentration is more significant than that of the diluting gas (N<sub>2</sub> or CO<sub>2</sub>) on the combustion profiles. While combustion in O<sub>2</sub>/N<sub>2</sub> and O<sub>2</sub>/CO<sub>2</sub> mixtures with identical oxygen concentrations

results in only slight differences in combustion characteristics of lignite, elevated oxygen levels in combustion environment shift the weight loss curves to lower temperature zone. First step of the weight loss accounts for the moisture release in the first 200 °C temperature range and the corresponding weight loss due to moisture release is found approximately 10% for all cases. The second step represents the weight loss due to devolatilization and char burning. Total weight loss of samples is found to be almost the same in all combustion cases.

Fig. 6 demonstrates comparison between DTG curves of combustion in different atmospheres. First peak within 200 °C and the second peak within the temperature range 225–600 °C represent moisture release and devolatilization and char burning, respectively. In air firing case, devolatilization and char burning steps

Table 3

Combustion characteristics of Çan lignite in different atmospheres.

	21% O <sub>2</sub> –79% N <sub>2</sub>	30% O <sub>2</sub> –70% N <sub>2</sub>	21% O <sub>2</sub> –79% CO <sub>2</sub>	30% O <sub>2</sub> –70% CO <sub>2</sub>
T <sub>in</sub> (°C)	224.0	226.1	225.8	202.8
T <sub>max</sub> (°C)	426.2	314.5	347.1	317.2
T <sub>10</sub> (°C)	297.1	265.3	308.8	264.1
T <sub>50</sub> (°C)	546.8	530.0	550.0	535.6
(dm/dt) <sub>max</sub> (%/min)	11.0	20.5	12.3	19.0
Total weight loss up to 950 °C	59.2	59.3	59.6	61.2

Please cite this article in press as: N. Selcuk, N.S. Yuzbasi, J. Anal. Appl. Pyrol. (2010), doi:10.1016/j.jaap.2010.11.003



Figure B.1 Continued

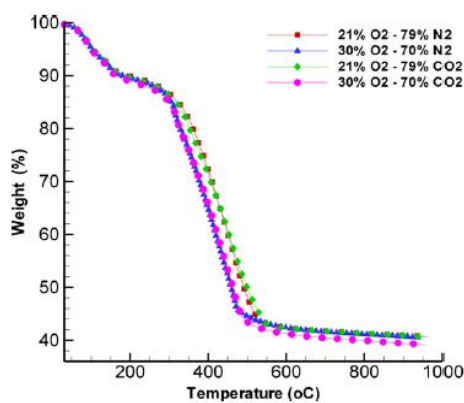


Fig. 5. TGA profile of Çan lignite in different combustion atmospheres.

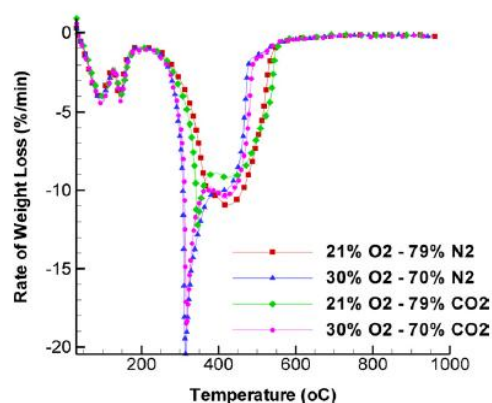


Fig. 6. DTG profile of Çan lignite in different combustion atmospheres.

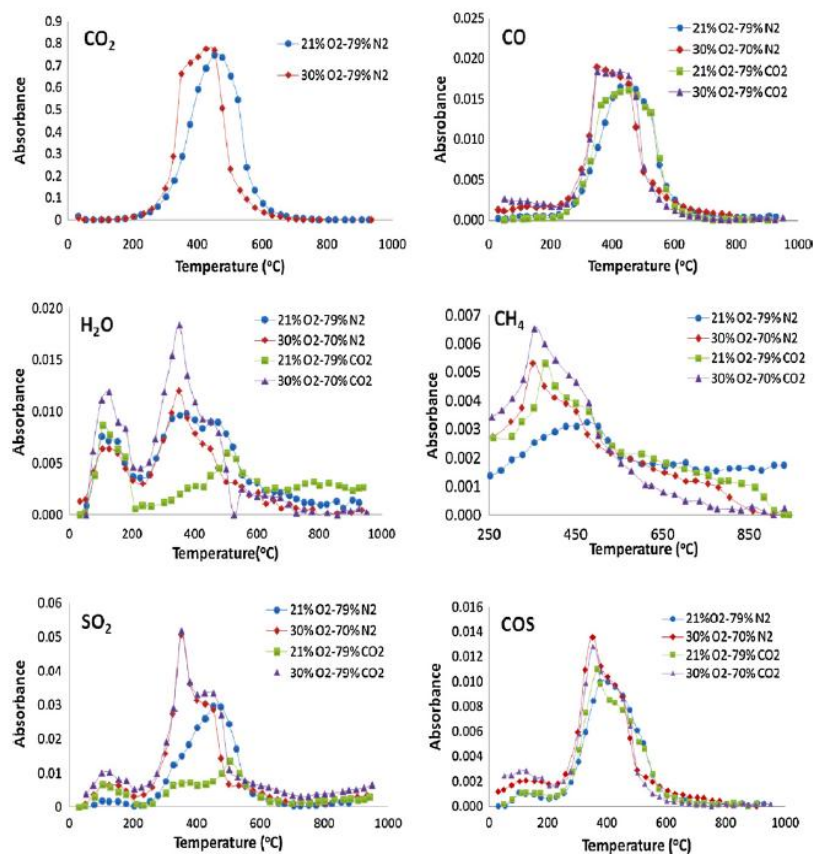


Fig. 7. Formation profiles of evolved gases during combustion tests.

Figure B.1 Continued

G Model  
JAAP-2504; No. of Pages 7

## ARTICLE IN PRESS

6

N. Selcuk, N.S. Yuzbasi / Journal of Analytical and Applied Pyrolysis xxx (2010) xxx–xxx

are not discretely separated; however, the shoulder around 370 °C can be attributed to volatile release. In oxy-fuel case the DTG profile of the lignite sample differs from the air-firing case with a small peak indicating the volatile matter release and a shoulder in 370–570 °C temperature interval indicating char burning which takes place within the same temperature interval in both cases. In oxygen-enriched conditions (30% O<sub>2</sub>–70% N<sub>2</sub> and 30% O<sub>2</sub>–70% CO<sub>2</sub>) the DTG profiles are similar with distinct volatile release peaks and characteristic temperatures as shown in Table 3. The similarity in DTG profiles obtained at the same oxygen concentration levels but with different diluting gas environments is an expected result. In TGA technique combustion temperature of the sample is controlled by electrical heating and sample temperature is not affected by combustion environment. Therefore, different heat capacities of diluting gases in combustion environment has no significant effect on combustion in contrast to practical tests as also confirmed in other studies [9,10,13]. Slightly higher burnout temperature in the CO<sub>2</sub> environment is indicative of slightly delayed combustion.

Effect of higher oxygen concentration on the combustion process is investigated with the tests under 30% O<sub>2</sub>–70% N<sub>2</sub> and 30% O<sub>2</sub>–70% CO<sub>2</sub> environments. Similar trends in the early stage of the process (up to 250 °C) in both environments reveal that initiation of the combustion process is not affected by oxygen concentration level. But at higher temperatures, more significant differences are displayed in DTG curves. In oxygen-enriched conditions, weight loss steps including volatile matter release and char burning are separately displayed in the DTG profile. In oxygen-enriched conditions a sharper peak that is observed in 250–400 °C temperature interval with a weight loss of 24%, is attributed to volatile matter release since weight loss value is in accordance with the one determined in pyrolysis conditions. Sharper peak is observed to continue with a distinctive shoulder up to 500 °C as represented in Fig. 6. In some studies it was demonstrated that the force of the fusion layer around solid particles is reduced by the presence of oxygen [17,18]. This situation also results in faster release of volatiles depending on the nature of solid particles and experimental conditions. High volatile matter content of lignite and the ease with which it is released, result in the formation of a sharper preliminary peak previously observed in low rank coals [19]. The shoulder following the peak is considered to account for weight loss due to burning of char in the sample. Increase in the oxygen concentration causes a shift of the burning profile to the lower temperature zone. Effect of oxygen concentration on characteristic temperatures is very clear. Characteristic temperatures including  $T_{ig}$ ,  $T_{max}$  and  $T_b$  are found to be lower in oxygen-enriched conditions. Moreover at higher O<sub>2</sub> concentrations complete combustion is achieved at lower temperatures and shorter times.

### 3.2.2. FTIR results of combustion tests

Fig. 7 displays formation profiles of gases evolved in different combustion environments. Gaseous species evolved during combustion tests were found to be CO<sub>2</sub>, CO, H<sub>2</sub>O, CH<sub>4</sub>, SO<sub>2</sub> and COS. As can be seen from the figure, the same specie evolves in different combustion environments.

H<sub>2</sub>O formation profiles show that moisture is released first in all combustion environments with further release in the temperature range of 200 °C to 550 °C. The major contributor to the evolved gases is found to be CO<sub>2</sub> with its higher absorbance intensity. The formation profile of CO<sub>2</sub> in oxygen-enriched air atmosphere shifts to lower temperature zone as elevated oxygen levels lead to faster burning and earlier release of CO<sub>2</sub>. CO formation profiles display similar trends in identical oxygen concentration levels while increase in oxygen level results in lower peak temperature. Methane evolution mainly takes place in the temperature range of 250–550 °C. In oxygen-enriched conditions, maximum

release is observed around 350 °C which corresponds to the peak in DTG profile of volatile matter. In the case of sulphur containing gases, SO<sub>2</sub> and COS appear in the FTIR spectra. Trend of SO<sub>2</sub> evolution in FTIR spectra are found to be in accordance with the DTG curves. SO<sub>2</sub> release starts around 200 °C and displays different formation profiles depending on the combustion environment. Maximum release takes place at about 500 °C in air- and oxy-firing cases and 350 °C in oxygen-enriched firing conditions. COS formation is observed in all combustion tests in the temperature range of 200–550 °C with sharper peaks in oxygen-enriched conditions.

## 4. Conclusions

Pyrolysis and combustion characteristics of a typical indigenous lignite is investigated in air and oxy-fuel conditions by using a combined TGA–FTIR system. In pyrolysis tests, similar profiles are observed up to 720 °C in N<sub>2</sub> and CO<sub>2</sub> environments. However, at high temperature zone, further weight loss is observed due to CO<sub>2</sub>–char gasification reaction in CO<sub>2</sub> atmosphere. Combustion tests were carried out in O<sub>2</sub>/N<sub>2</sub> and O<sub>2</sub>/CO<sub>2</sub> mixtures with oxygen concentrations of 21% and 30%. Results indicate that combustion in O<sub>2</sub>/CO<sub>2</sub> environment is delayed to a small extent compared with that in O<sub>2</sub>/N<sub>2</sub> environment at the same oxygen concentration. It is important to note that higher oxygen content in the combustion environment is the dominant factor affecting the combustion rather than the diluting gas. As oxygen concentration increases, DTG profiles shift to lower temperature zone, combustion rate increases and burnout time gets shorter. CO<sub>2</sub>, CO, H<sub>2</sub>O, CH<sub>4</sub>, SO<sub>2</sub> and COS are clearly identified in the FTIR spectra. Significant amount of CO due to char–CO<sub>2</sub> gasification reaction and consecutively COS is evolved in CO<sub>2</sub> atmosphere. In combustion, formation profiles displayed similar trends in oxygen-enriched conditions regardless of diluting gas in combustion environment. The current results add to previous literature data pyrolysis and combustion behaviour of indigenous lignite in air and oxy-fuel conditions.

## Acknowledgements

Financial support of TUBITAK through 109M401 project is gratefully acknowledged. The authors also wish to express their gratitude to Central Laboratory of the Middle East Technical University for the support provided during the TGA–FTIR tests and to Prof. Dr. Necati Ozkan for the valuable discussions.

## References

- [1] BP Statistical Review of World Energy, September 2010, [www.bp.com](http://www.bp.com).
- [2] D. Singh, E. Croiset, P.L. Douglas, M.A. Douglas, *Energy Convers. Manage.* 44 (2003) 3073–3091.
- [3] B.J.P. Buhre, L.K. Elliott, C.D. Sheng, R.P. Gupta, T.F. Wall, *Prog. Energy Combust.* 31 (2005) 283–307.
- [4] T. Wall, Y. Liu, C. Spero, L. Elliot, S. Khare, R. Rantham, F. Zeenathal, B. Moghtaderi, B. Buhre, C. Sheng, R. Gupta, T. Yamada, K. Makino, J. Yu, *Chem. Eng. Res. Des.* 7 (8) (2009) 1003–1016.
- [5] M.B. Toftegaard, J. Brix, P.A. Jensen, P. Glarborg, A.D. Jensen, *Prog. Energy Combust.* 36 (2010) 581–625.
- [6] Y. Tan, E. Croiset, M.A. Douglas, K.V. Thambimuthu, *Fuel* 85 (2006) 507–512.
- [7] H. Liu, R. Zailani, B. Gibbs, *Fuel* 84 (2005) 833–840.
- [8] Q. Li, C. Zhao, X. Chen, W. Wu, Y. Li, *J. Anal. Appl. Pyroly.* 85 (2009) 521–528.
- [9] R.K. Rantham, L.K. Elliott, T.F. Wall, Y. Liu, B. Moghtaderi, *Fuel Process. Technol.* 90 (2009) 797–802.
- [10] H. Liu, *Energy Fuels* 3 (2009) 4278–4285.
- [11] L. Duan, C. Zhao, W. Zhou, C. Liang, X. Chen, *J. Anal. Appl. Pyroly.* 86 (2009) 269–273.
- [12] L. Duan, C. Zhao, W. Zhou, C. Qu, Z. Chen, *Energy Fuels* 23 (2009) 3826–3830.
- [13] C.R. Bozzuto, N. ya Nsakala, D.G. Sloan, R. MacWhinnie, J.L. Marion, *Engineering Feasibility and Economics of CO<sub>2</sub> Capture on an Existing Coal Fired Power Plant Report*, vol. II, Alstom Power Inc., June 2001.
- [14] J. Yu, J.A. Lucas, T.F. Wall, *Prog. Energy Combust.* 33 (2007) 135–170.
- [15] D. Vamvuka, E. Kakaras, E. Kastanaki, P. Grammelis, *Fuel* 82 (2003) 1949–1960.

Please cite this article in press as: N. Selcuk, N.S. Yuzbasi, *J. Anal. Appl. Pyroly.* (2010), doi:10.1016/j.jaap.2010.11.003

Figure B.1 Continued

G Model		ARTICLE IN PRESS	
JAAP-2504; No. of Pages 7			
<i>N. Selcuk, N.S. Yuzbasi / Journal of Analytical and Applied Pyrolysis xxx (2010) xxx–xxx</i>		7	
[16] R. Basilakis, Y. Zhao, P.R. Solomon, M.A. Serio, <i>Energy Fuels</i> 7 (1993) 710–720.	[19] J.W. Cumming, <i>Thermochim. Acta</i> 155 (1989) 151–161.		
[17] G.H. Liu, X.Q. Ma, Z. Yu, <i>Waste Manage.</i> 29 (2009) 792–796.	[20] L. Jia, E.J. Anthony, I. Lau, J. Wang, <i>Fuel</i> 85 (2006) 635–642.		
[18] M.X. Fang, D.K. Shen, Y.X. Li, C.J. Yu, Z.Y. Luo, K.F. Cen, <i>J. Anal. Appl. Pyrol.</i> 77 (2006) 22–27.	[21] P.A. Morgan, S.D. Robertson, J.F. Unsworth, <i>Fuel</i> 65 (1986) 1546–1551.		
	[22] S. Su, J.H. Pohl, D. Holcombe, J.A. Hart, <i>Prog. Energy Combust.</i> 27 (2001) 75–98.		

## APPENDIX C

### FTIR Profiles of Imported Coal

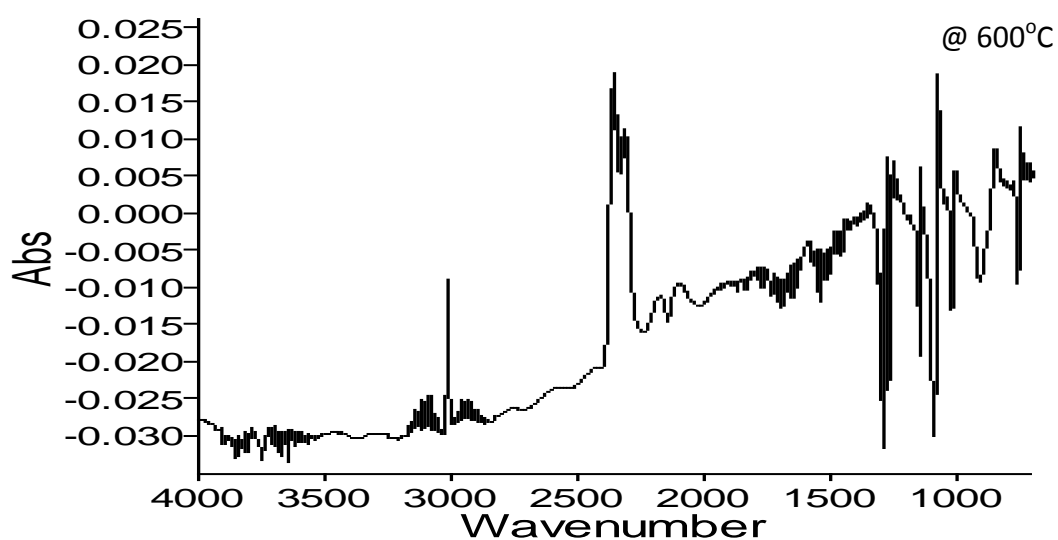


Figure C.1: FTIR profile of pyrolysis of imported coal in N<sub>2</sub> atmosphere.

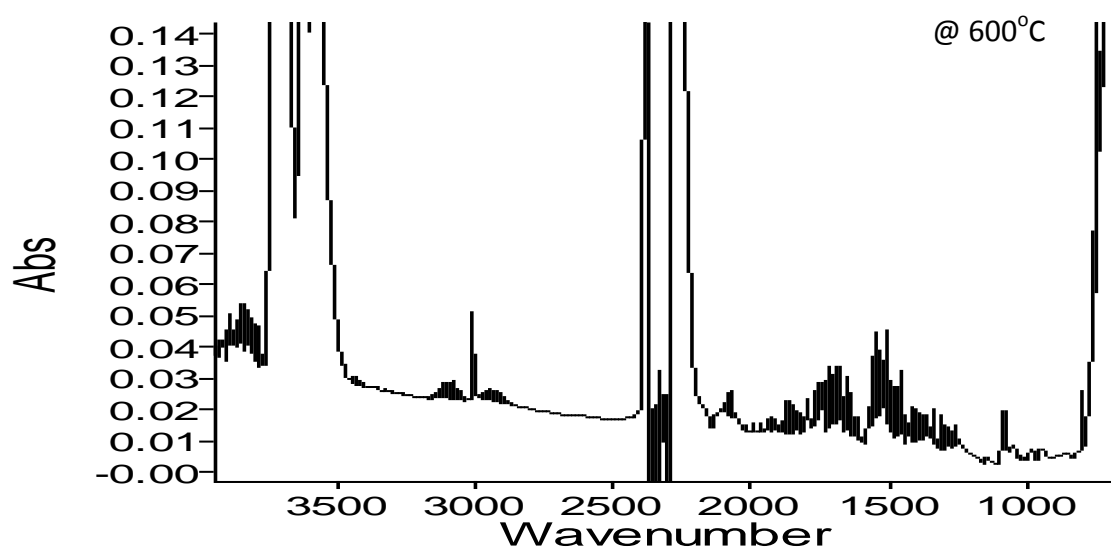


Figure C.2: FTIR profile of pyrolysis of imported coal in CO<sub>2</sub> atmosphere.

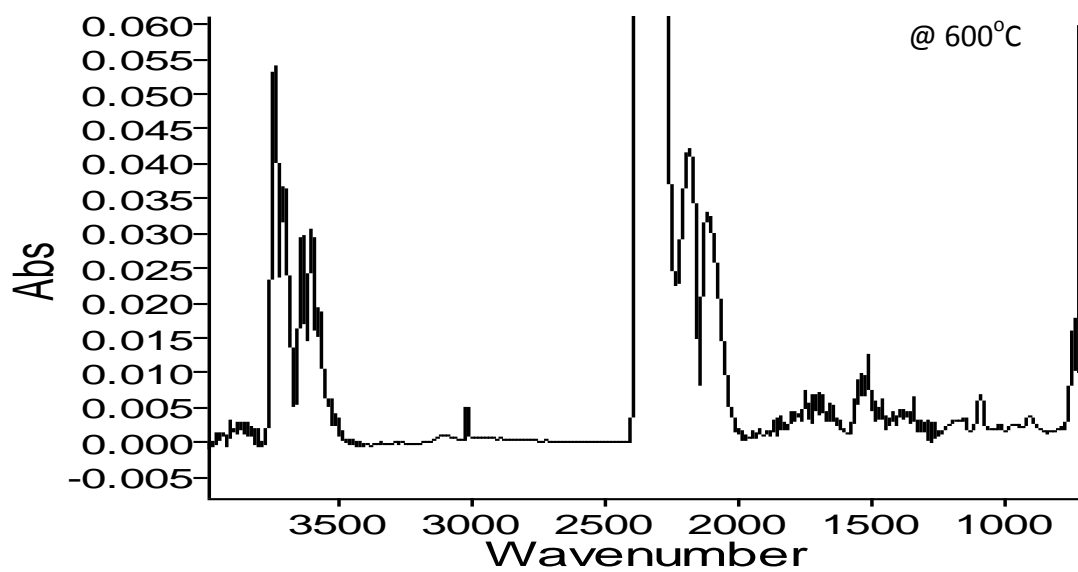


Figure C.3: FTIR profile of combustion of imported coal in 21% O<sub>2</sub> – 79% N<sub>2</sub> atmosphere.

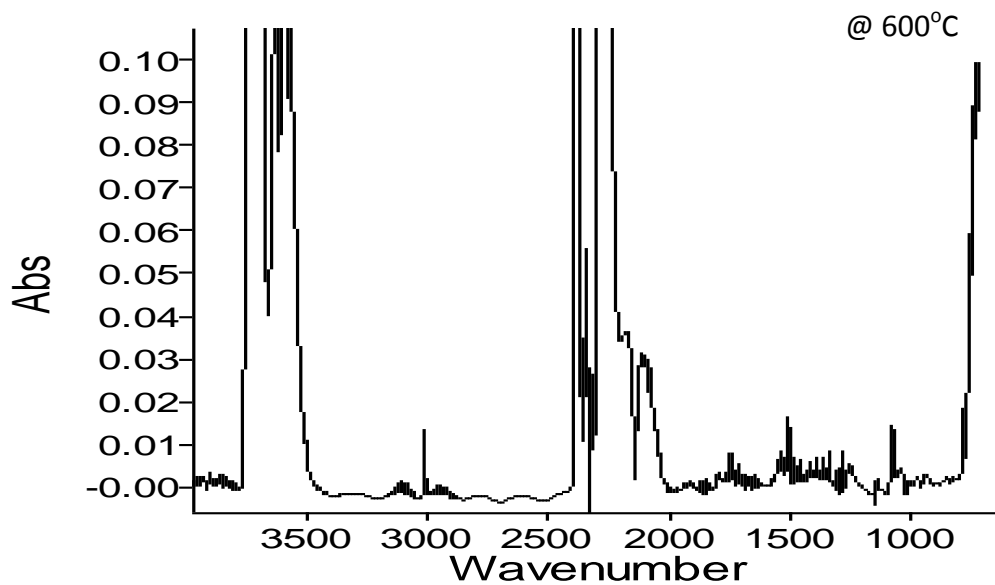


Figure C.4: FTIR profile of combustion of imported coal in 21% O<sub>2</sub> – 79% CO<sub>2</sub> atmosphere.

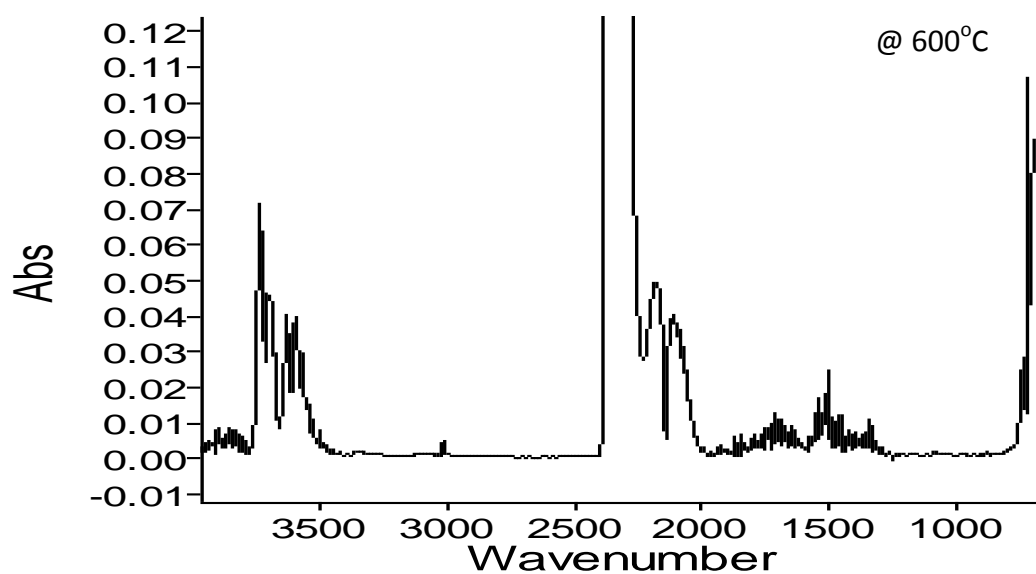


Figure C.5: FTIR profile of combustion of imported coal in 30% O<sub>2</sub> – 70% N<sub>2</sub> atmosphere.

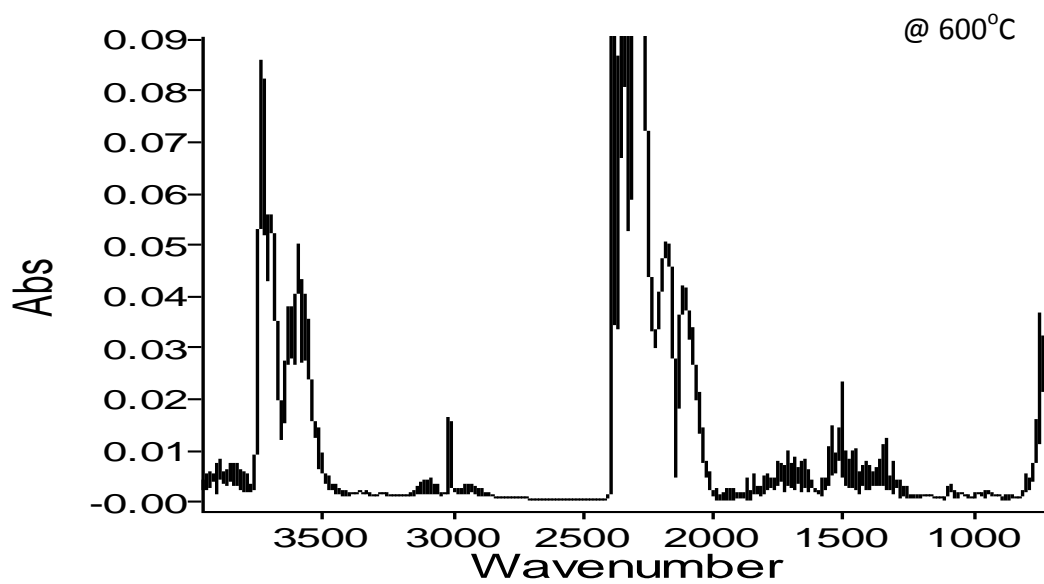


Figure C.6: FTIR profile of combustion of imported coal in 30% O<sub>2</sub> – 70% CO<sub>2</sub> atmosphere.